School of Geography, Archaeology and Environmental Studies

University of the Witwatersrand, Johannesburg

Monitoring biomass burning emissions using satellite imagery for Southern Africa

Candice-Joy McKechnie

0002111F

Supervisors: Prof. Stuart Piketh

Dr Kristy Ross

A dissertation submitted to the Faculty of Science, University of the Witwatersrand

for the degree of Master of Science

October 2010

Declaration

I declare that this dissertation is my own unaided work in fulfilment of the degree of Master of Science in the School of Geography, Archaeology and Environmental Studies at the University of Witwatersrand, Johannesburg. It has not been submitted previously for any degree or examination in any other university.

_____

(Candice-Joy McKechnie)

_____day of_____2010

Dedication

To my parents,

Kenneth Hugo and Marijke McKechnie

Abstract

Biomass burning contributes significantly to the global concentrations of greenhouse gases and aerosols in the atmosphere (Fishman et al., 2003, Kaufman et al., 1998). The African continent is responsible for a large proportion of these emissions, especially due to savanna burning (Scholes et al., 1996a). Due to extensive burning on the African continent, monitoring fires and quantifying their emissions has become important and relevant especially in southern Africa. Moderate Resolution Imaging Spectrometer (MODIS) daily active fire counts are used as a proxy for burning to provide insight into spatial and temporal distribution of fires and estimate biomass burning emissions over southern Africa. The burning season in southern Africa occurs during winter and spring and coincides with the dry season (May to October). Fires start in the western part of the sub-continent in March and spreads south and east throughout the burning season. Conditions are most conducive to fire occurrence when a particularly wet season follows an extended or particularly dry season. Anthropogenic burning is emphasised by the inconsistent correlation between rainfall and burning. The pattern for interannual and seasonal burning emissions is similar for carbon dioxide (CO_2), carbon monoxide (CO), methane (CH_4), ammonia (NH_3), total particulate carbon (TPC) and organic particulate carbon (OPC), with greatest quantities emitted from woodland fires, followed by forest and savanna, and lastly agriculture. Biomass burning emissions (189 $TgCO_2.yr^{-1}$) constitute approximately one quarter of the CO_2 emissions released by the industrial and the energy sector combined (843 $TgCO_2.yr^{-1}$) in South Africa. This study estimates twice the amount of particulates (610.yr^{-1}) released by biomass burning in South Africa as the industrial and energy sector combined (331. yr^{-1}). CH_4 emissions from biomass burning (approximately 463 $GgCH_4.yr^{-1}$) makes a considerable contribution to total CH_4 emissions (approximately 844 $GgCH_4.yr^{-1}$) for South Africa. The accuracy of greenhouse gas and aerosol estimates can be refined by using improved burned area estimates, consistent vegetation maps and standardised emission factors.

Preface

Biomass burning has been identified as a significant source of aerosol and trace gases (Scholes and Andreae, 2000), such as carbon dioxide (CO_2), methane (CH_4), nitrogen oxides (NO_x), carbon monoxide (CO) and hydrocarbons (Levine *et al*., 1996; Piketh and Walton, 2003). The African continent is responsible for a large contribution to global emissions especially due to savanna burning (Scholes *et al.*, 1996a and b). Biomass burning also contributes to the formation of tropospheric ozone (O_3) (Levine *et al*., 1996; Piketh and Walton, 2003). The peak of the burning season in southern Africa coincides with the dry season, which occurs during the southern hemisphere winter and spring (Christopher *et al.*, 1998). It is important to research trace gas and aerosol emission estimates because of their contribution to the regional air pollution (Guild *et al*., 1998) and the significant effect on climate and hence climate variability.

There are a number of parameters needed to calculate the emissions from biomass burning, namely burning efficiency, burned area, biomass density and emission factors. In this study biomass burning emissions for southern Africa (southern hemisphere Africa) between September 2002 and November 2006 are calculated using Moderate Resolution Imaging Spectroradiometer (MODIS) as a proxy for burned area. There are many uncertainties regarding emission calculations and parameters and further studies within this field are required to refine emission estimates.

This dissertation is divided into four chapters. In **Chapter 1** the background of this study is introduced and the aims and objectives are presented. A general literature review includes the contribution of biomass burning to regional and global emissions, and the transport and climatic effects of biomass burning emissions. A review of the use of various remote sensing and satellite products for fire detection is given. In **Chapter 2** the origin of the data used and the methods used to investigate the interannual and seasonal variations are outlined. The methods and data used to calculate the burnt biomass and resultant emissions are also described. In **Chapter 3** a discussion of the interannual and seasonal variations in burning patterns throughout southern Africa is presented, as well as the factors driving these patterns. In **Chapter 4** the seasonality of emissions from biomass burning and the variation in chemical species according to vegetation type are discussed. Biomass burning emissions calculated in this study are compared to results from global

studies, comparative studies for southern Africa and to other sectors to establish an estimated contribution of biomass burning emissions to regional air quality. In **Chapter 5** a summary of the findings of this research are presented and conclusions are provided.

This work contributes to refining the quantification of the contribution of biomass burning to ambient air quality. Training with regards to biomass burning, satellite products and emission calculation and representation was conducted at the Naval Research Laboratory (NRL), Monterey, United States of America. The Centre for Scientific and Industrial Research (CSIR) provided the MODIS active fire data that forms part of the Advanced Fire Information System (AFIS). Sections of this work have been presented at local conferences including the South African Society of Atmospheric Sciences (SASAS), held in Richards Bay, September 2005, Bloemfontein, October 2006 and in Johannesburg, September 2007.

I would like to thank the National Research Foundation (NRF), the University of the Witwatersrand, Johannesburg and the Climatology Research Group (CRG) for financial support throughout the duration of this research. Thanks to Phillip Frost from CSIR for MODIS active fire data. A special note of appreciation goes to Dr Jeff Reid and Betsy Reid for hosting me in their home and at the NRL, Monterey in December 2005. Many thanks to my fellow students at the CRG who have assisted in my research in many regards, as well as making the time with the CRG incredibly memorable. Extended thanks are given to Dr Kristy Ross for her knowledge, guidance, support, patience, encouragement and friendship throughout my involvement in the Climatology Research Group and beyond. This research was done under the guidance of Professor Stuart Piketh and Dr Kristy Ross. An exceptional note of thanks goes to Professor Piketh who opened a whole new world of science to me and provided many opportunities that broadened my horizons, knowledge and self. His advice, influence and guidance will always be held in high regard beyond my time with the CRG and this project. A special thanks to my parents who have supported and encouraged me and have provided the tools necessary for me to reach my goals.

TABLE OF CONTENTS

LIST OF FIGURES

List of Tables

CHAPTER 1

OVERVIEW

In this chapter, biomass burning in southern Africa is discussed. This includes findings from previous studies, climatic implications, and emission factors used to calculate emissions. Satellites used in fire monitoring and various products and applications using satellite imagery and remote sensing are examined.

Introduction

Biomass burning has been identified as a significant source of aerosol and trace gases, especially greenhouse gases such as carbon dioxide (CO_2) and methane (CH_4), and nitrogen oxides (NO_x), carbon monoxide (CO) and hydrocarbons. Biomass burning also contributes to the formation of tropospheric ozone (O_3) (Levine *et al*., 1996; Piketh and Walton, 2003) and to regional air pollution (Guild *et al*., 1998). Satellite observations have identified Africa as a region where fires are most persistent (Chandra *et al*., 2002). Biomass burning emissions for southern Africa mirror the seasonal pattern of fires, which occur most frequently in the dry season (Andreae, 1991; Cahoon *et al*., 1992). There are still uncertainties regarding the interannual variability of burning and the fundamental activities influencing the variability especially at a continental scale (van der Werf *et al*., 2006).

It is important to quantify and refine the estimates of aerosols and trace gases emitted from biomass burning. Biomass burning emissions contribute to the increasing degradation in air quality due the elevated levels of aerosols and trace gases, which has significant health effects. Trace gas and aerosol emissions have a significant effect on climate and hence climate variability.

Satellite remote sensing provides a practical opportunity to calculate emissions remotely for more than one burning season, for an area as extensive as southern Africa (Roy *et al*., 2005a). Numerous studies on emission estimates for southern Africa have been undertaken (especially under the Southern African Fire-Atmosphere Research Initiative (SAFARI) campaigns and Southern African Fire Network (SAFNet) (Roy *et al*., 1995a)). These studies have taken place over climatologically different years and have used different methods to calculate burning emissions. For practical purposes, this study uses the Moderate Resolution Imaging Spectroradiometer (MODIS) active fire product to calculate burnt area and subsequently biomass burning estimates. MODIS provides twice daily active fire observations at a 1 km^2 resolution (Kaufman *et al*., 1998; Moeller *et al*., 2003), which can be used as a proxy for burned area. Burned area, burning efficiency, biomass density and emission factors are used to calculate emission estimates for southern Africa (defined as Africa south of the Equator in this study).

Aims and Objectives

This project will provide insight into the distribution and characteristics of fires occurring on the southern African sub-continent by using the MODIS active fire product. Total emissions of aerosol and trace gas emissions from biomass burning in southern Africa (defined as Africa south of the Equator) will be calculated.

The objectives of the study are:

- To determine the spatial and temporal distribution of fires over southern Africa (defined as Africa south of the Equator) by identifying the interannual and seasonal pattern of burning

- To refine estimates of aerosol and greenhouse gas emissions from biomass burning. This is executed by using the MODIS active fire product as a proxy for burned area and calculating the biomass density and combustion efficiency and using previously calculated emission factors

- Provide a comparison of biomass burning emissions with emissions from other sectors

Literature Review

Biomass Burning

Savanna is the single largest source of burned biomass globally (Andreae, 1991), as it constitutes at least half of tropical biomass burning (Cachier *et al*., 1996). Two thirds of the world's savanna is found in Africa (Andreae, 1991; Scholes *et al.*, 1996a&b), and satellite observations have identified Africa as the region where fires are the most persistent, especially the region just north and south of the Equator (Chandra *et al*., 2002). At least 90% of biomass burned on the African continent has an anthropogenic origin, in the form of forest-clearing and domestic burning (wood and charcoal) (Andreae, 1991; Cachier *et al*., 1996; Delmas, *et al*., 1999) and agricultural burning associated with subsistence farming and ranging livestock (Edwards *et al*., 2006) or by lightning (Roy *et al.*, 2005a). These practices are a significant source of greenhouse gases and aerosols and therefore contribute to regional air pollution, and lead to a decrease in terrestrial carbon and nutrients originating from vegetation that would normally be recycled to the soil (Guild *et al.*, 1998). The consumption of biomass is important in ecological processes especially with regards to biogeochemical cycles of carbon, nitrogen and water (Kaufman *et al*., 2003). Biomass burning activities are part of very strong traditional agricultural and cultural practices throughout Africa and the increase in these activities is a response to social pressures of an ever-increasing population and the state of economies and socio-political forces (Anderson *et al*., 1996; Guild *et al*., 1998). Quantification of the effect of emissions on atmospheric chemistry and the radiative budget is inaccurate due to uncertainties in knowledge of the magnitude, spatial and temporal location of emissions (IPCC, 2001).

Fire Emissions

Atmospheric aerosols and trace gases originating from biomass burning play an important role in the chemistry of the troposphere and climate (Christopher *et al.*, 1996). Emissions vary according to the intensity and temporal variability of burning (Ichoku *et al.*, 2003). In the southern African region, fire is the dominant process producing hydrocarbons and aerosols (Swap *et al*., 2003) and burning is a significant source of greenhouse gases, especially carbon dioxide (CO_2) and methane, and photochemical gases (nitrous oxide (NO_x), carbon monoxide (CO) and hydrocarbons) that lead to the production of tropospheric ozone (O_3) (Levine *et al.*, 1996; Piketh and Walton, 2004). The properties of emissions are directly related to the type of burning process, fuel type and age of the smoke (Li *et al*., 2003). The temperature of the fire is dependent on the stage of the fire, i.e., smouldering or flaming (Prins and Menzel, 1994). Combustion Completeness (CC) is defined as the fraction of the dry biomass fuel consumed by the fire (Shea *et al*., 1996). It is dependent on the fuel load, the moisture content of the vegetation and the prevailing weather conditions (Ward *et al*., 1996; Korontzi *et al*., 2003a). Smouldering fires (less efficient) have less complete combustion and release more CO, whereas, flaming (intense, efficient) fires have more complete combustion and release more CO_2 (Ward *et al*., 1996; Scholes *et al*., 1996a). Flaming combustion usually dominates in the early burn of savanna and scrubland where emissions such as NO_x are favoured over CO or CH_4 (Barbosa *et al*., 1999). This is followed by a smouldering stage that can continue for a number of days or possibly weeks (Edwards *et al*., 2006). Fires with a lower fraction of biomass consumed (usually associated with deforestation) have a lower combustion efficiency, especially during the long cool smouldering stage, where organic carbon and CO are the main products released (Edwards *et* al., 2006). Fully oxidised products such as CO_2 and NO_x usually result from the combustion of grasslands, whereas the smouldering nature of leaf litter and twigs in woodland beds generate more products of incomplete combustion (Korontzi *et al*., 2004).

Southern African burning season

Fire activity in Africa south of the Equator is strongly seasonal (Figure 1) as biomass burning reaches a maximum in the dry season, before the first rainfall (Andreae, 1991; Cahoon *et al*, 1992). The burning season takes place between May and October, with concentrated burning between July and October (Christopher *et al*., 1998). At the beginning of the dry season, fuel is still relatively moist, which reduces combustion completeness and subsequently the amount of CO_2 emitted. Vegetation dries out as the dry season progresses, and CO_2 emissions increase and products of incomplete combustion (PIC) decrease (Justice *et al.*, 2002). During the dry season, an accumulation of easily-combustible dry fuel is available from dried out or dormant herbaceous vegetation and leaves shed by deciduous vegetation (Scholes, 1997 and Frost, 1999). Burning during the late dry season exhibits larger and more intense fires due to the increased amount of dry available fuel and is often accentuated by the dry and windy conditions that prevail and allow fires to spread and become uncontrollable (Roy *et al*., 2005a). There is a high interannual variability in burned areas as vegetation patterns and spatial distributions are sensitive to climate variability, particularly rainfall (Anyamba *et al*., 2003). This dependence on rainfall affects mainly the distribution and concentration of emissions (Hély *et al*. 2003). The intraseasonal variability of burning highlights the complexity of burning patterns in Africa.

Influence of vegetation on fire characteristics

The type and amount of pyrogenic emissions is greatly dependent on the spatial distribution and extent of the fires and biomass (fuel) (Anyamba *et al*., 2003). Fire incidence is dependent on weather conditions, progression of vegetation moisture and the fire source (Mbow *et al*., 2004). Fire is less common in arid regions in the west and south-west interior of southern Africa, as there is insufficient available biomass fuel (e.g. dead wood, grass, shrubs and litter) (Roy *et al*., 2005a). Surface fires (charcterised by scar burns of less than 20 cm on trees) are the most common type of fire in arid-savanna regions (Scholes and Walker, 1993). In closed canopy forest and woodland areas with prolonged moist conditions, fires tend to be small and spatially

fragmented by roads, field boundaries, fire breaks and lower fuel load due to grazing and firewood collection. Forests and woodlands are very low risk areas for burning (Mbow *et al*., 2004; Roy *et al*., 2005a). The amount of grass biomass varies with vegetation type (Mbow *et al*., 2004). The largest fires occur in vegetation areas with an intermediate amount of annual rainfall (550-770 mm), such as open savanna woodlands, grasslands, tree-shrub savanna and shrub savanna (Mbow *et al*., 2004). In this environment there is sufficient grass production for fuel, but insufficient rainfall for the canopy to close, to reduce grass production. This allows for large adjacent burned areas (Roy *et al*., 2005a). Areas with a continuous grassy layer that dries out very quickly after the rainy season, accentuated by plateaus and slopes with sandy-stony soils, are very high risk fire areas (Mbow *et al*., 2004). In shrubby grassland, where rainfall is below 550 mm, fire follows periods of above-average rainfall as grass production is dependent on rainfall, hence fire events are intermittent but burned areas are large and widespread (Roy *et al*., 2005a). African savanna fires are predominantly surface fires, therefore only grass, litter, and small woody debris under trees are considered as fuel (Scholes and Walker, 1993; Hély *et al*., 2003a).

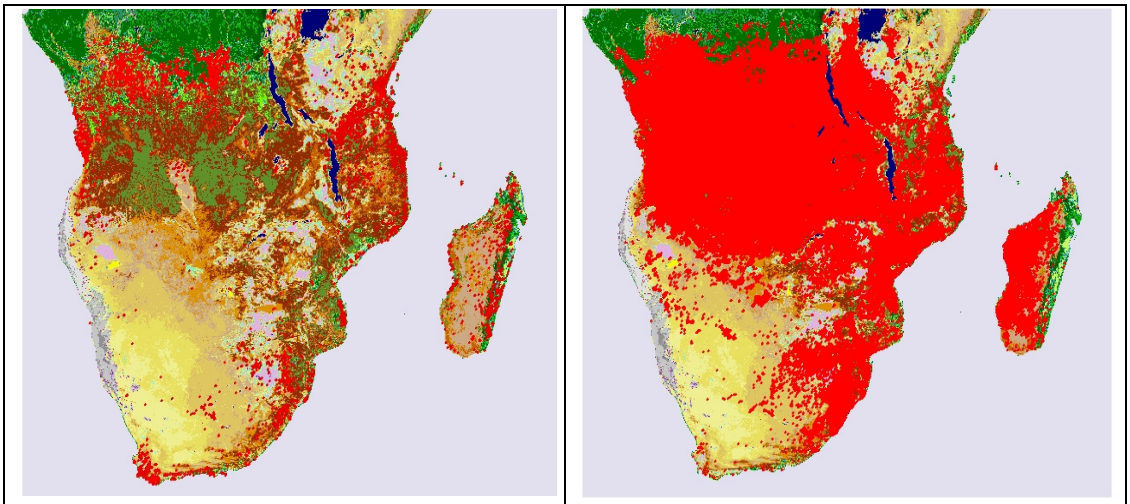

MODIS fires for Summer 2006	MODIS fires for Winter 2006

Figure 1: MODIS active fires for summer and winter 2006 showing the seasonal flux of burning (adapted GLC 2000 map (Mayaux *et al*., 2003) and MODIS active fire counts (red dots), created in ARCVIEW in 2007).

Factors influencing fire occurrence

Rainfall

The amount of rainfall decreases and the dry season lengthens with increasing distance from the Equator in Africa (Waugh, 1995). The onset of the spring rains is in June-July (in the lower latitudes) north of 20°S and progresses towards the higher latitudes in October-November (Swap *et al*., 1996). Higher amounts of rain fall in the Equatorial region, with a decrease in a southerly direction. South of 20°S the progression is east to west (Swap *et al*., 1996). Little rain falls on the west coast, and dry conditions spread eastward as the dry season progresses. A high (>1000mm) and consistent amount of rain falls all year round between 0°S and 12°S along the west coast of southern Africa and the western half of the interior (Waugh, 1995). During spring there is an increase in rainfall that spreads from the east coast between 20°S and 30°S and from the north west coast to the interior of the of the sub-continent. On the east coast between 7° and 17°S and 25°S and 30°S the rainfall is high (>1000mm) and occurs throughout the year (Waugh, 1995). Fire incidence is high when rainfall is low during the dry season, and decreases as moist conditions become prevalent with the increase of rainfall.

Ocean currents

The ocean currents influence the temperature and rainfall of the adjacent land mass. The warm Aghulas current flows south from the Equator along the eastern side of the sub-continent. Summer rainfall development is assisted by easterly winds that advect moister air from over the warm ocean to the sub-continent (Walker, 1990). Off the west coast of the sub-continent the cold Benguela current flows to the north bringing cold polar water towards the Equator. This hinders convection and subsequently reduces the rainfall on the west coast. This lack of rainfall causes deserts to form on the west coast, especially where there is a great deal of cold water upwelling. The air from over the oceans contains a great amount of moisture, which increases the possibility of rainfall and causes conditions that are not conducive to fire spreading.

Vegetation type

The higher the biomass density of a vegetation type, the more fuel it provides for burning. Forests have the highest biomass densities (Brown and Gaston, 1995) therefore even though the Tropics have a high amount of rainfall, the dense forests in this area provide a continuous supply of fuel, especially under dry conditions. People burn certain vegetation at particular times of the year, depending on the purpose of burning. The type of vegetation burnt will determine the nature of the fire and the type of emissions released.

Previous Studies

The Southern African Fire-Atmosphere Research Initiative (SAFARI-92) allowed for the investigation of the characteristics of savanna fires, and provided information about the emissions when burning was at its highest, namely between August and October, in the austral spring of 1992 (Piketh *et al*., 1996; Lindesay *et al*., 1996). The global and regional significance of African burning was realised through the SAFARI-92 campaign (Swap *et al.*, 2003) and consequently led to the South African Regional Science Initiative SAFARI 2000 (Swap, 2002; Keil and Haywood, 2003). The recognition and classification of regional emissions from biomass burning, biogenic, mineral and industrial sources, particularly in the dry season, was one of the main objectives of SAFARI 2000 (Swap *et al*., 2002b, Hély *et al.*, 2003a; Swap *et al*., 2003). The importance of gaining a greater understanding of the burning process as well as the completeness of burning was also recognised (Swap *et al*., 2003; Alleaume *et al*., 2005). It is evident from SAFARI-92 that the entrapment, transport and recirculation of aerosols and trace gases over thousands of kilometres is an important feature of the atmospheric characteristics over southern Africa (Garstang *et al*., 1996).

Transport of aerosols and trace gases

The southern African sub-continent has a unique set of meteorological and physical characteristics which significantly affect the emissions, transport and climate forcing of aerosols and trace gases (Garstang *et al*., 1996; Ichoku *et al*., 2003). Stable layers

and anticyclonic circulation increase the pollution problem over southern Africa by preventing vertical mixing (Tyson and Von Gogh, 1976; Tyson *et al.,* 1996a; Piketh and Walton, 2004). Aerosols transported in continental highs follow an annual cycle which peaks in winter (Tyson *et al*., 1996a).In southern Africa aerosol transport is a function of a distinct wet and dry season (Tyson, 1986).

Vertical Transport

The subsiding limb of the Hadley cell dominates regional circulation over southern Africa and semi-permanent subtropical anticyclones dominate lower tropospheric circulation (Tyson *et al*., 1996b) over the interior plateau (Piketh *et al.,* 1999). This circulation pattern over southern Africa (especially south of northern Zambia) results in similar climatic conditions (Tyson and Gatebe, 2001). Consequent adiabatic drying and warming of descending air allows for a highly stable thermodynamic structure of the atmosphere (Tyson *et al*., 1996b) which strongly influences the vertical transport of aerosols in the atmosphere (Zunckel *et al*., 1999). These conditions result in the development of the African haze layer capped at 500 hPa or 700 hPa (Piketh *et al.,* 1999; Tyson and Gatebe, 2001, Piketh and Walton, 2004). Multiple persistent stable layers are able to control transport over the sub-continent as air masses become trapped between stable layers after convection has occurred from the lower troposphere (Garstang *et al*., 1996, Piketh *et al*., 2002). Four stable layers are present over southern Africa, three of which lie over the interior plateau. The first is situated at the top of the midday mixing layer at 700 hPa. The second occurs at 500 hPa, and is most persistent as it is produced and sustained by large-scale subsidence. This layer is has been observed to persist for 40 days (Tyson and Gatebe, 2001) and can extend across most (up to 30° latitude) of the sub-continent (Garstang *et al*., 1996, Tyson *et al*., 1997, Tyson and Gatebe, 2001). The third layer exists at 300hPa but is less pertinent for aerosols and carries more significance for the transport of O_3. A fourth stable layer lies between the plateau and ocean, over the plateau slopes and coastline at 850 hPa (Tyson *et al*., 1996b). The 500hPa stable layer prevents vertical transport, however, frontal disturbances allow for vertical mixing to occur in the 700 hPa and 800 hPa layers (up to 500 hPa) over the central and southern parts of the region (Tyson and Gatebe, 2001).

Horizontal transport

Medium to long range transport (Freiman and Piketh, 2003) of aerosols is influenced by the anticyclonic mean circulation in the troposphere over the sub-continent, which varies according to wet and dry spells (Tyson, 1986, Piketh *et al*., 2002, Freiman and Piketh, 2003).). Horizontal transport is controlled by the dominance of anti-cyclonic wind curvature in the wind field, except near the Equator, where the influence of the Intertropical Convergence Zone (ITCZ) prevails (Tyson and Gatebe, 2001). Emissions from biomass burning in southern Africa are identified by Garstang *et al*., (1996) as being transported in five major pathways (Figure 3), namely direct easterly or westerly transport, easterly and westerly advection out of an initially anticyclonic circulation, and anticyclonic recirculation (Tyson *et al*., 1996b). Anticyclonic circulation and westerly wave disturbances are associated with conditions which result in the seasonal transport of aerosols and trace gases away from Africa and over the Indian Ocean (Figure 3) (Piketh *et al.,* 1999; Swap *et al*., 2003; Edwards *et al.*, 2006). Alternatively, easterly wave perturbations transport material west over central southern Africa and over the Atlantic Ocean (Piketh and Walton, 2004; Garstang *et al*., 1996), following the trade winds (Edwards *et al.,* 2006, Tyson and Gatebe, 2001). The meteorological conditions during the austral spring over the southern African region allow for much of the mixing of emissions from various sources across the region, particularly those from biofuels and biomass burning, before flowing out towards the east (Pak *et al*., 2003). Emissions from savanna fires are usually confined to the lower troposphere, as they are unable to generate high amounts of sustained energy to produce convection columns of 3-4 km (Lindesay *et al.*, 1996). Low-level recirculating transport re-enters the continent at 20ºS and 35ºS along the anticyclonic trajectory (Garstang *et al*., 1996). Re-circulation of aerosols generally occurs within a week, depending on their residence times in the atmosphere (Tyson *et al*., 1996a). The residence time of aerosols in the atmosphere is dependent on the frequency of precipitation, as well as the place, height and time of emission and chemical composition (Tyson *et al*., 1996b). Although the suggested global-mean residence times for aerosols in the lower troposphere is 2-7 days, under stable conditions, residence times can be lengthened to weeks or even longer (Tyson *et al*., 1996b).

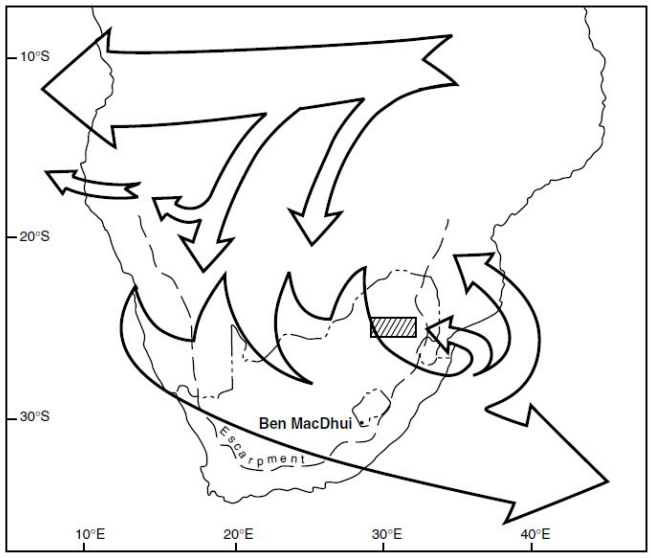

Figure 2: Major horizontal transport pathways of aerosols over the southern Africa subcontinent. The hatched area indicates the South African industrialized Highveld region (Piketh *et al*., 2002).

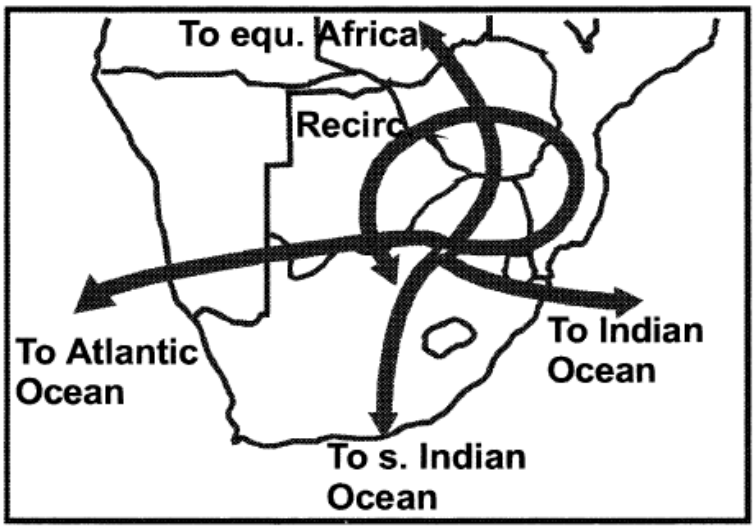

Figure 3: The main horizontal transport pathways of emissions for southern Africa (Freiman and Piketh, 2003).

Climatic Effects

Radiative forcing at the top of the atmosphere (TOA) represents the influence that aerosols and greenhouse gases have on climate (Keil and Haywood, 2003). Sulphate and organic particles from fossil fuel combustion and smoke particles from biomass

burning are believed to be the main contributors to aerosol radiative forcing (Hobbs *et al*., 1997). Greenhouse gases exhibit a positive radiative forcing (i.e. warming) and have a relatively uniform spatial and temporal distribution (IPCC, 2001). An increase in trace gases means an increase in precursor gases (namely, CH_4, NO_x, CO and VOCs) for tropospheric O_3 formation (Diab *et al.,* 1996a&b; Thompson *et al*., 1996; IPCC, 2001). During SAFARI-92 it was found that O_3 measurements reach a maximum in spring, when there is an abundance of precursor gases (Diab *et al*., 1996). This peak also coincides with the stable layers present over the sub-continent in winter (Diab *et al*., 1996b). Although stratospheric O_3 occurs naturally in the stratosphere and filters harmful ultraviolet (UV) radiation, tropospheric O_3 is mainly anthropogenic in origin and results in negative effects on health and air quality (IPCC, 2001). Photochemical O_3 formation in the 0-4 km altitude range was observed during the SAFARI-92/TRACE-A campaigns (Thompson *et al*., 1996). O_3 concentrations increase with height in the atmosphere O_3 is a strong indication of the emissions at the surface, and fluctuations in O_3 concentration have been positively correlated to variability of precursor gases, including those released from fires (Chandra *et al*., 2002).

Indirect aerosol effect

The indirect radiative effects of biomass burning aerosol, i.e. their role as cloud condensation nuclei (CCN), may be as important climatologically as the direct aerosol effect (Penner *et al.*, 1992). Biomass burning smoke particles can act as effective CCN and change cloud albedo through altering microphysics (Reid *et al.*, 1999) and hence cloud radiative properties (Anderson *et al*., 1996). Cloud albedo is increased through the increase in the number of cloud droplets (Keil and Haywood, 2003). The precipitation efficiency is reduced due to the decrease in mean droplet size, allowing for longer cloud lifetimes and a longer period of time required for precipitation to form, particularly in warm clouds (Albrecht, 1989). The indirect effect of aerosols on the radiative properties of clouds is known as the Twomey effect. Kaufman and Fraser (1997) used Advanced Very High Resolution Radiometer (AVHRR) data to confirm that biomass burning aerosol concentrations affect the effective radius of cloud droplets. There are still, however, significant uncertainties regarding the precise role

of biomass burning and the indirect effect on radiation (Reid *et al.*, 1999). A global and regional climate effect comparable to sulphate aerosol can result from the indirect effect of clouds and the direct radiative effect of biomass burning particles (Li *et al*., 2003). Biomass burning particles have approximately the same particle size distribution and atmospheric lifetime as sulphate aerosols (Christopher *et al*., 1996). Between 80-100% of submicrometer particles from biomass burning act as CCN (Li *et al*., 2003), which can alter the lifetime, formation and coverage of clouds and might impact on rainfall formation processes.

Direct aerosol effect

Aerosols alter the earth's radiation balance by scattering and absorbing solar and infrared radiation (Haywood and Boucher, 2000; Haywood *et al*., 2002). Radiative forcing by biomass burning aerosols, is strongly dependent on the presence of clouds (Keil and Haywood, 2003). Reflection of the aerosol layer is enhanced when the aerosol layer occurs above the cloud (Keil and Haywood, 2003). The effect of aerosols is difficult to quantify due to the uncertainties regarding the physical and radiative properties and the spatial variation of the type of aerosols (Haywood *et al*. 2002). Aerosols can have a cooling effect (Christopher *et al*., 1996), as they directly force climate through the reflection of shortwave radiation back into space, increasing the planetary albedo and possibly reducing temperatures at the surface (Charlson *et al*., 1992). This cooling effect is difficult to quantify due to the short and unpredictable lifetime of aerosols in the atmosphere (Penner *et al*., 1992). The particle size distribution, refractive index and optical depth are needed to determine the single-scattering albedo of aerosol particles (Reid *et al*., 1998). The single-scattering albedo of biomass burning aerosols generally lies between 0.7 and 0.9. This has been previously suggested (Hansen *et al*., 1997) to change the sign of direct radiative forcing from cooling to heating (Reid *et al*., 1998) in the region where the biomass burning aerosol is emitted. The absorbing properties of aerosols (Penner *et al*., 1992; Dubovik *et al*., 2002) affect the temperature lapse rate by converting the energy into heat, and consequently affecting convective activity and atmosphere dynamics (Anderson *et al*., 1996; Keil and Haywood, 2003).

Biomass burning products have varying radiative properties, since both coarse and fine-mode particles are emitted (Watts *et al*., 2000). The optical properties of biomass burning aerosols are determined by the vegetation type burned and the phase of the fire during burning (Dubovik *et al*., 2002). Fine mode particles and high aerosol optical thickness (AOT) values in the tropical regions of southern Africa can particularly be attributed to biomass burning emissions (Queface *et al*., 2003). A high aerosol optical depth (AOD) exists during the peak of the burning season (Holben *et al*., 1996, *et al*., Eck *et al.*, 1999). Biomass burning aerosols dominated the thick aerosol layer identified during SAFARI-2000 (Schmid *et al*., 2003). Fine-mode particles are optically far more important, and play a greater role in global radiation budget, than coarse mode particles, which exhibit a greater amount of variability and unpredictability in their variation over space and time due to their short life-span in the atmosphere (Watts *et al*., 2000). Remote sensing systems are able to measure regional optical depths fairly accurately (Reid, 2002), but the retrieval of AOT is sensitive to assumptions of single-scattering albedo and the assumed composition of aerosols (Christopher and Zhang, 2002). The Moderate Resolution Imaging Spectroradiometer (MODIS) allows for the observation of AOT over both the ocean and land (Ichoku *et al*., 2003). The MODIS AOT product (Figure 4) indicates the high AOT values over the African subcontinent, during the burning season (September 2004). When investigating the direct radiative impact of aerosols from biomass burning, Christopher and Zhang (2002) show that AOT values from Geostationary Operational Earth Satellite-8 (GOES-8) and the ground-based Aerosol Robotics Network (AERONET) correlate well. A north-south gradient in AOT has been suggested to exist over southern Africa in the burning season, which corresponds with a similar gradient in rainfall and vegetation, and therefore biofuel (Holben *et al*., 2001; Queface *et al*., 2003). Nonetheless, satellite observations (Figure 4) indicate that this gradient is rather from north-west to south-east.

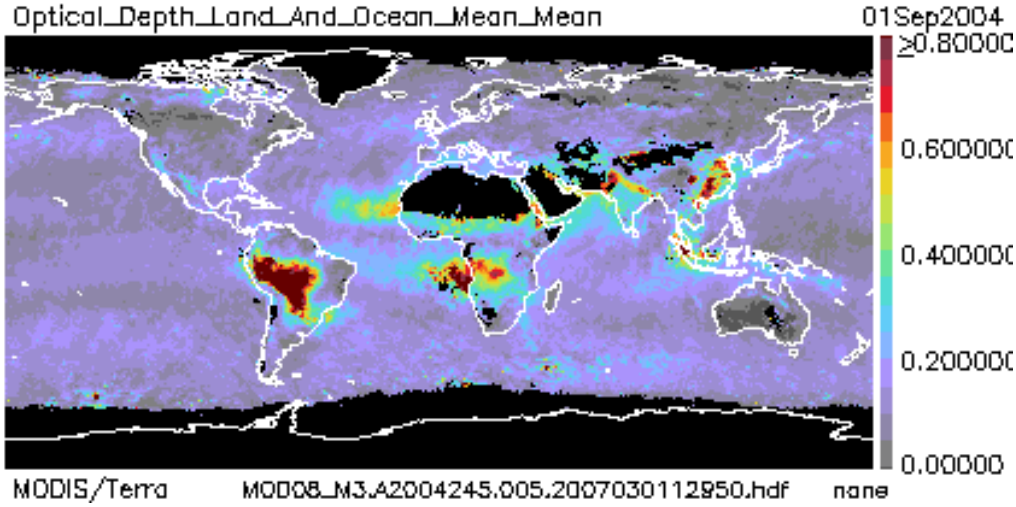

Figure 4: MODIS AOT product for September 2004 (burning season) showing high AOT values over southern Africa (http://modis-atmos.gsfc.nasa.gov/MOD04_L2/Indexhtml).

Emission Factors

Fuel load, vegetation composition, the total area burned and the combustion completeness determine the amount and type of emissions released into the atmosphere (Lindesay *et al*., 1996). There is a large uncertainty in emission estimates due to uncertainties in the quantification of these factors (Alleaume *et al*., 2005). Uncertainties regarding estimates of biomass burning emissions arise due to the large variations of burned areas at a regional scale over time and when estimates are based on qualitative descriptions of vegetation (Hély *et al*., 2003a). The spatial distribution of the burning has significant implications for emissions quantification (Korontzi *et al*., 2004).

An emission factor (EF) is required to calculate the total amount of aerosols and trace gases released during a fire once the area, type of fuel burnt, completeness of combustion and nature (smouldering or flaming) of the fire is known.

The emission factor for a given compound is defined as the amount of that compound released per amount of fuel consumed (g/kg) (Scholes et al., 1996a and Ward et al., 1996).

Sinha *et al*. (2003) calculate EF using the carbon mass balance method (Radke *et al*., 1988; Ward and Radke, 1993), based on the principle that the total carbon emitted from a fire into the smoke plume is emitted as carbon dioxide (CO_2,), carbon monoxide (CO), methane (CH_4), nonmethane organic carbon (NMOC), and particulate carbon (PC). The carbon mass balance method used to estimate fire-average, assumes that 50% of carbon mass is burned. Sinha *et al.* (2003) defines the emission factor (EF) of a species X as the ratio of excess mass concentration of a particular species (X) emitted and the excess mass concentration of total carbon emitted by the fire, expressed in units of grams of X emitted per kilogram of carbon burned;

$$EF(X) = \frac{[\Delta X]}{[\Delta C]_{CO_2} + [\Delta C]_{CO} + [\Delta C]_{CH_4} + [\Delta C]_{NMOC} + [\Delta C]_{PC}} \qquad \text{(Equation 1)}$$

Where [ΔX] and [ΔC] are the excess mass concentration of species X and total carbon emitted by the fire respectively.

Scholes *et al*., 1996a calculate EF as a linear function of Combustion Efficiency (CE) (Equation 2). The combustion efficiency (CE) is the amount of CO_2 emitted by the fire in proportion to the total gaseous carbon ($CO+CO_2$) emitted, and is related to the oxidation conditions in the fire (Scholes *et al*., 1996a). When a carbon content of 50% of the fuel is assumed (same as carbon balance method), a = 0 and b = 1.83 x 10^3. In these calculations approximately 49% error is assumed.

$$E_{gas} = a + bCE \qquad \text{(Equation 2)}$$

Ward and Hardy, 1991 describe the CE as the molar fraction of fuel carbon emitted that is completely oxidized to CO_2. It is difficult to measure all of the individual carbon species released from a fire, since CH_4, NMOC and PC are emitted in relatively small quantities compared to CO_2 and CO. Similarly, the modified combustion efficiency (MCE) used by Sinha *et al*. (2003) indicates the relative amounts of flaming and smouldering combustion (Ward and Hao, 1992; Ward and Radke, 1993) and can be calculated by using the molar ratio of excess carbon (C) emitted by the fire as CO_2 or CO (Sinha *et al*., 2003, Yokelson *et al*., 2003). The

difference between CE and MCE is usually only a few percent and both are useful as indicators of the relative amounts of flaming and smoldering combustion (Sinha *et al*., 2003). The MCE of Sinha *et al.* (2003) is essentially the same as the CE used by Scholes *et al.* (1996a).

Sinha *et al.* (2003) allow for modified combustion efficiency (MCE) and error in their calculations by including the standard deviation in the average emission factors for the initial smoke from savanna burning for a wide range of species (Table 1). Scholes *et al.* (1996a) cover a wide range of vegetation types, but fewer chemical species, and incorporate CE in their calculations. Yokelson *et al*., (2003), Bertschi *et al* (2003) and Sinha *et al*., (2003) all use the carbon balance method to calculate EF. Yokelson *et al*. (2003) determine initial emission factors for observed trace gases by calculating initial emission ratios using this method. Bertschi *et al.* (2003) calculate the total emission factor for specific compounds measured in the lofted emissions during residual smouldering combustion (RSC). Yokelson *et al*. (2003) incorporate RSC from Bertshi *et al*. (2003). Measurements that included RSC have shown significant differences particularly for $PM_{2.5}$ and some trace gases for fires consuming aboveground fine fuels (Bertschi *et al.,* 2003).

A comparison of emission factors measured in African savanna, Brazil and globally is presented in Table 1. Various authors use different methods for calculating emissions from fires and biomass, depending on the requirements of their study.

Barbosa *et al*. (1999) calculate the amount of biomass burned in Africa using the sum of the area burned, the ground biomass density and the burning efficiency for the given vegetation class. The product of an emission factor and the mass of burnt fuel provides a value for the amount (g) of the specific species released during combustion. The same methodological approach is used in this study.

Andreae and Merlet (2001) provide emission factors for tropical and extra tropical forest, agricultural residue and savanna and grasslands (Table 2).

Scholes *et al*. (1996a) calculate emission factors for grassland, forest and savanna (Table 1 and Table 2). Sinha *et al*. (2003), Yokelson *et al*. (2003) and Ferek *et al.* (1998) only calculate emission factors for savanna (Table 1), although the emission factors for Ferek *et al*. (1998) are applicable to Brazil, not southern Africa and Sinha *et al.* (2003) provides emission factors for more species than Yokelson *et al*. (2003) for southern Africa. The modified combustion efficiency (MCE) (Sinha *et al*., 2003) and Combustion efficiency (CE) (Scholes *et al*., 1996a) allow emission calculations to include the flaming and smouldering phases of burning and gaseous released by the fire thereby taking into consideration the amount of carbon released in relation to all the gases released by the fire. Bertschi *et al*. (2003) calculate the emission factors for compounds during residual smouldering combustion (RSC) and Yokelson *et al*. (2003) use fire-average emission ratios (calculated using the carbon balance method) and MCE. In this study emission factors from Sinha *et al*. (2003), Scholes *et al*. (1996a) and Andreae and Merlet (2001) will be applied to calculate emissions from biomass burning.

Table 1: Emission factors (EF) for savanna burning in southern Africa (Sinha *et al.,* 2003; Yokelson *et al*., 2003), burning of grasslands in Brazil (Ferek *et al.*, 1998) and global savanna burning (Andreae and Merlet, 2001).

	Emissions g/kg fuel					
Species	**Southern African savanna (Sinha *et al* ., 2003)**	**Southern African savanna (Yokelson *et al* , 2003)**	**Southern African savanna (Scholes *et al* ., 1996)**	**Grasslands, South Africa (Scholes *et al* ., 1996)**	**Grasslands, Brazil (Ferek *et al.*, 1998)**	**Global savanna (Andreae and Merlet, 2001)**
Carbon Dioxide (CO_2)	1700 ± 60	1734			1700	1613 ± 95
Methane (CH_4)	1.70 ± 0.98	1.16	1.7 – 3.4	1.8 – 2.3	2	2.3 ± 0.9
Carbon Monoxide (CO)	68 ± 30	55.7	59 - 97	63 – 73	75	65 ± 20
Non-Methane hydrocarbons (NMHC)	3.4 ± 2.3				3.5	3.4 ± 1.0
Total Particulate Matter (TPM)	10.0 ± 7.5		5.1 – 6.6	5.3 – 5.6	8	8.3 ± 3.2
Total Particulate Carbon (TPC)	2.7 ± 1.4				5.9	3.7 ± 1.3
Organic Particulate Carbon (OPC)	2.3 ± 1.2				5	3.4 ± 1.4
Black Carbon (BC)	0.39 ± 0.19				0.65	0.48 ± 0.18
Nitrous oxides (NO_x) as NO	3.3 ± 0.6	3.14	4.2 – 6.8	4.4 – 5.1		3.9 ± 2.4
Ammonia (NH_3)	0.26 ± 0.14	0.27			-	0.6 – 1.5
Condensation Nuclei (CN)	3.0 ±1.7 x 10^{16}				-	3.4×10^{15}
Formaldehyde (HCHO)	1.1 ± 0.38	0.63			-	0.26 – 0.44
Hydrogen Cyanide (HCN)	0.53 ± 0.15	0.35			-	(0.15)[a]

Table 2: Emission factors for pyrogenic species emitted from biomass burning from different vegetation types (adapted from Scholes *et al*. 1996a and Andreae and Merlet, 2001).

	Emission Factor (g/kg)						
	Sinha *et al*. (2003)	Scholes *et al*. (1996a)		Andreae and Merlot (2001)			
	Savanna	Grassland	Forest	Tropical forest	Extratropical forest	Agricultural residues	Savanna and Grassland
Carbon Dioxide (CO_2)	1700 ± 60			1580 ± 90	1569 ± 131	1515 ± 177	1613 ± 95
Methane (CH_4)	1.70 ± 0.98	1.7 – 3.4	9.47	6.8 ± 2.0	4.7 ± 1.9	2.7	2.3 ± 0.9
Carbon Monoxide (CO)	68 ± 30	59 - 97	230	104 ± 20	107 ± 37	92 ± 84	65 ± 20
Non-Methane hydrocarbons (NMHC)	3.4 ± 2.3			8.1 ± 3.0	5.7 ± 4.6	(7.0)[b]	3.4 ± 1.0
Total Particulate Matter (TPM)	10.0 ± 7.5	5.1 – 6.6	12.3	6.5 – 10.5	17.6 ± 6.4	13	8.3 ± 3.2
Total Particulate Carbon (TPC)	2.7 ± 1.4			6.6 ±1.5	6.1 – 10.4	4	3.7 ± 1.3
Organic Particulate Carbon (OPC)	2.3 ± 1.2			5.2 ± 1.5	8.6 - 9.7	3.3	3.4 ± 1.4
Black Carbon (BC)	0.39 ± 0.19			0.66 ± 0.31	0.56 ± 0.19	0.69 ± 0.13	0.48 ± 0.18
Nitrous oxides (NO_x) as NO	3.3 ± 0.6	4.2 – 6.8	16.1	1.6 ± 0.7	3.0 ± 1.4	2.5 ± 1.0	3.9 ± 2.4
Ammonia (NH_3)	0.26 ± 0.14			(1.30)a	1.4 ± 0.8	(1.30)a	0.6 – 1.5
Condensation Nuclei (CN)	3.0 ±1.7 x 10^{16}			3.4×10^{15}	3.4×10^{15}	3.4×10^{15}	3.4×10^{15}
Formaldehyde (HCHO)	1.1 ± 0.38			(0.14)[b]	2.2 ± 0.5	(0.14)[b]	0.26 – 0.44
Hydrogen Cyanide (HCN)	0.53 ± 0.15			(0.15)[a]	(0.15)[a]	(0.15)[a]	(0.15)[a]

[a] Best value guess

[b] Extrapolation based on emission ratios to CO

Satellite Imagery and Remote Sensing

Remote sensing is a useful device for monitoring fires. The sensitivity of certain channels to thermal anomalies has facilitated the use of remote sensing in fire detection and monitoring. The investigation of the distribution and frequency of fires via satellite data facilitates the refinement of estimates of trace gases and aerosols emitted via burning (Kiehl, 1999). There is an awareness of an increase in the severity, incidence and extent of uncontrolled burning, and therefore a great need to refine fire estimates and strengthen reliable fire information (Roy *et al*., 2005b). Much of the biomass burning occurs in developing countries, which are not equipped to monitor fires (FLAMBÉ, 2003). Although satellite observations have been used to monitor fires for two decades and there are many approaches and sensors that have been used to map fires and affected areas, an agreement has not been reached on one well-validated effective global product (Roy *et al*., 2005b). However, the Southern African Fire Network (SAFNet) has implemented a protocol to validate fire and burnt area products by integrating high resolution imagery and observations with fire and burned area products (Roy *et al*., 2006). Daily global fire product information facilitates the monitoring of the spatial and temporal distribution of fires in various ecosystems, the detection of changes in fire distribution and the identification of new fire frontiers, changes in the frequency and intensity of fire incidence (Kaufman *et al*., 2003). Satellites used for fire analysis are discussed below.

AVHRR

The Advanced Very High Resolution Radiometer (AVHRR) on the National Oceanic and Atmospheric Administration (NOAA) satellites provides fire data either on a global scale with a spatial resolution of 4 km or through Local Area Coverage (LAC) at a spatial resolution of 1 km (Moula *et al.,* 1996). Fires are detected with the AVHRR 3.7 μm channel, which has an increased response to fires when compared to the background (Christopher *et al*., 1998). The infrared channel on the AVHRR is often saturated below the temperature of the fires and the exact fire count is occasionally difficult to determine (Christopher *et al*., 1998). During SAFARI 2000 fire count data was derived from the 3.9 μm channel of the NOAA AVHRR and

active fires in the region were identified daily, at a spatial resolution of 8 km (Anyamba *et al*., 2003). Fires that are burnt for agricultural purposes are often smaller than the resolution of the minimum detectable fire size of 1 km^2 (Hély *et al.*, 2003a), and the spatial resolution of the AVHRR is inadequate to identify small fires and acquire specific information of individual fires, such as fire spread and temperature (Moula *et al*., 1996).

GOES

The Geostationary Operational Earth Satellite (GOES) offers an increased temporal resolution and has a higher saturation level in the infrared band than AVHRR, but it may not detect smaller fires, due to its coarse spatial resolution (4-8 km in thermal bands) (Christopher *et al*., 1998). GOES visible infrared spin scanner radiometer atmospheric sounder (VAS) investigations have been undertaken since the 1980's over South America (Prins *et al.*, 1998). The GOES VAS imagery manually identifies fires by identifying hot spots in the 4 μm channel, and then verifies the presence of fires through the identification of a smoke plume in visible imagery (Prins and Menzel, 1994). The spatial resolution (7-14 km) of GOES VAS imagers is limited in comparison to that of AVHRR (4 km), but its high temporal resolution allows for the diurnal monitoring of fires (Prins and Menzel, 1994). GOES data is available for the western hemisphere on a half-hourly basis (Reid, 2002), as GOES is centred over the Americas.

The initial GOES VAS algorithm developed by the Cooperative Institute for Meteorological Satellite Studies (CIMSS) allows for limited fire detection and characterisation and the observation of the path of smoke transport (Prins *et al*., 1998). The GOES-8 Automated Biomass Burning Algorithm (ABBA) was developed from sampled data sets from 1994 (after the burning season), and used for the 1995 burning season (Menzel and Prins, 1996). ABBA supplies information regarding size, temperature and location of sub-pixel fires (Prins and Menzel, 1996). GOES-8 ABBA provides a more realistic estimate of burned areas and represents a more realistic idea of what is expected from the intervals of diurnal imagery (Prins *et al*., 1998). The algorithm uses brightness values from the 4- and 11 μm

bands, in a thresholding technique to exclude pixels that contain cloud or fire and calculates the average background temperatures from 150 km by 150 km segments within the area of study (Prins and Menzel, 1994). GOES Wild Fire Automated Biomass Burning Algorithm (WF_ABBA) has so far allowed for a preview of the type of information that could possibly be available on a global scale and has offered insight into diurnal, spatial, seasonal and inter-annual biomass burning activity throughout the North, Central and South America (Reid, 2002). Since this data is not available for Africa, it is necessary to use another sensor that scans the African continent, for example, Moderate Resolution Imaging Spectroradiometer (MODIS) or Meteosat Second Generation (MSG).

MSG

Meteosat Second Generation (MSG) is the most advanced geostationary satellite since the launch of GOES-8 and functions through the European Space Agency (ESA) and European Organisation for the Exploitation of Meteorological Satellites (EUMETSAT) (Schmetz *et al.,* 2002). It is situated over the Equator and the Greenwich Meridian. The continuous observation of the earth is achieved through the Spinning Enhanced Visible and Infrared Imager (SEVIRI), which scans from south to north and east to west in a fifteen minute repeat cycle. The twelve channels that are available on MSG allow for extensive information on clouds, water vapour, ozone, atmospheric instability and the earth's surface (Schmetz *et al.*, 2002). EUMETSAT has recently (April 2007) released a 3 km operational active fire monitoring algorithm (FIR) which is based on similar principles to those already in use for GOES, AVHRR and MODIS 'hot spot' detection (EUMETSAT, 2007). The MSG algorithm uses a combination of the brightness temperatures in channel 4 (IR3.9 μm) and channel 9 (IR10.8 μm), their differences and standard deviations over a 3x3 pixel array. The foundation of the algorithm is the detection of increases in brightness temperature in the 3.9 μm channel in relation to the surrounding pixels (EUMETSAT, 2007). There are a number of threshold tests that are carried out using the 3.9 μm and 10.8 μm channels to filter out active fires and compensate for errors due to water attenuation, CO_2 and water vapour absorption, solar reflectance and sub-pixel clouds over hot surfaces (EUMETSAT, 2007).

MODIS

Moderate Resolution Imaging Spectroradiometer (MODIS) was launched by National Aeronautics and Space Administration (NASA) on the polar orbiting Earth Observation System (EOS) (Kaufman *et al.,* 1998). MODIS data is calibrated and processed using cloud screening, geo-location and atmospheric correction and is available on the World Wide Web (http://modis-atmos.gsfc.nasa.gov) (Roy *et al*., 2005b). MODIS on the TERRA spacecraft offers daily global coverage in 36 reflectance and thermal infrared (TIR) spectral bands at a resolution of 1 km or better (Moeller *et al*., 2003). NASA launched a second MODIS product on the AQUA satellite, which allows for further comparison and validation for the MODIS product (Moeller *et al*., 2003). MODIS has the ability to detect sub-pixel (smaller) fires, which will provide a greater understanding of the extent of human influence on fires (Hély *et al.*, 2003a). A fire at a given location can, however, be observed in two adjacent pixels along the scan line (across the orbital swath), known as the triangular response of MODIS (Kaufman *et al.,* 2003).

Routine fire products for the entire globe are available four times a day from MODIS (twice from Terra and twice from Aqua) at a 1 km resolution (Kaufman *et al*., 1998). These global fire products are available on the web at http://modis-fire.umd.edu/MOD14.asp. MODIS is able to recognize mottled or moderate fires, that AVHRR, Along Track Scanning Radiometer (ATSR), GOES and Defense Meteorological Satellite Program (DMSP) are unable to, due to the low saturation capacity of the brightness temperature (325-335 K) in their fire detection channel (Kaufman *et al*., 2003). The MODIS sensor has a higher saturation temperature at 1 km in the 3.9 μm and 11 μm channels, than the AVHRR sensor, which will result in a reduced chance of ambiguities with false alarms (Giglio *et al.*, 2003).

Fire detection via satellite in South Africa

The Council for Scientific and Industrial Research (CSIR) Satellite Applications Centre (SAC), in conjunction with Eskom and the Department of Agriculture has developed a fire monitoring system, the Advanced Fire Information System (AFIS).

The AFIS product has been developed with the assistance of the NASA and the University of Maryland and uses MODIS and MSG data, and applies the WF_ABBA fire detection algorithm to the satellite data. This near-real time monitoring system provides fire information to disaster management centres, fire protection agencies, Eskom's national control centre and researchers, in an attempt to document and monitor the frequency and distribution of natural and man-made fires and allow for early fire detection. The products generated are displayed as regional maps and are accessible on the World Wide Web (www.wamis.co.za/eskom/checkboxes/eskom.htm). The fire products used in this project are derived from the MODIS algorithm in the AFIS project and were obtained from the CSIR SAC.

Satellite Fire Products and Applications

Long-term observations of active fire data are extensively available (Giglio *et al*., 2006). There are two main strategies that are used to assess a burned area, namely hot-spot analysis (active fire detection based on thermal anomalies) and post-burn, which detects the damage or change of vegetation after the fire. Active fire locations provide limited information on spatial extent and timing of burning whereas burn scars use multi-temporal data to observe a fire (Roy *et al*., 2005a).

Burned area products

Burned area identification uses change techniques based on classification and thresholding techniques that rely on the relationship between the actual signal and the change of features compared to the previous scene (Roy *et al*., 2002). Burnscars are classified by identifying areas that were previously associated with active fires and have a spectral signature that corresponds with that of a burn scar (Chu *et al.,* 2002). Although these methods provide valuable information on the characteristics of fires and the spatial extent of burning, they cannot present absolutely accurate results (Roy *et al*., 2002). Burned areas algorithms document fire-induced changes that are persistent over time and are insensitive to the satellite overpass, unlike mapping hotspots (Roy *et al*., 2002).

The satellite-based burned area products such as Global Burnt Area (GBA-2000) (Tansey *et al*., 2004), GLOBSCAR (Simon *et al*., 2004) and MODIS burned area product (Justice *et al*., 2002, Roy *et al*., 2002) have been developed using data from 2000 but have not been thoroughly validated (Korontzi *et al*., 2004) and are not yet available on a multi-year basis (Giglio *et al*., 2006). Area burned, biomass density, and combustion completeness are factors that are extremely variable and burned area is especially difficult to estimate because of the potentially high spatial and interannual variability at continental to global scales (Giglio *et al*., 2006). Cloud shadows, sunglint (especially off water surfaces) and very bright land surfaces, may interfere with classification of burned and unburned areas (Chu *et al.,* 2002). The temporal discontinuities and high data volumes limit global validation of burned area estimates via Landsat imagery (Giglio *et al*., 2006). Giglio *et al*. (2006) have presented a global method for estimating monthly burned area at a 1° spatial resolution with additional data on vegetation cover available at http://modis-fire.umd.edu/products.asp#8.

The MODIS burned area product combines a bi-directional reflectance model with inverted multi-temporal 500-m land surface reflection observations, identifying the position of a fire and approximate day of burning, as well as uncertainties for the subsequent observations (Justice *et al*., 2002). Automated techniques fail to account for the difference between old and new burns; spectrally similar unburned features and burned features; and may overlook small and spatially fragmented fires or burns with low combustion completeness (Roy *et al*., 2005a). In addition to this, the exact day of burning cannot always be accurately determined due to cloudy or missing data (Korontzi *et al*., 2004). The validation of MODIS burned area products during fieldwork 2000 and 2001 under SAFNet, indicate that a high accuracy in location and day of burning, however, detection is unreliable with smaller fires that have burns with small axis dimensions and areas smaller than approximately 500 m and 1 km^2 respectively (Roy *et al.,* 2005a).

For the years 2001-2004, global estimates of the total burned area ranged between 2.97 million km^2 in 2003 and 3.74 million km^2 in 2001 (Giglio *et al*., 2006). Cumulatively, the total area burned in Africa (northern and southern hemisphere) and Australia from 2001-2004 comprised 80% of the total area burned globally (Giglio *et al*., 2006).

Active fire detection

There are a number of fire products available at the moment (Table 3). The active fire algorithm identifies thermal anomalies in separate pixels which indicate fires, as well as other high temperature sources, such as gas flares and power plants (Justice *et al*., 2002). Active fire detection algorithms are used to determine the location of hotspots using satellite data, emphasising the practicality of using satellite remote sensing as a method to monitor biomass burning over an extensive area (Roy *et al*., 2005a). Even though fire count data cannot be directly converted into the amount of burnt material and emissions released, fires are a good proxy of the variability in burned areas and hence emissions (Schultz, 2002; Korontzi *et al,* 2004). Active fire monitoring can serve as an interim product until long-term burned area data sets become available (Giglio *et al.*, 2006), if there is little change in the amount of biomass burned and the vegetation cover annually (Schultz, 2002). Satellite observations are capable of detecting the location of a fire, but cannot provide information regarding the fire intensity, amount and type of biomass burned without additional data (Edwards *et al*., 2006). The level 2 MODIS global fire product generates daily global browse images at a spatial resolution of 5 and 20 km (Justice *et al*., 2002) and archived at a spatial resolution of 1 km (Kaufman *et al*., 2003). Validation of the product took place using data that has a reliable and known level of accuracy, such as other fire products, ground validation and a global sample of Advanced Spaceborne Thermal Emission and Reflection Radiometer (ASTER) data, due to its high resolution of fire detection (Justice *et al*., 2002).

Table 3: A summary of active fire products

Product name	Resolution	Frequency	Agency	Products available at
NOAA-AVHRR	1 km	Global active fire day & 10 day	JRC	http://www-gvm.jrc.it/tem/
ERS-ATSR-AATSR	1 km	Global active fire day & 10 day	ESA	http://shark1esrin.esa.it/ionia/FIRE/AF/ATSR/
ENVISAT-AATSR				
TRMM-VIRS	2.2 km	+/-40º from Equator active fire day & night	NASA	http://earthobservatory.nasa.gov/Observatory/Datasets/fires.trmm.html
	0.5º	Monthly		
GOES WF_ABBA	1 km	Western hemisphere active fire day & night	CIMMS	http://www.nrlmry.navy.mil/flambe/
MODIS-AQUA, TERRA	250 m Lat long	Global active fire day and night	MODIS team	http://rapidfire.sci.gsfc.nasa.gov/
MSG FIR	3 km	MSG coverage Active day & night	EUMETSAT	http://eumetsat.int
AFIS	1 km	Southern Hemisphere active day & night	CSIR NASA Eskom	www.wamis.co.za/eskom/checkboxes/eskom.htm

Origin of the MODIS fire algorithm

The original MODIS algorithm was based on the algorithms developed for the AVHRR and VIRS (Giglio *et al*., 2003; Morisette *et al.*, 2005). The original algorithm was developed from the contextual daytime algorithm; however, rather than relying on the background brightness temperatures in a very heterogeneous area, the improved spectral capacities of MODIS have been utilised by using the mid-infrared reflectances and identifies individual per-pixel locations of fires (Justice *et al*., 2002). The algorithm uses the brightness temperatures from the 4 μm and 11 μm channels. The warm part of a pixel will emit more radiance in the shorter wavelengths in the thermal infrared than in longer wavelengths (Dozier, 1981). The development of the original fire detection algorithm, was based on the fact that the 3.8 μm brightness temperatures accentuate areas of high temperatures, and was found to be 34.5°C higher than the brightness temperatures in the 11 μm channel (Matson and Dozier, 1981). The theory of fire detection means that channel 3, rather than channel 4, on AVHRR records the maximum amount of infared radiation emitted, as the

maximum of the emission curve shifts towards shorter wavelengths, with increasing intensity and increasing temperature of the fire (Chrysoulakis and Cartalis, 2000, Dozier, 1981).

MODIS Fire Algorithm

Algorithms developed and used by the MODIS Fire Science Team (MFST) use thermal signatures to separate the fire signal from the background signal (Kaufman *et al*., 2003). The MODIS instrument has two channels (21 and 22) that lie at the wavelength (4 μm) used for global fire monitoring (Kaufman *et al*., 1998). Channel 22 saturates at 331 K and is less noisy than channel 21, and is therefore used as the 4 μm temperature (T_4) value whenever possible. Channel 21 saturates at almost 500 K, is not affected by water vapour or the absorption of other gases and, and is used when there is data missing from channel 22 (Giglio *et al*., 2003).

A number of threshold tests are carried out on the potentially active fire using the brightness temperature from the 4 μm channel, as well as the difference in brightness temperatures of the 4 μm and 11 μm channels to differentiate the fire pixel from the non-fire background. Additional specialised tests are applied to the data to eliminate false detections that can be attributed to sun glint, desert boundaries and errors in the water mask. At the end of the process, pixels are assigned to a class as missing data, clouds, water, nonfire, fire or unknown (Morisette *et al*., 2005). The 250-m near-infrared channel (channel 2) averaged to 1 km resolution, is used to reduce false alarms by identifying highly reflective surfaces (Kaufman *et al*., 2003) and absolute criteria are used to identify larger and more intense fires, whereas relative criteria are used to identify smaller fire by accounting for natural variability in temperature and emissivity of surface reflection by sunlight. Sun glint rejection is performed on all daytime observations, taking into consideration the satellite and sun geometry (Kaufman *et al*., 2003). Different thresholds are used at night because of the solar contamination in the 3.8 μm channel (Matson and Dozier, 1981; Roberts *et al.*, 2005). A detection confidence is also implemented to provide an estimate of the quality of individual fire pixels for the user (Kaufman *et al*., 2003).

False alarms and clouds are detected using the brightness temperatures of the 250-m red ($\rho_{0.65}$) and near-infrared ($\rho_{0.86}$) channels. Water-induced false alarms are detected by the 500-m 2.1 μm band ($\rho_{2.1}$) (Giglio *et al*., 2003). Despite this false alarms do still exist, most of which can be attributed to the absolute threshold tests (Justice *et al*., 2002) and the sensitivity of the algorithm to smaller and cooler fires, which result in fewer obvious false alarms (Justice *et al*., 2002). These fire products capture much of the seasonality and spatial distribution of fires, but actual burned area is difficult to estimate, due to inadequate temporal sampling, cloud cover, variability in vegetation/fuel conditions, variations in fire behaviour and issues with spatial resolution (Scholes *et al*., 1996b, Eva and Lambin, 1998a&b, Kaisschke *et al*., 2003). To avoid over-estimating fire occurrence, it is important to have good band to band, and scene to scene registration (Kaufman *et al.*, 1998).

Biomass burning contributes a significant amount of trace gas and aerosols into the atmosphere. There is a distinct burning season for southern Africa and the emissions have both indirect and direct climatic implications. The development of the field of remote sensing and the use of satellites in fire detection has allowed for the continuous monitoring of burning, improving the temporal and spatial scale of monitoring fires and biomass burning emissions.

Chapter 2

Data and Methods

In this chapter the fire count and land cover data used in the dissertation are discussed. The method used to separate fire data into seasons and years is described here. This is to depict the pattern of interannual and seasonal variations in burning and highlight the spatial and temporal distribution of fires. The method used to calculate biomass burned and the emission factors used to calculate the emissions released from biomass burning are presented in this chapter.

Methods

Fire data

Processed MODIS fire data from September 2002 to November 2006 is used in this project. All the data is used to calculate emissions; however, for the interannual spatial and temporal distribution of fires, only data for 2003 – 2006. The MODIS daily fire counts were obtained from the CSIR SAC, generated as part of the AFIS project. The fire data were imported into the ARCVIEW GIS program, ARCMAP, to produce maps to demonstrate the spatial and temporal distribution of the fires over the given time period. The extensive data set was separated, first into yearly fire counts for 2002, 2003, 2004, 2005 and 2006, and then into monthly fire count data. This was achieved by using Structured Query Language (SQL), using ARCVIEW's "SELECTION BY ATTRIBUTE". The displayed map with selected data was then exported as a shapefile for each month for every year (Figure 5).

The fire data sets include seasonal, monthly and yearly fire counts in the form of shapefiles. Even though 2003, 2004 and 2005 were the only years with a complete data set, the data set used is from September 2002 to November 2006 (Spring 2002 to

Spring 2006). In order to assess the seasonal and interannual changes of the fires over the given study period, Africa south of the Equator was divided into six sub-regions, namely, East Africa, Congo, Zambezi, Namibia, Angola and South Africa (Figure 6). These sub-regions were defined using the shapefile of SAFARI-2000 vegetation species composition map. This map was developed by the National Botanical Institute (NBI) in South Africa (Rutherford *et al*., 2000). The map consists of six individual sub-regions (Otter *et al*., 2003), namely 1)South Africa- South Africa Lesotho and Swaziland (Low and Rebelo, 1998), 2)Namibia (Wild and Barbosa *et al*., 1968), 3) Zambezi-Botswana, Zimbabwe, Zambia, Malawi and Mozambique (Barbosa, 1970), 4) East Coast-Tanzani, Kenya, Uganda, Somalia, 5)Congo-Ruanda, Burundi, Congo, Gabon, Democratic Republic of Congo and 6)Angola (White, 1983).

For practical purposes, the fires were divided into seasons, for each year, where summer months include the December of the previous year to the following February, autumn includes March to May, winter includes June to August and spring constitutes September to November. Fires were overlaid onto the map indicating the sub-regions, to ascertain the number of fires in each sub-region. The same seasonal divisions were assumed for the whole of Africa south of the Equator with the aim of outlining the progression of the burning season across the sub-continent, the seasonality of burning and interannual differences of the burning season.

Fire density (number of fires/km^2) was calculated by dividing the number of fires by the total area of each region. To compare the relationship between rainfall rate (mm/day) and fire density, a seasonal average of fire density was obtained by averaging the fires for each season over the four year period. The same process was carried out to calculate a seasonal average of rainfall rate (mm/day). The mean was calculated by finding the mean of the annual totals of rainfall rate and fire density for the four year period. The deviation from the mean was calculated by subtracting the annual totals from the mean to illustrate the interannual variability in rainfall rate and fire density for each region. Monthly fire density totals were summed to calculate the seasonal fire density total for each region for each year. Seasonal totals for estimated emissions were calculated in the same way, where the total monthly emissions from

each land cover type, for each year were added.

The method used to calculate biomass burned and consequently emission estimates for this study followed the method used by Barbosa *et al*., (1999). Barbosa *et al*., (1999) distinctly outlines the method used to calculate emissions from burned biomass and was applied to studies spanning multiple years of data, extending across southern Africa. The calculation of biomass density according to Barbosa *et al.,* 1999 does not require field or lab work, which was relevant to the scope of this remote-based study. The method is most applicable to the available data for this study and can be applied to the entire southern African (Africa south of the Equator) region. Biomass density and combustion efficiency are considered by Barbosa *et al*., (1999) in calculating burned biomass estimates due to variable nature of fire. This is beneficial to calculating emission estimates. Total error can be calculated, as Barbosa *et al*., 1999 calculate present percentage error for emission estimates, which given the nature of the study is pertinent to include.

Biomass Burned

The large variation in emission estimates is due to the large uncertainty in quantification of biomass burned in vegetation fires. Burned biomass estimates presented by various authors (Hao *et al*., 1996, Scholes *et al*., 1996a, Ward *et al*., 1996) are determined by using the classification method, which uses the area burned, biomass density and burning efficiency for a particular vegetation type. This study follows the method used by Barbosa *et al.* (1999) which uses NDVI values to calculate biomass density values and burning efficiency and makes use of biomass density, burning efficiency and burned area to calculate burned biomass (Equation 3) estimates. The method Barbosa *et al.* (1999) uses to calculate biomass density is based on NDVI values, which are readily accessible for southern Africa, and calculating biomass density values for each season and vegetation type is more accurate than extrapolating values calculated for the northern hemisphere.

$$\text{Biomass Burned} = \sum A_v \times B_v \times C \qquad \text{(Equation 3)}$$

where A_v is the burned area (m^2), B_v is the above ground biomass density ($g.m^{-2}$), C is the burning efficiency ($g.g^{-1}$) and *v* is the vegetation class.

Biomass burned was calculated for each month in the four year study period for each of the twelve (12) land cover classes and then summed to result in five land cover classes. Monthly biomass burned totals were added to calculate seasonal biomass burned totals for each year for five land cover classes.

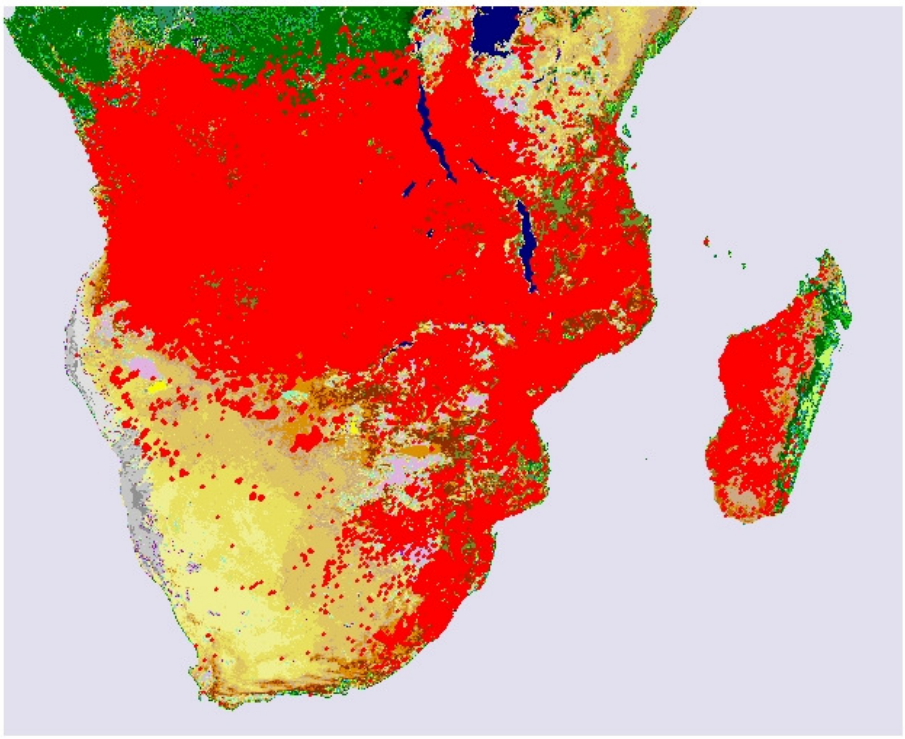

Figure 5: Shapefile showing the distribution of fires for August 2006 (adapted GLC 2000 map (Mayaux *et al*., 2003) and MODIS active fire counts (red dots), created in ARCVIEW in 2007)

Figure 6: Regions for observation of spatial and temporal distribution of fires

NDVI and land cover images for combustion efficiency and biomass density

NDVI and AVHRR UMD land cover images of the entire African continent were downloaded and the southern African region was "windowed" out from the full image, using latitude and longitude co-ordinates. However, the land cover image and NDVI images did not correspond if an overlay operation was carried out. The land cover map was therefore co-registered to the NDVI images using 23 ground control points (GCP), based on latitude and longitude co-ordinates. The images with corresponding sizes and the same co-ordinates in terms of rows and columns were used for analysis.

Biomass density

To account for interannual and interseasonal variability, an accumulated NDVI was computed for each season from spring 2002 to spring 2006, for each land cover type. This also reduces the effect of cloud cover on the NDVI. The NDVI images and land

cover image were imported into ENVI and saved as geotiff files. Interactive Data Language (IDL) was used to run a program that identified the land cover type with the corresponding NDVI values. Following Barbosa *et al.* (1999) the accumulated NDVI (∑NDVI) was calculated by finding the NDVI values between the maximum and minimum NDVI values found for each season. The values were summed on a pixel by pixel basis for each land cover type, for each season in the three year period. The biomass density for each season for the study period was then calculated by computing the linear relationship between 1) the minimum and maximum ∑NDVI values found for the 3 year study period for each vegetation type, and 2) the maximum and minimum biomass density values from previous studies (Table 4). Biomass density values were calculated for each vegetation type for each season for the three year period.

Burning efficiency

To account for the variation in moisture content of vegetation, a relative greenness index (RGI) (Equation 4) was computed for each vegetation cover, for each season from Spring 2002 to Spring 2006. RGI is assumed to have an inverse relationship with burning efficiency, i.e. when RGI is low, burning efficiency is high, and vice versa (Barbosa *et al*., 1999). RGI was calculated using the maximum ($NDVI_{max}$) and minimum ($NDVI_{min}$) NDVI value observed for each vegetation type during the entire three (3) year period and the median NDVI value ($NDVI_o$) for each vegetation type for each season, for each year:

$$RGI = \frac{\left(NDVI_0 - NDVI_{MIN}\right)}{\left(NDVI_{MAX} - NDVI_{MIN}\right)} \times 100 \qquad \text{(Equation 4)}$$

Table 4: Biomass density values from previous studies (adapted from Barbosa *et al*., 1999).

Vegetation types	Biomass density ($t.ha^{-1}$)	
	Minimum	Maximum
Sudanian Savanna[a]	2	5
Guinean Savanna[b]	4	8
Humid Miombo[c]	3	7
Dry Miombo[c]	3	7
South African Savanna[b]	1	5
[a]Menaut *et al* ., (1991)		
[b]The Net Primary Production Database available at http://www-eosdis.ornl.gov/npp/npp_home.html		
[c]Shea *et al* ., (1996)		

Burned Area

Active fire information can be used indirectly to reduce the uncertainties in estimates of burned biomass (Barbosa *et al*., 1999). Fires detected by the MODIS fire product can be used as a proxy for the amount of biomass burned. The spatial resolution of the fire product is 1 km^2, therefore for each fire detected, one square kilometre of vegetation can be assumed to be burned. This might result in an overestimate of the amount of biomass burned, as it is assumed that the entire pixel (1 km^2) is burning and this might not be the case. It is also possible that the algorithm is unsuccessful in detecting smaller fires that do not emit enough intense energy to be detected as a fire. This could possibly reduce some of the error in the overestimate of the area burned. The fire data for the study period were converted from shapefiles into raster files in IDRISI. The images were then resampled using twenty three (23) GCP so that the fire data correspond to the landcover and NDVI images used to calculate biomass density and combustion efficiency. The fire count data were saved in geotiff format to be used in a program written and run in IDL. This program cumulatively sums the number of fires that are detected in each vegetation class for each season from spring 2002 to spring 2006 to calculate the burned area, for each season for each year.

Aerosol and trace gas emission estimates

The amount of trace gases and aerosols released from biomass burning can be calculated by multiplying the amount of biomass burned with the emission factor for a specific vegetation type. A number of methods have been used to calculate emission factors. Sinha *et al.* (2003), Yokelson *et al.* (2003) and Ferek *et al*. (1998), calculate emission factors purely for savanna vegetation. Scholes *et al*. (1996) calculate emission factors for grassland, forest and savanna, and Bertschi *et al*. (2003) present emission factors for compounds released during residual smouldering combustion (RSC). Andreae and Merlet (2001) calculate emission factors for extra tropical and tropical forest, agricultural residue and savanna and grasslands. In this study emission factors calculated for southern Africa (Scholes *et al*., 1996a and Sinha *et al*., 2003) are used where available and emission factors calculated by Andreae and Merlet (2001) are used to complete the data set (Table 5).

The total number of emissions per compound for each vegetation class for every season, for each year is calculated using the amount of burned biomass (Equation 3) and multiplying it by an emission factor specific to the vegetation type (Equation 4). Monthly emission estimates for five land cover types were calculated and then summed to obtain seasonal emission estimates per land cover type for each year in the four year study period. The number of emissions released by each country is calculated by estimating the percentage of a particular land cover class present in the country and the emissions are calculated proportionally.

$$Emissions = B_v \times EF_x \qquad \text{(Equation 5)}$$

where B_v is the biomass burned for a specific vegetation and EF_x is the emission factor for a specific compound.

Monthly emission data for each land cover type was combined to demonstrate seasonal trends. Emission data for December, January and February were combined to display totals for summer, and March, April and May were combined for an autumn total. June, July and August were combined for winter totals. Emission totals for spring were calculated by summing emissions from September, October and November.

Table 5: Emission factors for the different vegetation types used in this study

Emissions (g/kg)					
Author	**Sinha *et al*. (2003)**	**Scholes *et al*. (1996a)**	**Andreae and Merlot (2001)**		
Vegetation Type / **Species**	**Savanna**	**Grassland**	**Tropical forest**	**Agricultural residues**	**Extratropical forest**
Carbon Dioxide (CO_2)	1700 ± 60		1580 ± 90	1515 ± 177	1569 ± 131
Methane (CH_4)	1.70 ± 0.98	1.7 – 3.4	6.8 ± 2.0	2.7	4.7 ± 1.9
Carbon Monoxide (CO)	68 ± 30	59 - 97	104 ± 20	92 ± 84	107 ± 37
Non-Methane hydrocarbons (NMHC)	3.4 ± 2.3		8.1 ± 3.0	(7.0)[b]	5.7 ± 4.6
Total Particulate Matter (TPM)	10.0 ± 7.5	5.1 – 6.6	6.5 – 10.5	13	17.6 ± 6.4
Total Particulate Carbon (TPC)	2.7 ± 1.4		6.6 ±1.5	4	6.1 – 10.4
Organic Particulate Carbon (OPC)	2.3 ± 1.2		5.2 ± 1.5	3.3	8.6 - 9.7
Black Carbon (BC)	0.39 ± 0.19		0.66 ± 0.31	0.69 ± 0.13	0.56 ± 0.19
Nitrous oxides (NO_x) as NO	3.3 ± 0.6	4.2 – 6.8	1.6 ± 0.7	2.5 ± 1.0	3.0 ± 1.4
Ammonia (NH_3)	0.26 ± 0.14		(1.30)a	(1.30)a	1.4 ± 0.8
Condensation Nuclei (CN)	3.0 ±1.7 x 10^{16}		3.4×10^{15}	3.4×10^{15}	3.4×10^{15}
Formaldehyde (HCHO)	1.1 ± 0.38		(0.14)[b]	(0.14)[b]	2.2 ± 0.5
Hydrogen Cyanide (HCN)	0.53 ± 0.15		(0.15)[a]	(0.15)[a]	(0.15)[a]

Data

Fire data

Daily fire count data from Moderate Resolution Imaging Spectrometer (MODIS) fire products were obtained from the Advanced Fire Information System (AFIS) project operated by the Council for Scientific and Industrial Research (CSIR). This system is based on the technology developed at the University of Maryland, USA and National Aeronautics and Space Administration (NASA). The project is a collaboration between the CSIR Satellite Application Centre (SAC), Eskom and the Department of Agriculture. Fires are detected by MODIS and Meteosat-8 Second Generation (MSG) satellites where the centre of a 1 km pixel contains one or more burning fires. The satellite data is processed by the Wild Fire Automated Biomass Burning Algorithm (WF_ABBA) to identify active fires and reduce the detection of false alarms. MODIS fire detection data is processed using a contextual thresholding algorithm that is based on the sensitivity of the mid-infrared channels to thermal anomalies. The detected fires can be viewed using the Advanced Fire Information System (AFIS) Geographical Information System (GIS) on the World Wide Web (AFIS User Guide, CSIR Satellite Application Centre, 2006). MODIS Terra and Aqua are polar orbiting satellites that pass over the southern African region daily between 10:00-11:30 and 14:00-15:30 respectively, whereas MSG produces a full scan of Africa every 15 minutes. Although MSG is currently available and has a better temporal resolution than MODIS active fire data, MSG still detects many false alarms and burning is overestimated. MODIS fire data from AFIS was therefore used for this project.

Rainfall rate data

Rainfall rate (mm/day) data from the Global Precipitation Climatology Project (GPCP) was used to investigate the correlation between rainfall and fire occurrence and consequently the relationship between fire occurrence and vegetation. The GPCP was developed and implemented by the World Climate Research Program and integrates precipitation information from a number of sources to provide a

monthly mean analysis of surface precipitation at a 2.5°longitude x 2.5°latitude resolution (McCollum *et al*., 2000). This information comprises low orbit satellite microwave data (Special Sensor Microwave/Imager (SSM/I)) from the Defense Meteorological Satellite Program (DMSP), infrared (IR) precipitation estimates from numerous geostationary and polar orbiting satellites (McCollum *et al*., 2000; Huffman *et al*., 1997) and the rain gauge data are assembled and analysed by the Global Precipitation Climatology Centre (GPCC) of the Deutscher Wetterdienst. (Huffman *et al*., 1997). The GPCP is a globally complete data set from January 1986 to present. (McCollum *et al*., 2000). Data is available through the World Climate Research Programme at http://cics.umd.edu/~yin/GPCP/main.html

Land cover map (UMD AVHRR 1 km)

The University of Maryland, Department of Geography (UMD) first generated a global land cover classification map in 1998, distinguishing 14 classes. The land cover classification map was created using Advanced Very High Resolution Radiometer (AVHRR) 1 km data between 1981 and 1994 to distinguish the classes (Hansen *et al*., 1998). More recently, UMD generated a land cover map with a spatial resolution of 1 km, using the one degree (DeFries and Townshend, 1994) and 8 km (DeFries *et al*., 1998) maps as a foundation (Hansen and Reed, 2000). The 1 km AVHRR UMD land cover map (Figure 7) was developed using a supervised classification method and Local Area Coverage (LAC) data. Data from Normalised Difference Vegetation Index (NDVI) images and five AVHRR bands (channel 1-5) between 1 April 1992 and 31 March 1993 were integrated into a tree classification algorithm to classify the globe (Hansen *et al*., 2000). The training data used for the UMD 1 km map is a combination of interpreted high resolution and co-registered coarse resolution data. The AVHRR data was divided into twelve (12) classes using a hierarchical tree structure classification (Hansen *et al.*, 2000). The decision tree creates a homogeneous class membership, where classification continues until each pixel is separated from another (Hansen *et al.*, 2000). The trees usually overgrow the training data, therefore two sets of data are used; one to grow the tree and one to prune the tree (by visual interpretation of global geographical distributions of vegetation) when too many errors or noise are generated (Hansen *et al*., 2000). For this study, twelve (12) classes were reduced to 5 land cover classes in order to

correspond with emission factors. Broad and needle leaf deciduous, evergreen and mixed forest were combined and named forest, savanna comprises open and closed shrubland, grassland constitutes grassland and wooded grassland, woodland remained woodland and cropland was combined with bareground and renamed as agriculture(Figure 7). For emission calculations savanna and grassland were combined and labelled savanna.

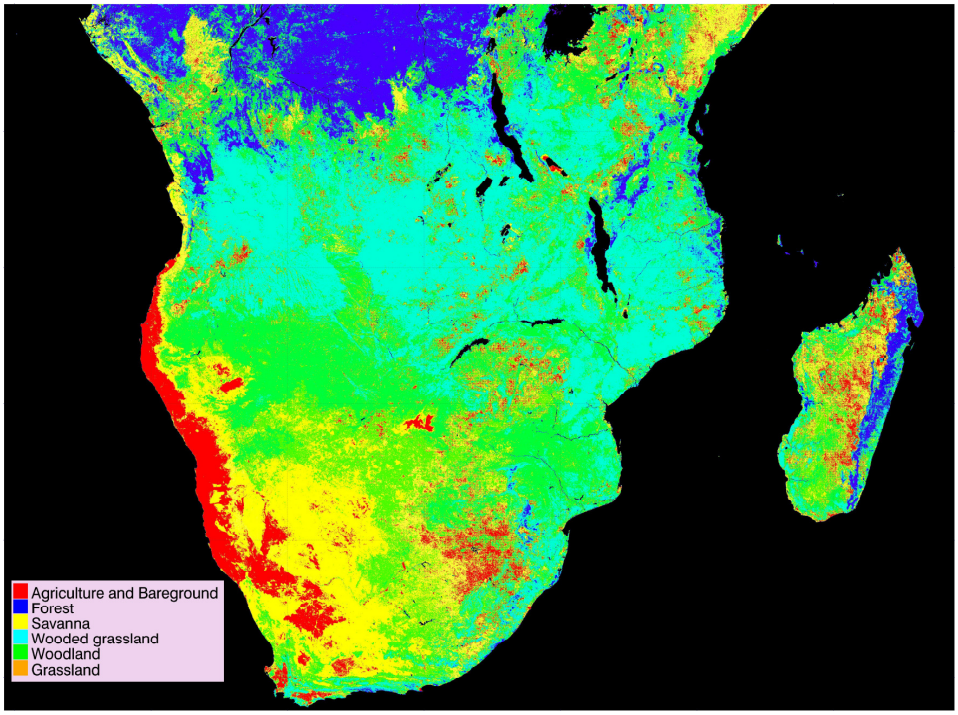

Figure 7: UMD AVHRR 1 km land cover map for southern Africa (Global Land Cover Facility, UMD AVHRR 1 km adapted in ENVI, created in 2007).

Normalised Difference Vegetation Index (NDVI) images

The VEGETATION instruments onboard the SPOT-4 and SPOT-5 satellite provide accurate operational measurements of fundamental characteristics of vegetation and vegetation canopies in order to monitor essential vegetation resources. The S10 NDVI product for Africa was downloaded from www.spot-vegetation.com for each season for the period between January 2003 and October 2005 in Geographic (lat/lon) projection. The S10 product uses atmospherically corrected segments over a ten day period, which are then compared on a pixel by pixel basis to acquire the optimum reflectance values for the given period. The S10 NDVI product uses only the NDVI data from the S10 product. The NDVI product has a spatial resolution of 1 km^2 and an

accuracy of 300m (www.VGT4AFRICA.org). VEGETATION data is distributed in Africa through EUMETCast. Further information about the VEGETATION products and downloads are available at www.VGT4AFRICA.org or www.spot-vegetation.com/vegetationprogramme/index.htm.

The data used in this study consist of MODIS daily fire count data from AFIS to explain the spatial and temporal distribution of fires over Southern Africa and a proxy for the area burned to calculate emissions from biomass burning. Ancillary data include the AVHRR 1 km landcover map and monthly NDVI images, which are used to calculate the biomass density per landcover type. Emissions released from biomass burning are calculated following the method of Barbosa *et al.* (1999), who calculates biomass density, area burned and the combustion efficiency to determine burned biomass. A combination of the most appropriate and available emission factors is applied to calculate the emissions released from biomass burning.

Chapter 3

Results: Spatial and Temporal Distribution of Fires

In this chapter the seasonal and interannual variability of fire distribution and occurrence in southern Africa, specifically in relation to vegetation, burning practices and rainfall, are examined.

The number of fires detected varies not only from one season to another, but from one year to another. The study period extends from the spring of 2002 to the spring of 2006. The number of fires detected can be influenced by a number of factors. Using remotely sensed fire data from this period, it is possible to provide insight into how rainfall and subsequently vegetation (biomass burning fuel) influence the number of fires that occur. A higher number of detected fires can be attributed to agricultural practices, a higher amount of available fuel load for burning, dry atmospheric conditions conducive to fires in the burning season and/or more cloud-free days.

Seasonal Variability in fire incidence

The burning season in southern Africa occurs during winter and spring and coincides with the dry season (Figure 8). A distinct seasonal pattern of burning and a progression in the spatial distribution of burning throughout the year are evident. In many areas of southern Africa, the wet season extends over five to seven months of the year during the summer months (Conley, 1996). Most of the annual rain falls during this period (Conley, 1996), and very little burning occurs in the wet season. Although this pattern stays consistent, there is variation in the amount of burning that takes place from one season to another and from one year to another. The mean annual rainfall in southern Africa is affected by the quasi-periodic 18-year oscillation, with nine years of above annual mean rainfall (wet years) and nine years of below annual mean rainfall (dry spell) (Tyson and Preston-Whyte, 2000). The effect of the quasi-periodic oscillation is most prominent in dry years and accounts for not more

than 20-30% of rainfall variability (Tyson and Preston-Whyte, 2000).

The period of burning spans May to October. There is a notable increase in fire counts in May and counts continue to increase, reaching a maximum in August and September. The highest number of fires and lowest rainfall rate (mm/day) (Figure 8) occur in winter throughout the region. There are few fire incidences during summer (Figure 9) in southern Africa, as this is when most of the rain occurs across the sub-continent.

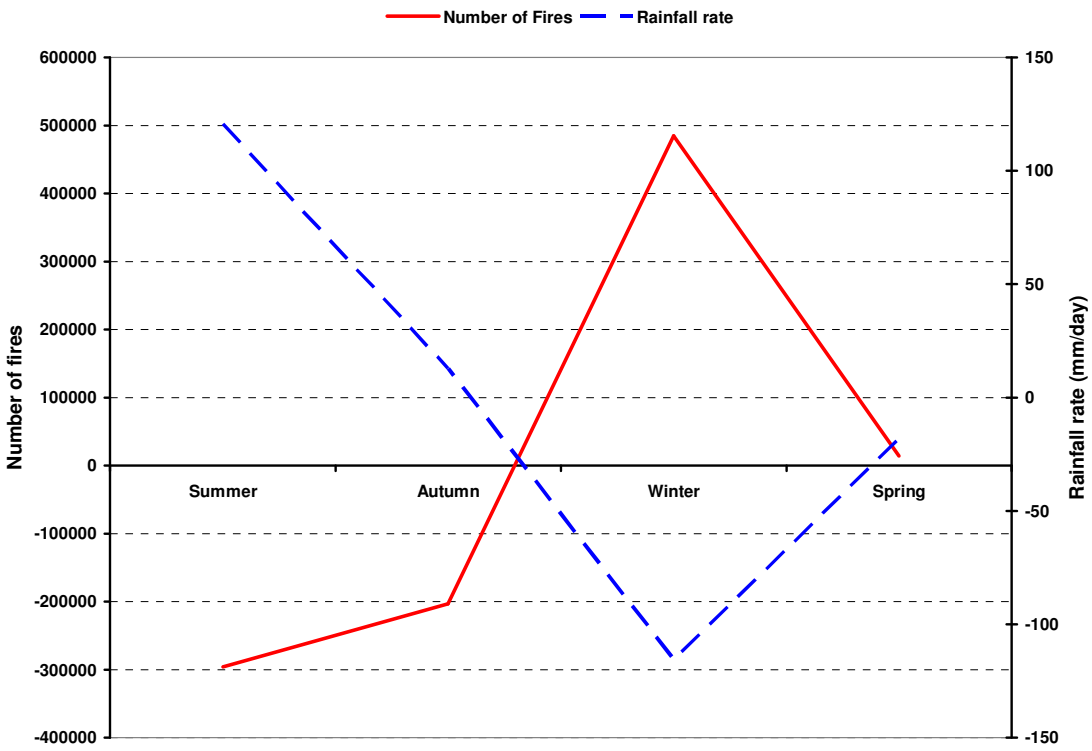

Figure 8: Average number of fires and rain rate (mm/day) in summer (December-February), autumn (March-May), winter (June-August) and spring (September-November) for Southern Africa (deviation from the mean for number of MODIS active fires and rainfall rate (GPCP)).

Fires start in the western part of the sub-continent in north-western Angola and the southern Democratic Republic of Congo (DRC) in March (Figure 10) and become more frequent in these areas during April. As drier conditions spread over the sub-continent from March to June, fires spread across the savannas from Namibia to the interior of southern Africa, especially to the south east of the Great Rift Valley and southwards (to 20°S) along the eastern coast (Edwards *et al.*, 2004). Fires burn

extensively in the Tropics throughout the winter period (Figure 11). From late winter/early spring (Figure 12) there is an increase in burning in the eastern countries and east coast (Tanzania/Mozambique) and a decline in burning in the west and interior as drier conditions extend to the eastern coast of southern Africa (Cahoon *et al*., 1992). By September fires are widespread across southern Africa, and burning is particularly intense in Angola, DRC, Zambia, Zimbabwe and Mozambique (Figure 12) (Cahoon *et al*., 1992) but are no longer burning as extensively in the northernmost parts of the Tropics, where burning was initiated. Fires continue to burn on the sub-continent, but not as extensively, as earlier in the winter months. By November most of the fires have ceased in the Tropics (Angola/DRC), except for isolated fires burning, as is the case in late summer and early autumn. The cycle of burning repeats from the point of initiation – eastern Angola (at approximately 10°S) and the southern parts of the DRC.

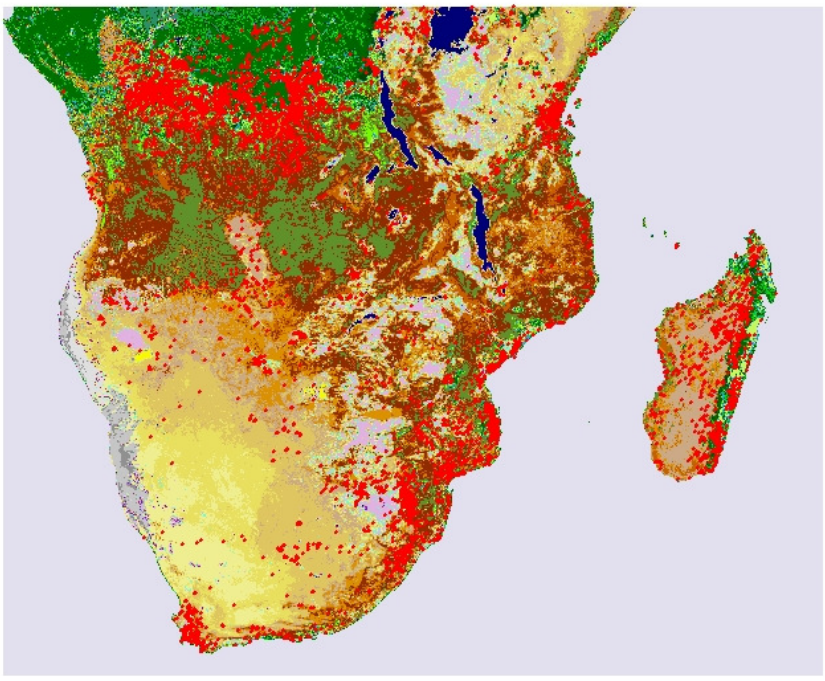

Figure 9: MODIS fire counts for summer 2005 (adapted GLC 2000 map (Mayaux *et al*., 2003) and MODIS active fire counts (red dots), created in ARCVIEW in 2007).

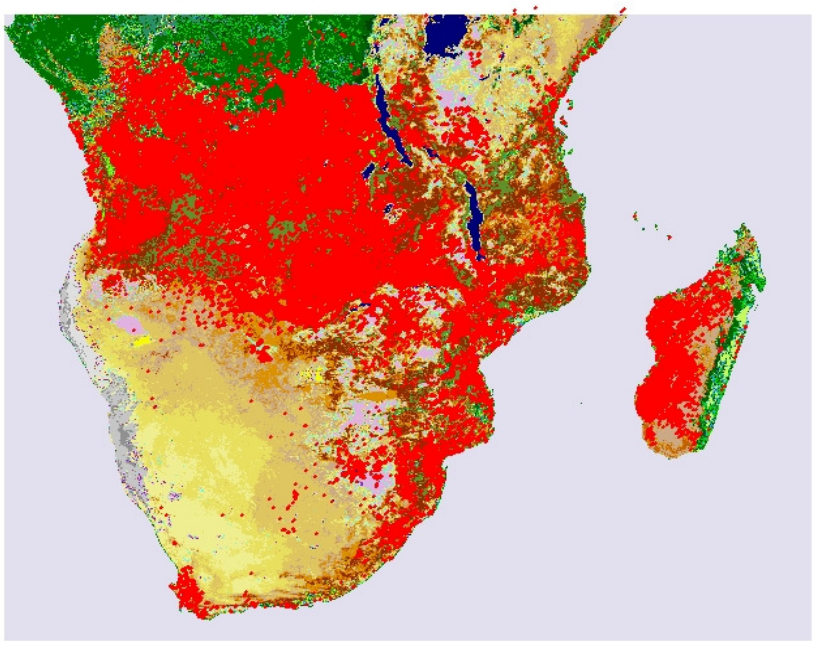

Figure 10: MODIS fire counts for autumn 2005 (adapted GLC 2000 map (Mayaux *et al*., 2003) and MODIS active fire counts (red dots), created in ARCVIEW in 2007).

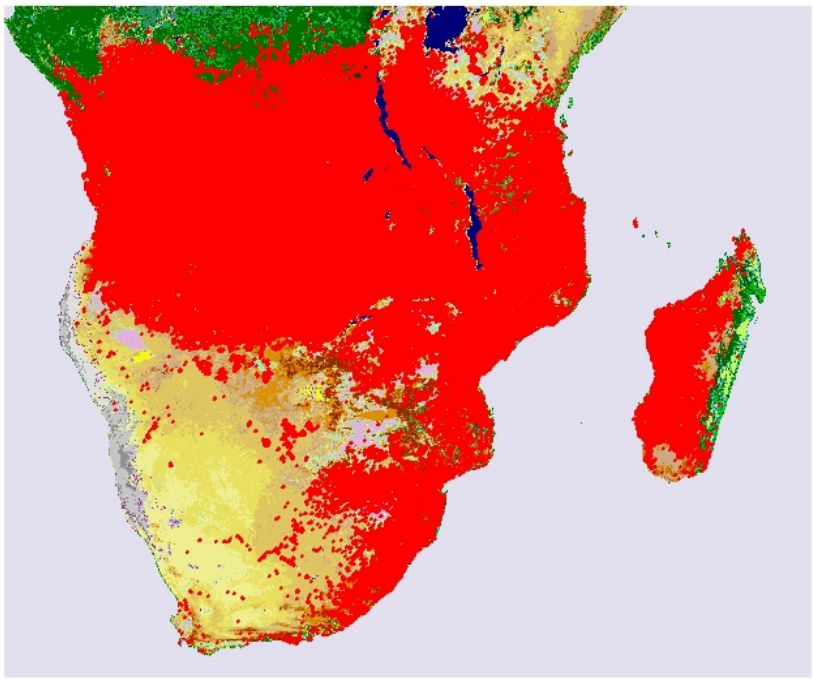

Figure 11: MODIS fire counts for winter 2005 (adapted GLC 2000 and MODIS active fires (red dots) in ARCVIEW, created 2007 adapted GLC 2000 map (Mayaux *et al*., 2003) and MODIS active fire counts (red dots), created in ARCVIEW in 2007).

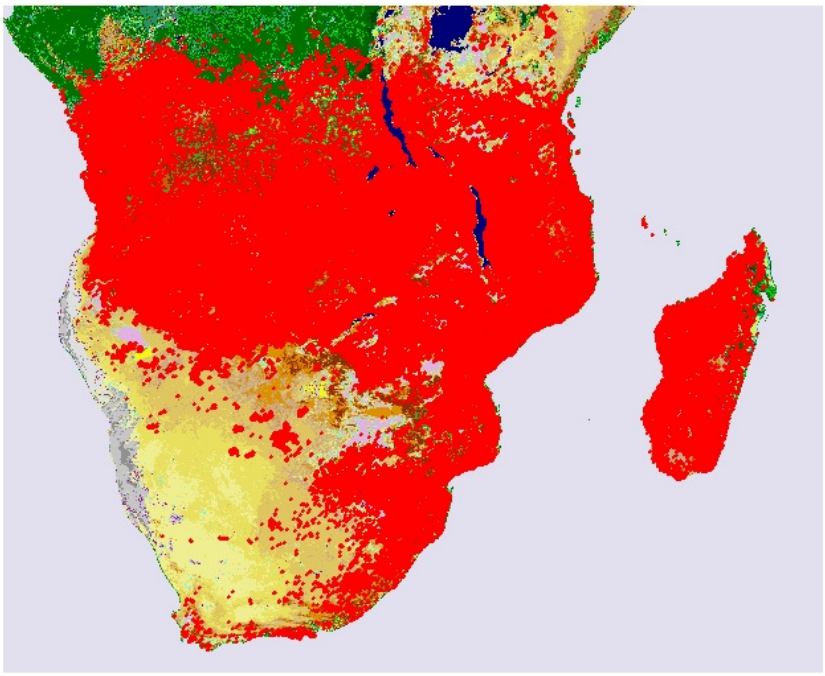

Figure 12: MODIS fire counts for spring 2005 (adapted GLC 2000 map (Mayaux *et al*., 2003) and MODIS active fire counts (red dots), created in ARCVIEW in 2007).

Angolan and Congo Region

The Angolan region has the highest fire density in southern Africa for autumn and winter (Figure 13). The Angolan and Congo region received the highest amounts of rainfall in the sub-continent. These areas have very little bare ground and are extensively covered with vegetation with a high biomass density, which provides a large amount of fuel to burn. Rainfall tends to be very high at the Equator where maximum rainfall is received during summer. Tropical regions experience dry winters and heavy convective rainfall during summer (Waugh, 1995). The rainfall in this region fluctuates with the north- and southward shift of the position of the Inter-Tropical Convergence Zone (ITCZ) throughout the year (McCollum *et al.*, 2000, Tyson and Preston-Whyte, 2000). During the southern hemisphere winter, the ITCZ migrates further north with the rain belts shifting accordingly. Conversely in summer, the ITCZ moves into the southern hemisphere and establishes a region of major latent-heat release in the tropical atmosphere of southern Africa (Tyson and Preston-Whyte, 2000). Rainfall is lowest during autumn and winter (Figure 14 and

Figure 15). There is a high incidence of fire in savanna, forest and woodland during winter in the Angolan region. A high amount of rain falls in spring and continues into summer on the west coast of Congo and northern Angola (0°S-15°S) then moves east and south to cover the sub-continent in summer. The Congo (0.37 fires/km^2), Zambezi (0.30 fires/km^2) and East African (0.22 fires/km^2) regions also have high fire densities in winter, but these regions experience between a third and a half of the burning experienced in Angola . There are many fires burned for land clearing for provision of agricultural needs in these regions, but particularly in Angola. In the Congo region, there is a slight increase in the number of fires in March and April, especially in the Tropics, where the number of fires increase and fires spread eastwards and southwards (Figure 15). Fires decrease in spring in the central Congo region due to an increase in precipitation, particularly if rains occur early in spring (Figure 15) (Cahoon *et al.*, 1992).

East Africa and Zambezi region

The Zambezi region has the highest incidence of fire per square kilometre in spring. The burning season for this region extends over winter and spring (Figure 16). Croplands, woodlands and forest constitute the vegetation classes affected by fire in the Zambezi region in spring. These vegetation types have high biomass density that provides a large amount of fuel for burning. Natural vegetation is burned to clear land for agricultural purposes and land use changes.

The interior receives the most rain during summer, although lower than the central DRC, east coast and west coast between 0°S and 7°S. There is a general decrease in rainfall over the sub-continent during autumn and winter. The burning season for East Africa occurs during winter when rainfall is at its lowest (Figure 17). In 2006 there was less burning in winter than in the preceding years. This could be due to the extended rainy season of 2004/2005, which delayed the onset of the dry season and hence burning. Ordinarily, the wet season spans summer and autumn, with the maximum amount of rain falling in summer; however, a small amount of rain fell in summer 2005 and the majority of rainfall was experienced in autumn 2005 (Figure 17). From November, a less dense pattern of fire incidence occurs and fire counts start

to decline until they cease in December, as the moist conditions start to settle into the interior and north western and southern coasts of the sub-continent (Cahoon *et al*., 1992). In January and February forest fires start to burn in the Tropics, particularly along the east coast of southern Tanzania, eastern Angola (at approximately 10°S) and in the southern parts of the DRC. There is an increase in grassland, woodland and forest burning in June and July on the northern coast of Mozambique, progressing southwards along the east coast from approximately 10°S-33°S in South Africa.

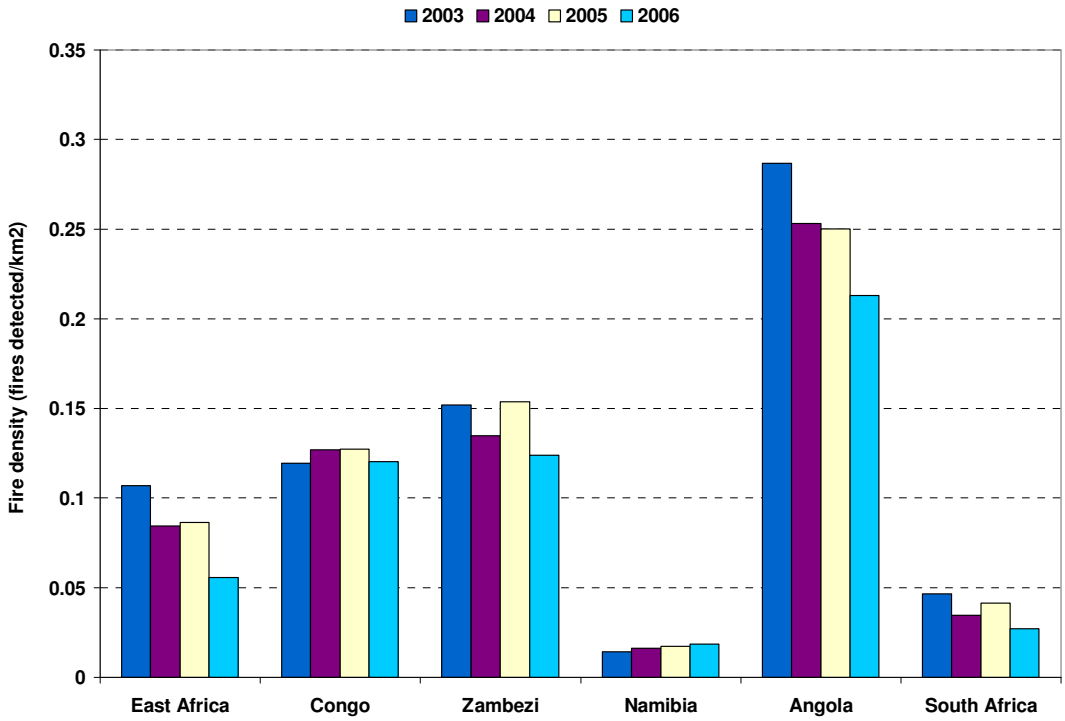

Figure 13: Annual fire density for regions within southern Africa between 2003 and 2006 for summer (December-February), autumn (March-May), winter (June-August) and spring (September-November) for southern Africa

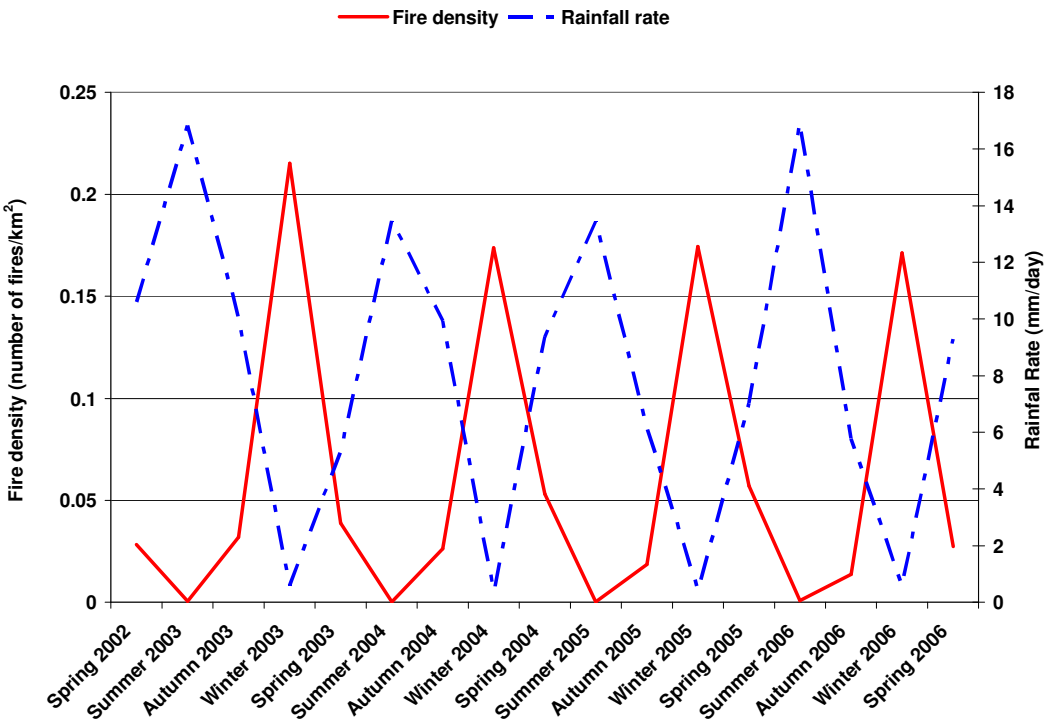

Figure 14: Relationship between fire density and rainfall rate for Angolan region

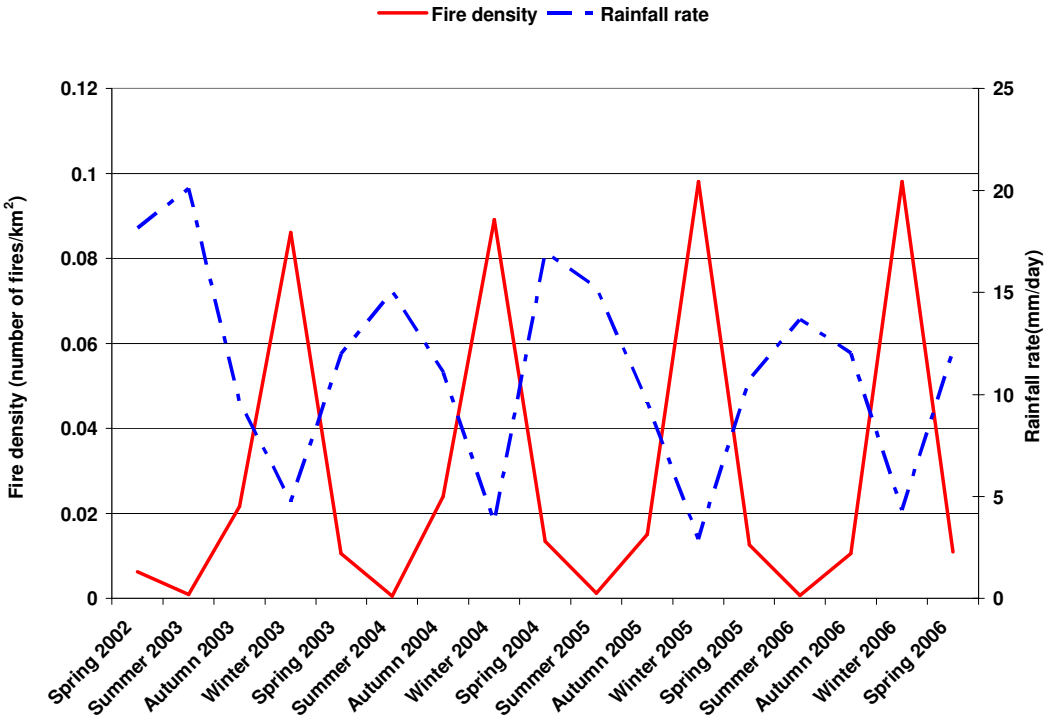

Figure 15: Relationship between fire density and rainfall rate for the Congo region

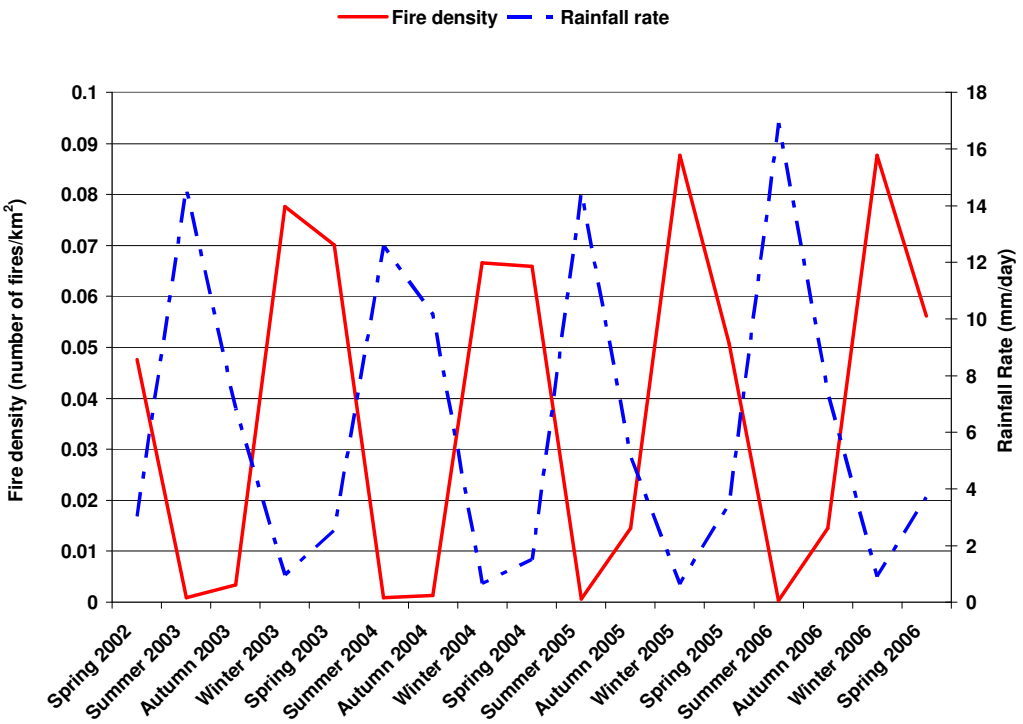

Figure 16: Relationship between fire density and rainfall rate for the Zambezi region

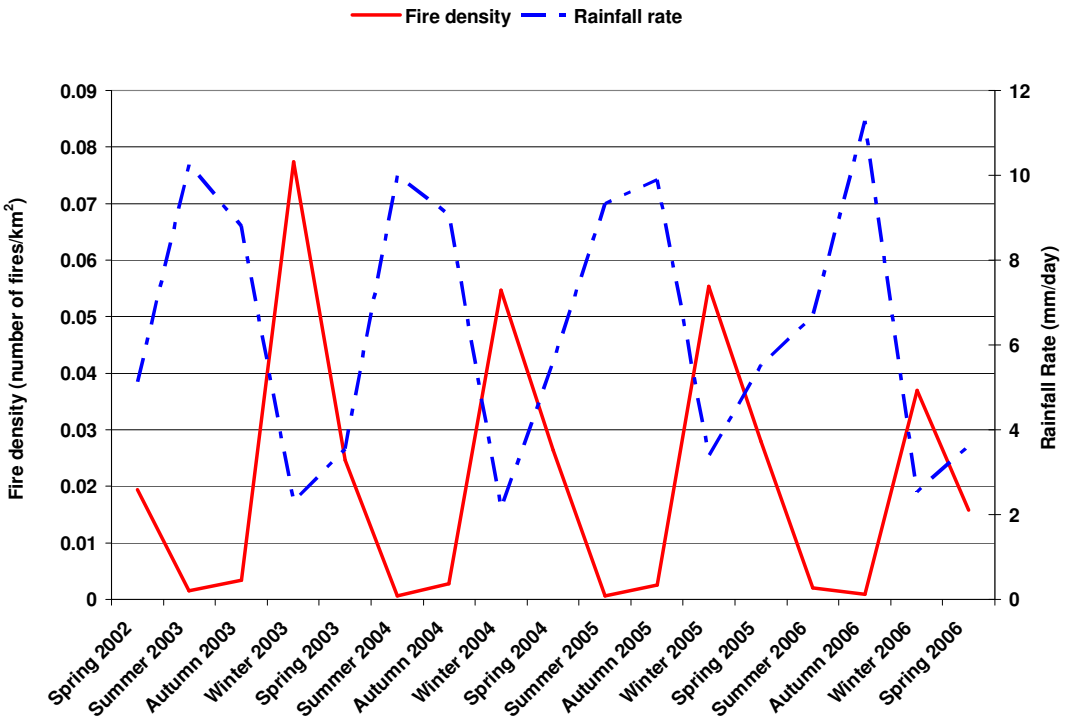

Figure 17: Relationship between fire density and rainfall rate for the East African region

Namibia and South Africa

The lowest fire density for the sub-continent for each season occurs in Namibia. The low fire density (Figure 13) can be attributed to the lack of vegetation and vast desert that extends across most of the country. Minimal rain falls in subtropical regions due to the subsiding limb of the Hadley and Ferrell cells at 30°S (Waugh, 1995). The west coast of Namibia and the western coast of South Africa remain dry during the summer, but experience an increase in rainfall during late autumn and winter. The greatest amount of burning in the central and eastern parts of the countries occurs during spring (Figure 18) in preparation for the growing season and just before the rainy season (summer) (Figure 16). The lowest fire density occurs in autumn (Figure 13) during harvest time. The primary vegetation type that burns in Namibia is croplands, and some forest and grassland further inland.

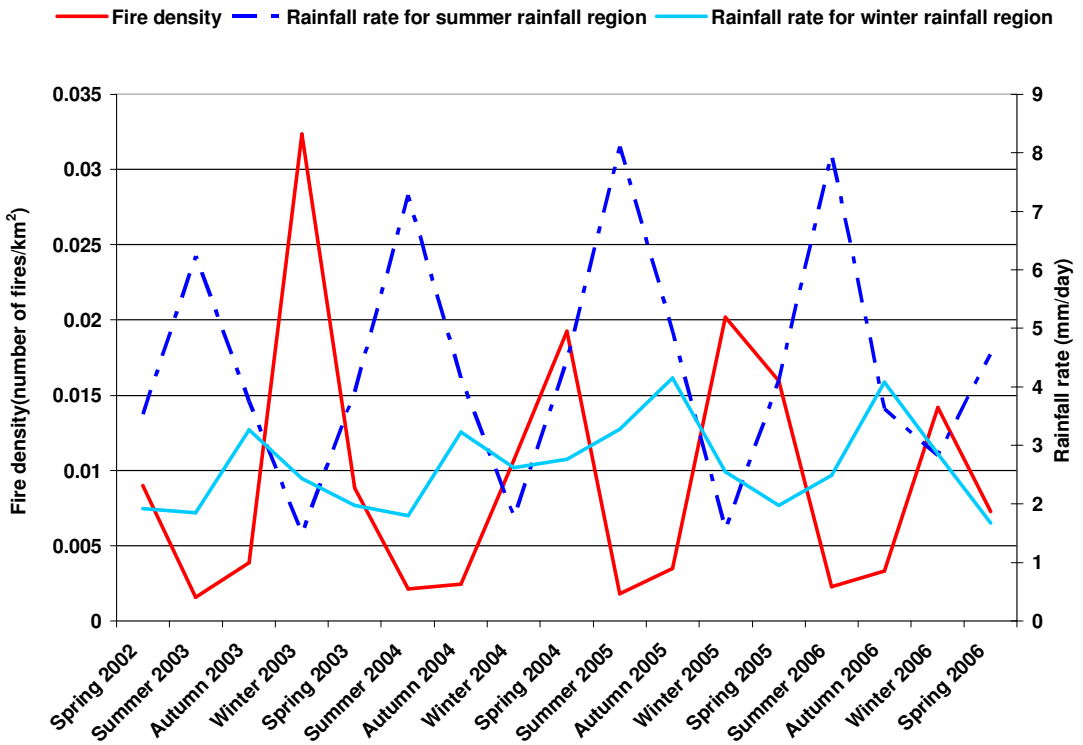

Figure 18: Relationship between fire density and rainfall rate for Namibia

The western cape region of South Africa experiences burning during the summer/autumn months, as this is the dry season for the south western coast and burning increases in this area from December through to February. In the rest of South Africa, the burning season occurs in winter and spring, but maximum burning

occurred in winter in 2003, 2005 and 2006, and in spring in 2004 (Figure 19). This is possibly due to the intense burning season of 2004 and an average wet season of 2004/2005 resulting in less available fuel. In November the fires mainly occur on the eastern coast of southern Africa, from approximately 15°S to 25°S, although they do not extend as far south as during the winter months. Little to no burning occurs on the south western coast of South Africa (25°S-35°S) in the winter months. The fires along the east coast of South Africa extend further into the interior (westwards) to Swaziland, KwaZulu Natal and the Highveld region of South Africa.

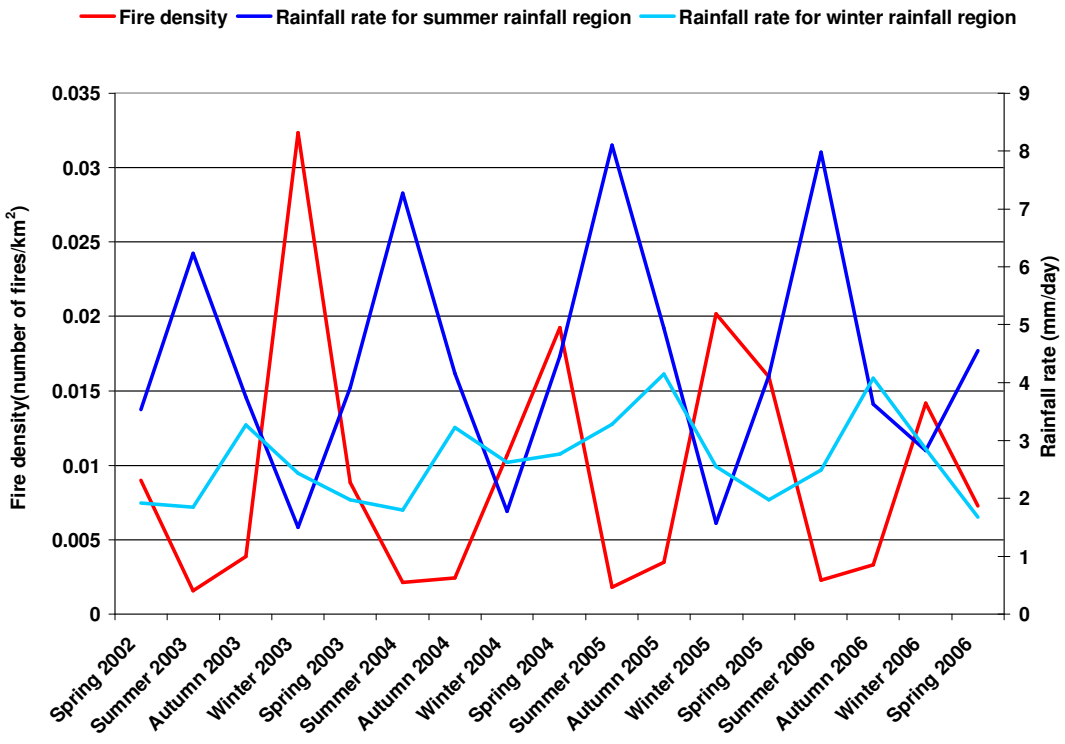

Figure 19: Relationship between fire density and rainfall rate for the South African region

Interannual variability of fire incidence

During the study period the greatest number of fires were detected in 2003, followed by 2005, 2004 and the least detected in 2006 for the southern African region (Figure 20). This pattern coincides with the extraordinarily wet rainy season of 2003/2004. An El Niño phase and consequently dry conditions were associated with the rainy season

of 2002/2003. Drier than normal conditions were prevalent in Angola, Namibia and Zambezi regions in 2004/2005, even though the regional rainy season of 2004/2005 was not exceptionally high, and the Congo, East Africa and South Africa regions experienced an abnormally wet rainy season, followed by a La Nina event in 2005/2006. A lower than normal amount of rain fell in the Congo and Angolan regions. The late spring rains of 2005/2006 resulted in an extended dry season of 2005, resulting in more fires in the Zambezi and East African regions (Figure 21). A particularly wet season followed by an extended or particularly dry season results in conditions most suitable for fire occurrence. The prevailing moist conditions and increased cloud cover during the wet rainy season result in fewer fires being detected via satellite. The greatest interannual variations in fire counts occur in autumn. The most biomass burning occurs during winter which means that the annual variations in burning reflect variations in winter burning.

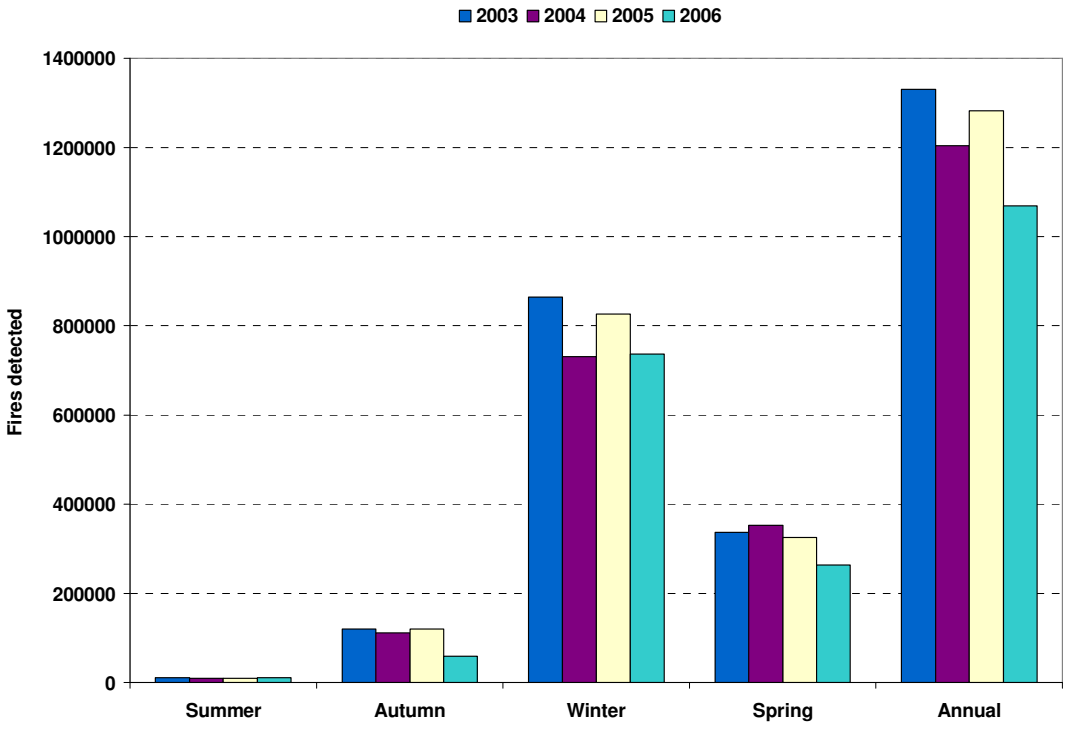

Figure 20: Interannual variabilty in the total number of detected fires in Africa south of the equator

Interannual variability for South Africa and the Zambezi region (Figure 21), follow a similar pattern to the regional trend (Figure 20), where fires occur later in the burning season in 2004, i.e. in spring rather than winter. The South African and Zambezi regions contain much of the savanna and woodland of the sub-continent. Woodlands and savanna are very susceptible to fires especially in dry conditions, and it can be said that in 2003 and 2005, there is an increase in savanna and woodland burning and hence burning across the sub-continent. There is an inverse relationship between fire incidence and rainfall in the Zambezi region (Figure 16). In 2003 and 2004 the burning and dry seasons are longer than in 2005 and 2006 but burning is not as extensive.

Fires that occur in regions of predominantly savanna are dependent on rainfall of the preceding rainy season and the dry conditions of the dry season. A wet preceding rainy season allows for a greater amount of available biomass and a greater potential for burning. A particularly dry burning season allows fire occurrence to be wide spread. This can also be said for regions that consist predominantly of woodlands, as fire incidence corresponds inversely to rainfall. Fire incidence in regions covered mainly by forest is dependant more on the dryness of the preceding rainy season, which allows the vegetation to dry out enough by the burning season and allow for extensive burning. Although crop burning follows a seasonal pattern according to the season of growing and harvest, fires lit for agricultural purposes are not correlated with rainfall, as these have an anthropogenic origin.

South Africa has a more complex relationship between fire incidence and rainfall (Figure 19). This is a consequence of winter rainfall and summer/autumn burning on the south west coast, and summer rainfall and winter/spring burning over the rest of the country. There was higher rainfall in the 2004/2005 and 2005/2006 rainy seasons in South Africa (Figure 19). The irregular pattern of rainfall in the winter rainfall region of South Africa can account for the erratic pattern of burning (Figure 19). The burning seasons of 2003, 2005 and 2006 correlate well with the rainy seasons of 2002/2003, 2004/2005, 2005/2006 in the summer rainfall region. There is an inverse relationship between rainfall and fire counts, where fewer fires detected in

summer/autumn when rainfall is high. In 2004 maximum burning occurs at the end of the dry season. Rainfall in the winter rainfall region does not decrease after winter rains in the 2003/2004 rainy season, but extends into spring.

The most consistent number of fires detected per square kilometre each year occurs in the Namibian region (Figure 18). This can be attributed to fires occurring mainly due to agricultural burning and the limited vegetation. There is a slight but progressive increase in the number of fires with each year. The Namibian region contains very little vegetation, as the majority of the country is desert. Between 15° and 25°S (over the Namib Desert) along the west coast, rainfall is low (<200mm per annum) and the region is very susceptible to drought (Anyamba *et al*., 2003). A similar amount of rain fell in 2002/2003 and 2003/2004; there was a decrease in rainfall in 2004/2005 and much higher rainfall in 2005/2006 (Figure 18). This does not correspond with the fire pattern, which suggests that factors other than rainfall influence burning in Namibia. The main vegetation cover is agriculture, with a small amount of grassland. Therefore the variation in burning between years can be attributed to changes in agricultural practices from year to year and burning of land to prepare the land for the growing season.

In the East African and Angolan regions the greatest amount of variability in fires occurred in 2003 and 2006, such that in 2003 a substantially above average number of fires were detected and in 2006 a substantially less than average number of fires occurred (Figure 20). The rainfall variability does not account for the vast variation in fire detection, since in East Africa an above average amount of rain fell in 2004/2005 (Figure 22). The vastly below average rain that fell in the 2002/2003 rainy season accounts for the large number of fires in 2003, as the particularly dry conditions are conducive to fire occurrence. The particularly low number of fires in 2006 can be attributed to other factors, such as atmospheric conditions and local burning practices. In Angola, an above average amount of rain fell in the 2002/2003 rainy season, and a below average amount of rain fell in the 2004/2005 rainy season (Figure 22), even though a similar number of fires are detected in 2004, 2005 and 2006 (Figure 21). This suggests that rainfall alone does not determine fire occurrence. A high amount of rain fell in the 2002/2003 and 2005/2006 rainy season (Figure 14) in Angola,

although the burning in winter differs between these two years, with more fires detected in 2003 (Figure 14). There is little variability in the number of detected fires during the burning seasons from 2004 to 2006, but there a higher number of fire counts in the burning season of 2003 than in the years that follow. Angola and East Africa have a range of vegetation types. The dominant vegetation type is woodland. It is evident that fires and rainfall are not consistently well correlated. This suggests that despite the many fires in this region are anthropogenic in origin, despite the strong relationship of fire and rainfall throughout the rest of southern Africa.

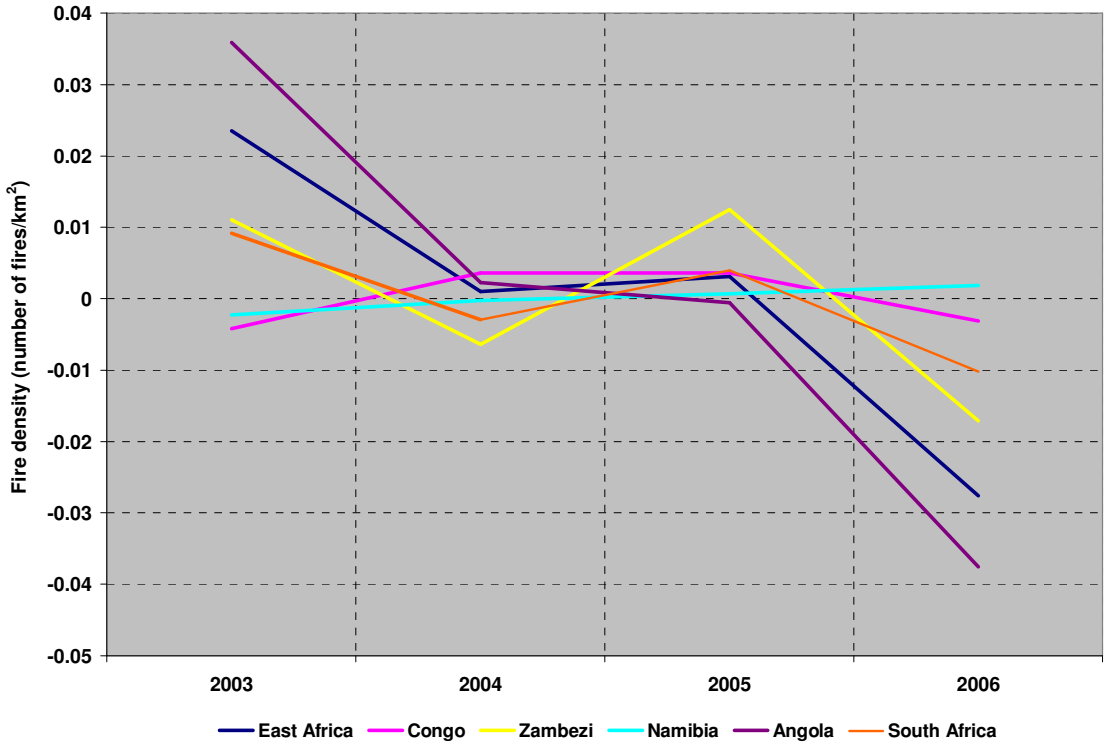

Figure 21: Interannual variability of fires detected per km^2 in each region, using the deviation from the mean for each region

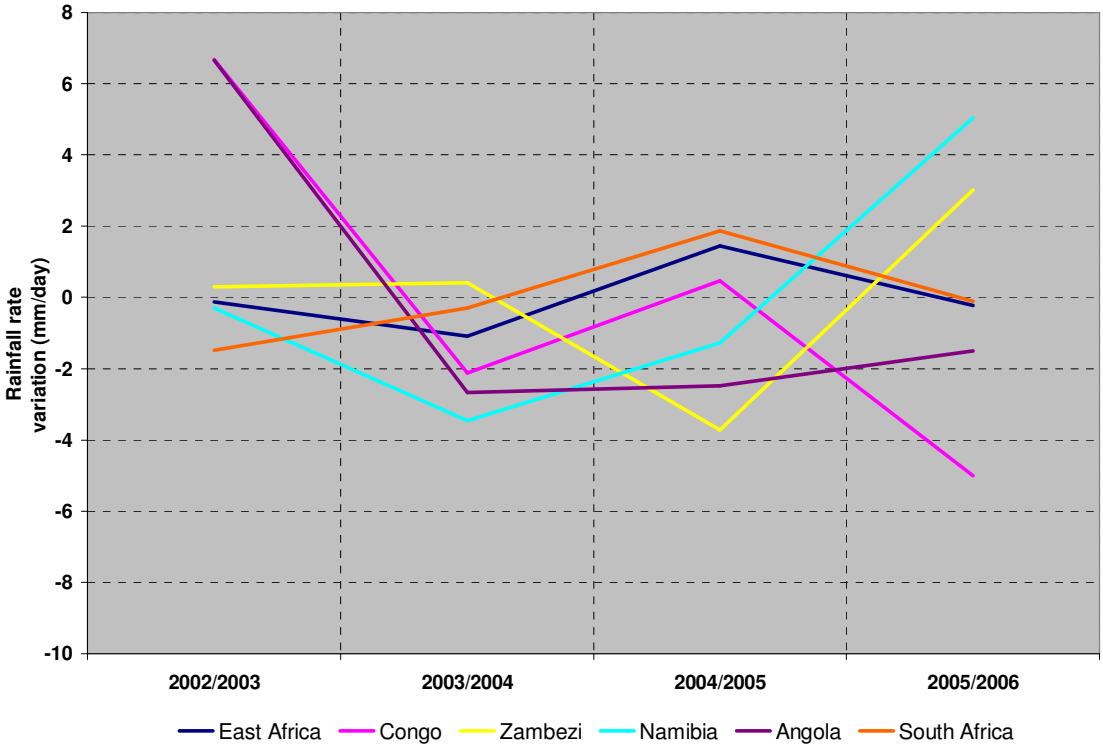

Figure 22: Interannual variability of rainfall rate per region, using the deviation from the mean for each region

There is little difference between fires detected between 2004 and 2005 in the Congo region, which shows a similar trend to many other regions on the sub-continent; however, the Congo region is the only region that has fewer fires detected in 2003 and 2006 (Figure 21). In the Congo region an above average amount of rain fell during 2002/2003 and 2004/2005 rainy seasons (Figure 22), although 2002/2003 was substantially higher. In the 2003/2004 rainy season and especially in the 2005/2006 rainy season a below average amount of rain fell. The drier conditions could account for the larger number of fires detected in 2004, although this does account for the decrease in fires in 2006 or the increase in 2005. Less rain fell during the 2003/2004 rainy season than in 2002/2003, yet there is little variability in the amount of detected fires in the burning season of 2003 and 2004 (Figure 22). Similarly there is a great difference between the rainy season of 2004/2005 and 2005/2006 rainy season yet only a slight difference in the amount of detected fires in the burning season of 2005 and 2006 (Figure 15). Fires in this area can be attributed to deforestation and land use changes, as the dominant vegetation type in the Congo region is forest.

Fire incidence corresponds with agricultural practices and with rainfall distribution and amount across southern Africa. Burning occurs during the dry season and is at a minimum during the rainy season. An exceptionally wet rainy season followed by a particularly dry season results in a high amount of detected fires. Variations in the pattern of burning can be attributed to local burning practices, such as land clearing and deforestation in order to use the land for agriculture. Interannual variations in burning can be explained by rainfall, atmospheric conditions, traditional burning practices and changes in seasonal burning. The burning season is initiated on the north west coast of southern Africa during late autumn/early winter. The fires spread in an easterly and southerly direction across the sub-continent. By spring, burning decreases in north west of the sub-continent, but the interior is burning, especially the Zambezi region. By summer burning has ceased over most of the sub-continent, except for the south western Cape.

Chapter 4

Results: Emissions

The seasonal and interannual distribution of biomass burning emissions, specifically by land cover type, is explored in this chapter. The emissions calculated in this study are compared to global emissions and other results for southern Africa. Biomass burning emissions are also compared to emissions from other sources in South Africa.

Emissions released from biomass burning are dependent on a number of factors, including the number of fires (burned area), biomass density, combustion efficiency, and quantity of aerosols and trace gases released when a specific vegetation type is burned (usually expressed as an emission factor). There are a number of methods used to calculate these parameters, which can result in different emission values.

Seasonality of emissions

The greatest number of fires in southern Africa burn in woodland and savanna (Figure 23). The biomass density for these two vegetation types is not particularly high, but emissions, especially for woodland, are the highest of all the vegetation types for most of the chemical species. Savanna and woodland dry out quickly and are easily combustible, which allows these two vegetation types to burn extensively and efficiently. Forests are not affected as much by fire as savanna (Figure 23), but release similar and often more emissions than savanna due to the large amount of fuel load available and higher density (Figure 24).

High biomass density values occur at the end of the rainy season (late summer, autumn) and low values during the dry season, especially when much of the biomass has been burnt (spring). Biomass density is closely related to rainfall as areas with high rainfall have a high biomass density, and areas with lower rainfall have a lower

biomass density. Forest has the highest biomass density of all the major vegetation types in southern Africa (Figure 24). Savanna has a considerably lower biomass density than that of forest (Figure 24). Even though biomass density is an important factor in burning (through the provision of fuel load) it is not necessarily the driving factor behind the amount of aerosols and trace gases released during burning, as the high density might result in smaller, smouldering fires rather than widespread flaming fires detected via satellite. Biomass burning estimates often underestimate emissions from surface fires as NDVI do not detect the corresponding fuel load (litter as dead tree leaves, twigs and grass) (Hély *et al.*, 2003b). In this study, it was found that the burning of forest releases per unit area less CO_2 (approximately 113 000 $kgCO_2.year^{-1}.km^{-2}$) and CO (approximately 48 $kgCO.year^{-1}.km^{-2}$) than woodland (180 000 $kgCO_2.year^{-1}.km^{-2}$ and 540 $kgCO.year^{-1}.km^{-2}$), even though forest has a higher biomass density. This highlights that there are a number of factors that determine the amount of emissions released from burning.

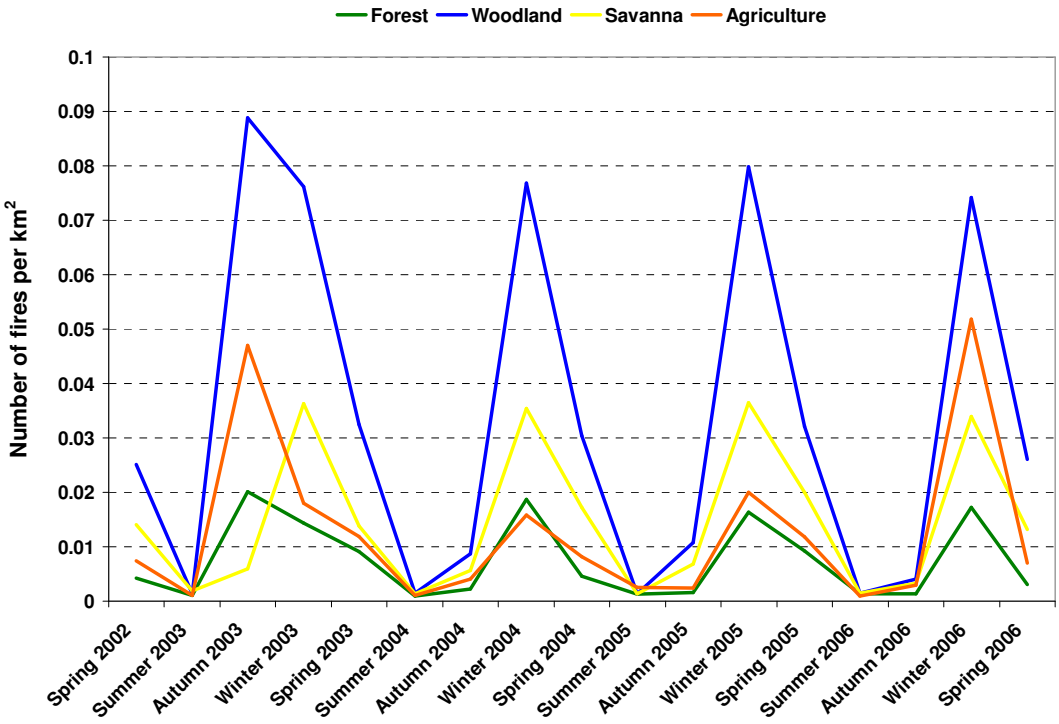

Figure 23: Number of fires in 2002 to 2005 per square kilometre for each vegetation type in southern Africa, as detected by MODIS active fire product

Biomass burning emissions in southern Africa peaked during winter (Figure 25 to Figure 28). High measurements of Aerosol Optical Depth (AOD) indicate strong increases in aerosol loading from August to October (Edwards *et al*., 2006) during the peak of the burning season (Holben *et al*., 1996). In this study emissions are calculated based on fire incidence as a proxy for burned area, rather than emissions observed via remote sensing. This highlights the correspondence between the peak of emissions and fire incidence. The seasonal emission pattern follows the pattern of the burning season where burning progresses from the north west of the sub-continent, in a southerly and easterly direction. Efficient burning from flaming combustion usually dominates in the early burn in woodland and savanna and results in a higher release of CO_2 (Korontzi *et al*., 2003, Ward *et al*., 1996). This is followed by a later smouldering stage that can continue for days and even weeks (Sinha *et al*., 2003) and a higher release of CO. Towards the end of the burning season, the smouldering phase and smaller undetectable (via satellite) fires burn.

The interannual and seasonal variations in emissions are primarily due to the occurrence of rainfall, the number of fires burning and agricultural practices. Fires occur during the dry season and are more prevalent after a particularly wet rainy season (Figure 23). Variations in emissions per land cover type can be attributed to the burning and prevalence of a particular land cover type on the sub-continent. The difference in emissions between land cover types could be as a consequence of vegetation-specific emission factors and different biomass densities. For most trace gases, the highest emissions originate from woodland, followed by either savanna or forest.

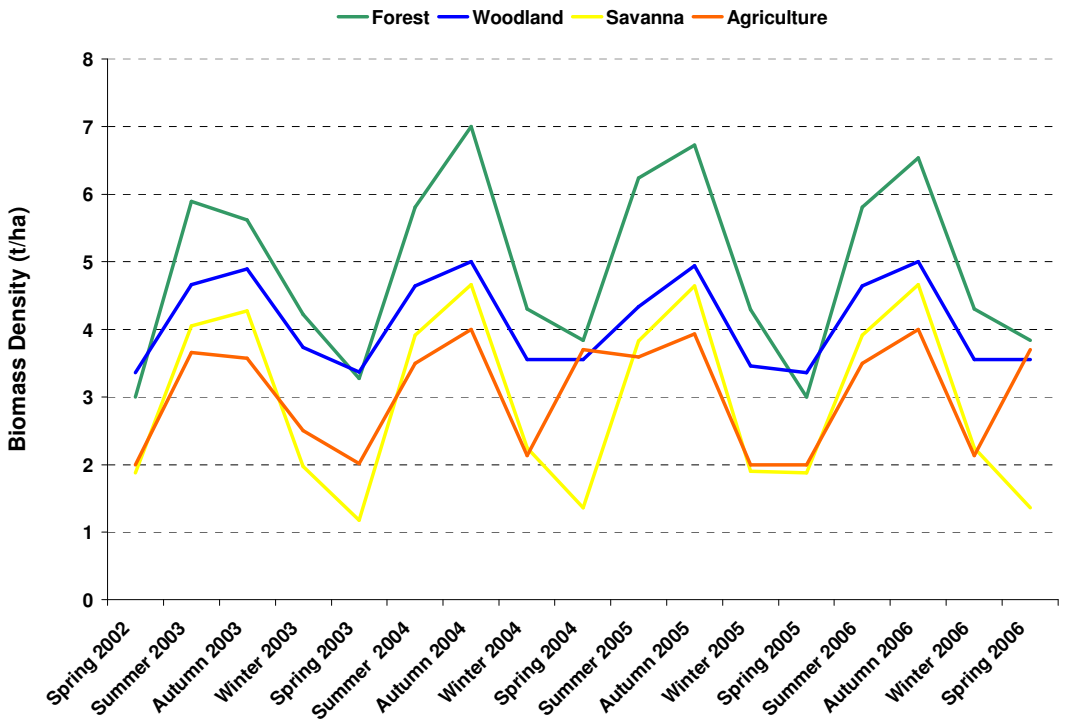

Figure 24: Biomass density for common vegetation types in southern Africa

Variations in the emission of chemical species due to vegetation type

Carbon dioxide (CO_2), carbon monoxide (CO), methane (CH_4), ammonia (NH_3), total particulate carbon (TPC) and organic particulate carbon (OPC) (Figure 25 and Figure 26) exhibit a very similar pattern of burning interannually and seasonally, with woodland emitting the most, followed by forest and savanna and lastly agriculture. These trace gases are the most abundant of emissions from biomass burning. CO_2 is released in the greatest amount of all the chemical species, mainly due to the high carbon composition of fuel. Some studies (van der Werf *et al.*, 2003 and Levine, 1990) calculate CO_2 emissions assuming 90% of the biomass burned is emitted as CO_2. The extensive amount of vegetation classified woodland and the burning of woodlands in southern Africa could result in woodland exhibiting the largest amount of emissions for most chemical species. The burning of woodland and savanna emits the most CO_2 per square kilometre (Figure 25) due to the large number of fires (woodland) and the high biomass density and subsequently fuel load (forest). In 2003 and 2005 burning continues peaking into spring. This is could be due to the prolonged dry season of the respective years.

The burning of savanna and woodland emit similar amounts of nitrogen oxides (NO_x) per square kilometre, considerably more than other land use types (Figure 27). Savanna burning also emits the largest amount of Hydrogen cyanide (HCN). In the winter of 2005, NO_x emissions from woodland were particularly high (Figure 27). This could be due to the increased amount of burning that took place in 2005 due to the extended dry season. Emissions of NO_x, organic compounds, and CO from biomass burning result in the formation of O_3.

Agricultural burning accounts for the lowest emissions per square kilometre for all trace gases, other than non-methane hydrocarbons (NMHC), total particulate matter (TPM) and nitrogen oxides (NO_x). Condensation nuclei (CN) emissions (Figure 28) follows a slightly different pattern to the regional pattern, where the maximum emissions originate from the burning of forest, followed by savanna, woodland and lastly agriculture. Formaldehyde (HCHO) is emitted predominantly from woodland burning, with minimal amounts released by other land cover types.

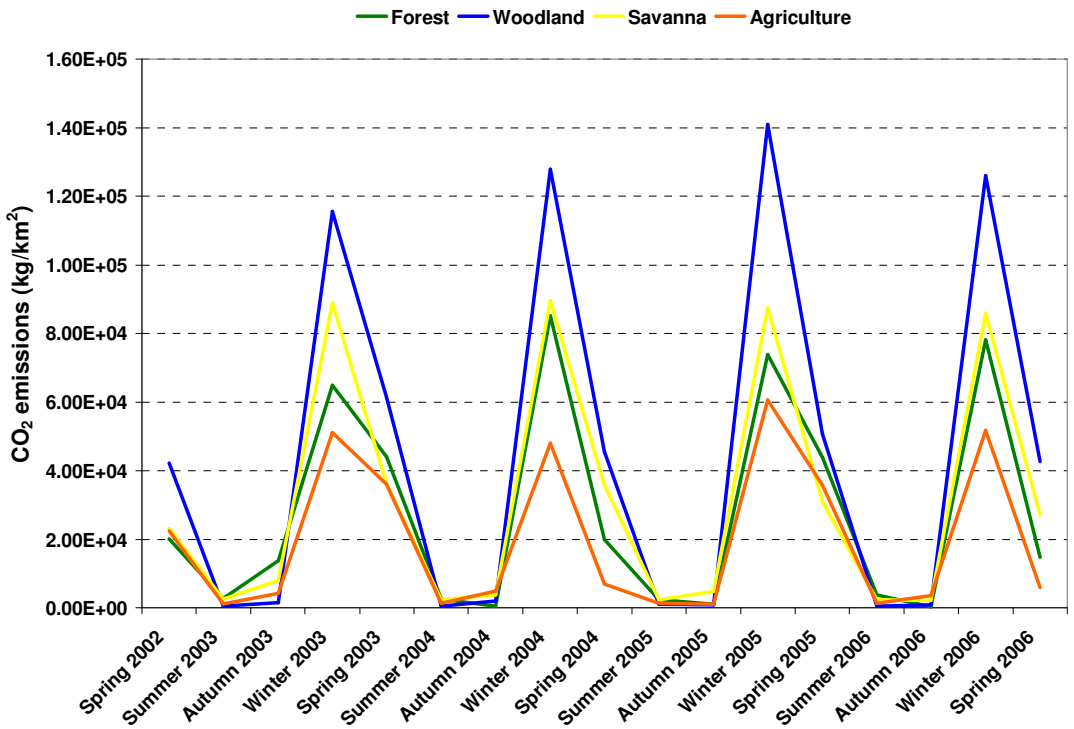

Figure 25: CO_2 emissions from biomass burning in southern Africa (30-35% error)

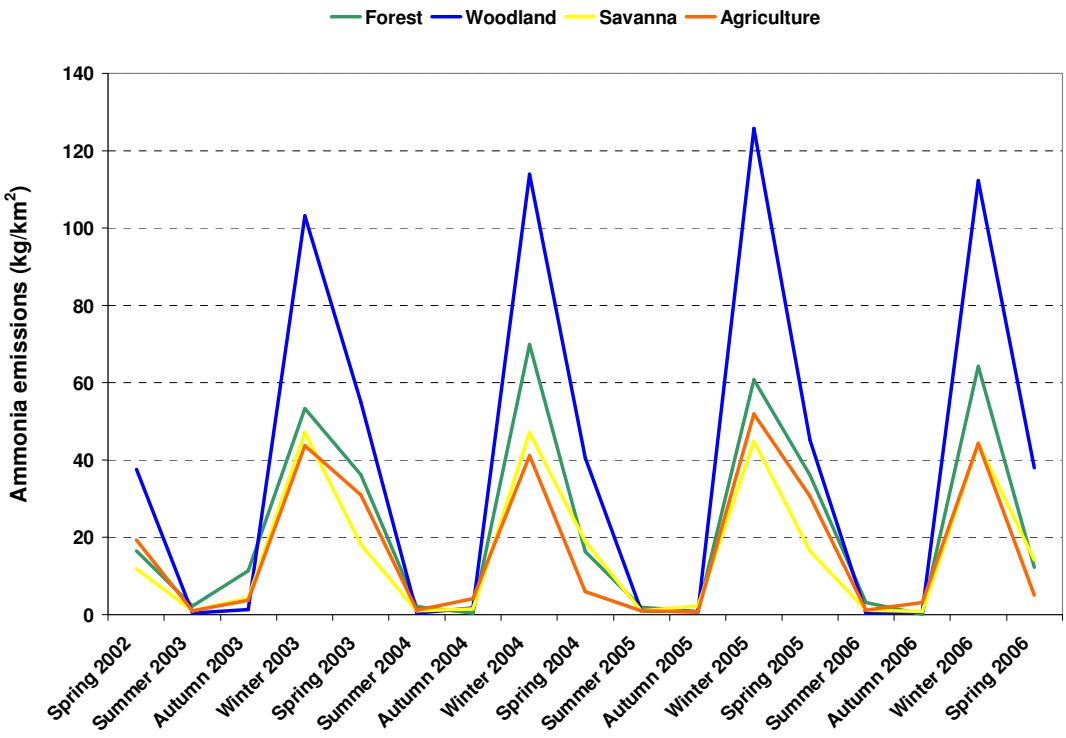

Figure 26: NH_3 emissions from biomass burning in southern Africa (>60% error)

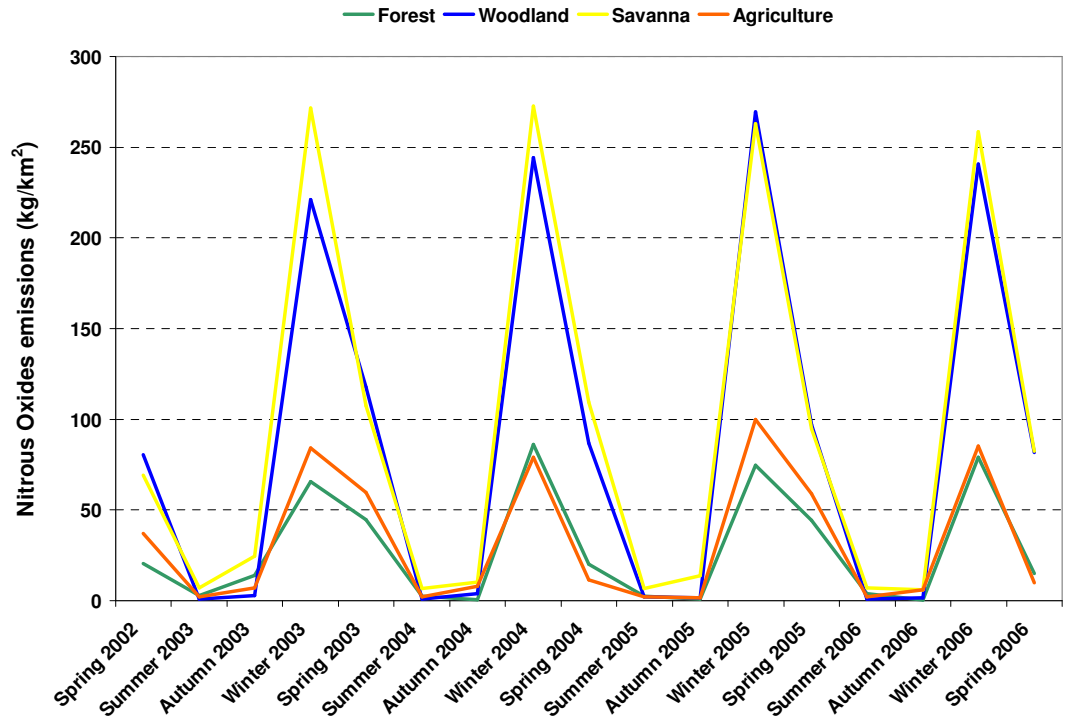

Figure 27: NOx emissions from biomass burning in southern Africa (50-55% error)

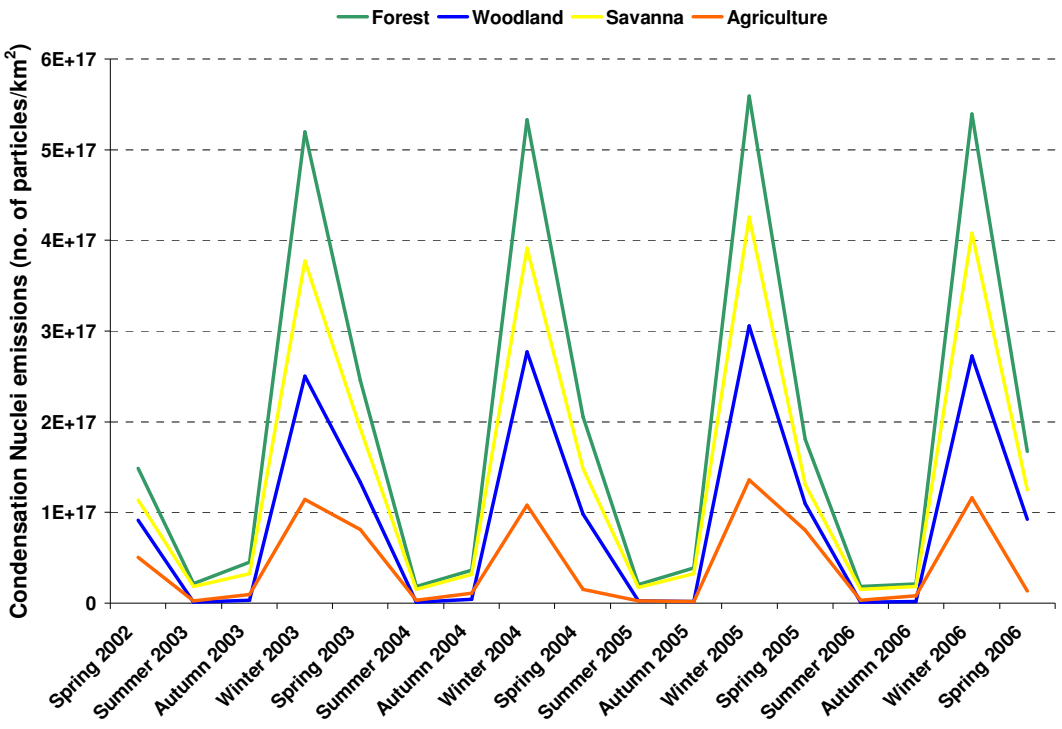

Figure 28: Condensation Nuclei emissions from biomass burning in southern Africa (>60% error)

Uncertainties

There are a number of uncertainties in estimating biomass burning emissions, especially since several parameters are used to calculate emission estimates.. In this study biomass burning emissions are calculated using biomass burned, biomass density, combustion efficiency and emission factors. Consistently, the largest uncertainty in calculating biomass burning emissions is burned area (Andreae and Merlet, 2001) which can hold a level of uncertainty of up to 50%. In this study, MODIS active fires are used as a proxy for burned area. The two main obstacles for using an active fire product to estimate burned area, is the overestimation of burned area through the assumption that the entire $1km^2$ pixel is burning and secondly the underestimation of fires due to the time of satellite overpass. Smaller fires are not easily detected (Hoelzemann *et al.*, 2004) and cloud cover can prevent fires from being detected (Hoelzemann *et al.*, 2004). The MODIS active fire product has a 50% probability in detecting a minimal flaming fire of $100m^2$ however, this probability increases to almost 100% for a $50m^2$ flaming fire under ideal atmospheric conditions

(AFIS User Guide). Burned area products are not without error either. Burned area products rely on a change analysis of imagery, which often has to be validated with higher resolution imagery (Roy *et al*., 2005a and 2006). The landcover change is not associated with fires early in the season and those that occur late in the season (Bucini and Lambin, 2002) which means burned area products dependent on change analysis of spectral signature will not underestimate the fires for the burning season. Burned area calculations can be refined by using a combination of a burned area and an active fire product (van der Werf *et al.,* 2003 and Ito and Penner, 2004), and validated using ground-based information and higher resolution images much like the protocol followed by SAFNet (Roy *et al*., 2005a).

Fuel load estimates and interannual differences in vegetation and burning also result in differences in emission estimates from biomass burning. Variation in rainfall and hence available fuel load will result in interannual differences in emission estimates. Various authors use different approaches when calculating emissions. For example, van der Werf *et al.*, (2003) use TRMM VIRS imagery and a biochemical model for 1998-2001, Scholes *et al*., (1996b) use the fuel consumption and emission factors from SAFARI-92 in a static model and Barbosa *et al*., (1999) use NDVI to calculate biomass density and combustion efficiency and subsequently estimate biomass burning emissions. Ideally validation of products and studies should be carried out for the same time period and defined area, using the same land cover classification system and emission factors.

Error

Barbosa *et al.,* (1999) suggest an error of 30% for biomass density values and 25 % for combustion efficiency. Hoelzemann *et al*., (2004) suggest an error of 12% in burning efficiency values for savanna and grasslands and up to 20% error in estimates for forests (Hoelzemann *et al*., 2004). Andreae and Merlet, (2001) highlight the problems with emission factors. In general, emission factors are calculated for specific regions and fire types (e.g. savanna) or for biomass burning as a whole, without considering different fuel types. Sufficient work on emission factors has been carried out for CO_2, CO, and CH_4 (Andreae and Merlet, 2001; Hoelzemann *et al*., 2004) where a 20-30% error can be assumed. An error of up to 50% is assumed for other emission factors that have not been investigated as

extensively (Andreae and Merlet, 2001). Barbosa *et al*., 1999 account for error in their biomass burning estimates using the following expression:

$$e_{total} = (e^2_{\text{burned area}} + e^2_{\text{biomass density}} + e^2_{\text{combustion efficiency}} + e^2_{\text{emission factor}}) \quad \text{(Equation 6)}$$

Following Equation 6 the total error for CO2, CO and CH4 in savanna and grasslands is 34% and for forest the total error is 35%. The total error for other chemical species for savanna and forest is 52% and 54% respectively. The emission factor for CN and NH3 is given with uncertainty (>60%) for forest and agriculture but with a 55% error for savanna and grassland, resulting in a total error of at least 60%.

Comparative studies and sources

In this study, the amount of biomass burned, biomass density and burning efficiency and were calculated according to the method used by Barbosa *et al.*, (1999), emissions are calculated using emission factors from a number of sources (Table 5) and fire counts used as a proxy for burned area. The biomass burning emissions calculated in this study are compared with global emission estimates, other estimates for southern Africa calculated using different methods or datasets, and emissions from other sources in South Africa.

Comparison of biomass burning emission estimates with previous studies

The total error in emissions for this study vary from 30% for CO_2, CO and CH_4 for savanna and grassland burning to >60% for CN and NH_3 in forest and agricultural burning. The total error for emission estimates calculated by Barbosa *et al*., (1999) is 58%. The main difference between Barbosa *et al*., (1999) and the study presented, is the method used for calculating burned area. Burned area estimates were derived by applying a multitemporal multithreshold technique to AVHRR images and validated by Landsat Thematic Mapper (TM) in Barbosa *et al*., (1999), whereas this study, used MODIS active fires as a proxy for burned area. Burned area estimates are one of the greatest uncertainties in calculating emission estimates. The different vegetation classification and differences in the regional climate for the respective study years can account for the variance in emission estimates. CO_2 emissions calculated in this study

fall within the average range of those calculated in other studies (Table 6). Burned biomass is higher than the average of that calculated in other studies for southern Africa (Table 6), however if a 30% error is considered for burned biomass for each of the studies, then the values are comparable. The error can account for some fires, especially smaller fires that are not detected with MODIS due to the resolution of the instrument and the time of the overpass of the satellite. A greater amount of biomass burned is detected due to the assumption that the whole pixel area is being burnt or the triangular response of MODIS, where a fire at the same location is detected twice in adjacent pixels along the scan line. Differences in burned area, burned biomass and CO_2 emissions calculated in the studies may also be partially due to interannual climatic differences.

Table 6: Comparison of annual estimates of burned areas, biomass burned and CO_2 emissions from open fires in southern Africa (Barbosa et al., 1999, van der Werf et al., 2003, Ito and Penner, 2004).

Study	Area Burned (10^3 km^2.yr^{-1})	Burned biomass (Tg)	CO_2 Emissions (Tg CO_2.yr^{-1})
This study	692	722	963
Ito and Penner (2004)	999	-	1644 – 2188[a] (1639 – 1786)[b]
Hao *et al.* (1990)		914	1508
Scholes *et al*. (1996)	1680	117	324
Barbosa *et al.* (1999)	1541	456	748
Justice *et al.* (2002)	-		1525
Van der Werf *et al*. (2003)	1160		1702[c]
Average	1345 ± 318		1242 ± 568[a]

[a] Statistics were estimated by using Sc1: RSF=1 and TFF=1 in only grid cells where ATSR fire counts are detected

[b] Values in parenthesis represented the Scenarios 3 and 4 (RSF=1 and TFF=1 in all grid cells, TFF = 0 in only grid cells where ATSR fire counts are detectable

[c] Estimated from the carbon emissions in van der Werf *et al*. (2003) assuming 90% is CO_2

The results in this study differ significantly from those in Scholes *et al.* (1996). Burned area calculated in this study is less than half of that calculated by Scholes *et al*. (1996), yet biomass burned is four times greater and CO_2 emissions are three times greater than in Scholes *et al*. (1996) (Table 7). Scholes *et al*., (1996) derived emission factors and used modified combustion efficiency values in a modelling method to estimate the amount of trace gases and aerosols released from biomass burning. Biomass burned values calculated in this study are most comparable with those in Hao *et al*. (1990), yet the emissions are approximately a third less, which could be due to the different emissions factors applied. CO_2 emissions and burned biomass calculated by Ito and Penner (2004) exceed estimates in this study by approximately a third, and CO_2 emissions and biomass burnt calculated by van der Werf *et al.* (2003) exceed those in this study by more than a half (Table 6). Ito and Penner (2004) use Global Burned Area (GBA)-2000 burned area estimates and Along Track Scanning Radiometer (ATSR) fire counts to compensate for smaller fires that are not detected by the burned area algorithm to calculate the burned area as the input into emission calculations. Van der Werf *et al*. (2003) use a combination of the Moderate Resolution Imaging Spectrometer (MODIS) 500-m burned area algorithm and Tropical Rainfall Measuring Mission (TRMM) fire counts to estimate burned area. The MODIS burned area algorithm detects a large amount of burned area, which explains the large amount of biomass burned calculated by van der Werf *et al*. (2003). Van der Werf *et al*. (2003) derive a vegetation map based on mean annual precipitation and satellite-derived tree-cover (DeFries *et al*., 1999) and use the Carnegi-Ames-Stanford Approach (CASA) to estimate net carbon fluxes from the terrestrial biosphere to model the flux of carbon from vegetation burning. The higher emission estimates could be accounted for by differences in the estimate of burned area, vegetation classification or model uncertainties. CO_2 emission estimates for this study are higher than those calculated by Barbosa *et al.* (1999), even though the method used for this study follows Barbosa *et al.* (1999). Barbosa *et al.* (1999) calculated burned area by applying a series of Advanced Very High Resolution Radiometer Global Area Cover (AVHRR-GAC) data to a multitemporal, multithreshold technique-burned area algorithm (BAA) and validated the burned areas with Landsat TM images. This study uses fire counts as a proxy for burned area. The variation between studies, highlights the possibility of error that can affect the final emission total due to the differences in emission factors and methods used to calculate

burned area and burned biomass totals. The discussed studies were not carried out in the same year or over the same time period. The interannual fuel load differences, in the amount of available fuel and the dominant vegetation type constituting the fuel for that period of time can have a considerable effect on emission estimates.

Contribution of CO_2 emissions from biomass burning in southern Africa to global biomass burning emissions

CO_2 emissions from biomass burning in southern Africa have previously been suggested to contribute 40% of global biomass burning emissions (Levine *et al*., 1995) since a large portion of biomass burning takes place on the African continent. If CO_2 emission estimates for biomass burning in southern Africa from this study are compared to global CO_2 emission estimates from biomass burning from Levine *et al*. (1995), it is calculated that biomass burning in southern Africa contributes approximately 30% of carbon released globally from biomass burning and approximately 10% of biomass burned globally (Table 7) The use of vegetation indices (this study) rather than dry matter (global estimates) can account for the difference between this result and that of Levine *et al.* (1995). The burning of agriculture in southern Africa constitutes 10% of global biomass burning. Woodland emissions of CO_2 exceed global estimates of tropical and boreal forests. This is possibly due to the manner in which biomass density is calculated, where global estimates use dry matter and this study uses vegetation indices. The difference can also be ascribed to a difference in the classification in vegetation type and the value of the emission factor applied to the biomass burned.

Comparison of emissions calculated using MODIS, GBA-2000, GLOBSCAR and in the current study for southern Africa

The MODIS 500m burned area product, GBA-2000, GLOBSCAR (Table 8) and MODIS fire products (this study) all have a pixel resolution of 1 km^2. Emissions were calculated from the MODIS 500m burned area product, GBA-2000 and GLOBSCAR using the same method used here, the only difference being area burned. The MODIS burned area product detects a much higher burned area (9 269 225 km^2) than this study (2 528 294 km^2), GBA-2000 (268 500 km^2) and GLOBSCAR (59 800 km^2) (Korontzi *et al.,* 2004). The three 2000 burned products are available yet none are

systematically validated (Korontzi *et al.*, 2004) and indicate very large discrepancies in burned area estimates. This is can be attributed to the different satellites used for detection and/or the burned area algorithm. The difference in emission estimates is predominantly due to the amount of area burned, the study period and emission factors used. In addition to this, the amount of atmospheric species emitted is not directly proportional to the area burned, in that there is not a consistency in the order of magnitude between the differences in the burned area products and the emissions. Emissions are dependent on the spatial distribution of burning relative to the fuel load amount and the composition of grassland and woodland (Korontzi *et al*., 2004).

Table 7: Estimates of biomass burnt annually and the associated emission of carbon and carbon dioxide (CO_2) to the atmosphere for southern Africa (this study) and globally (Levine, 1995).

Source of burning	Biomass burned (Tg/year)		Carbon Released (Tg(C)/year		CO_2 Released ($Tg(CO_2)$/year	
	Global[a]	Southern Africa	Global[b]	Southern Africa	Global[c]	Southern Africa
Savanna	3690	239	1660	440	1494	417
Agricultural waste	2020	21	910	42	829	39
Tropical forest	1260	87	570	170	513	156
Temperate and boreal forests/ Woodland (southern Africa)	280	318	130	587	117	537
Total	**7250**	**666**	**3270**	**1238**	**0**	**963**

[a] 1 Tg (teragram) = 10^6 metric tons = 10^{12}g

Based on carbon content of 45% in biomass material. In case of charcoal, the rate of burning has been multiplied

[b] Assuming that 90% of the carbon released is in the form of CO_2

[c] Sources: Seiler and Crutzen (1980), Crutzen and Andreae (1990), Hao *et al*. (1990), Andreae (1991).

The emissions from grassland (savanna) and woodland from this study are much greater for September than the emissions from the comparative products, especially for CH_4, CO, NMHC, OPC, BC, NO_x and HCHO. Emissions estimates for savanna are greater for all trace gases. This is could be attributed to the vegetation classification, for example, in this study, grassland is included in the savanna classification. The difference in detected burned biomass and emission factors used can account for the differences in emissions estimates. The values from this study compare well with MODIS 500m burned area product for woodland for CO_2, CO, BC, NO_x and TPM. MODIS 500m burned area product, GBA-2000 and GLOBSCAR made use of models comparing emission factors and modified combustion efficiency reported in literature (Korontzi *et al.,* 2003b, Sinha *et al*., 2003, Ward *et al*., 1996, Yokelson *et al*., 2003) whereas this study used a combination of emission factors (Table 5). MODIS 500m burned area, GBA-2000 and GLOBSCAR are all specific to one month, being September 2000, whereas this study averages the emissions for September from 2003-2006. GLOBSCAR estimates do not compare well with this study at all, other than HCN estimates. The main difference in the calculation of

emissions is the vegetation classification and the estimate of burned area. This study uses fire as a proxy for burned area, whereas the comparative products are all burned area products.

Comparison of emissions from biomass burning to emissions from other sectors in South Africa

Most CO_2 and NO_x in South Africa is emitted by the industrial and energy sector (Table 9). Vehicle emissions contribute a greater amount of NO_x than biomass burning, but still contribute approximately a quarter of what industry contributes (Table 9). Agricultural and cane sugar burning contributes the least emissions of all the sectors. The sector responsible for the largest amount of CO is veld and bush fires, whereas it was calculated in this study that biomass burning contributes the most to CH_4 emissions. Biomass burning also contributes a considerable amount of CO_2 even though it is only approximately one quarter of the CO_2 emissions released by the industrial and energy sector. Helas and Pienaar (1995) estimate CO emissions from veld and bush fires (Table 9) to be four times those from biomass burning, as calculated in this study (Table 9). Emission estimates for this study were calculated using emission factors, whereas emission ratios from SAFARI-92 were used by Helas and Pienaar (1995) to calculate estimates for veld and bush fires (Table 9). This together with the possibility of different spatial resolutions used, the detection of different detecting types of burning and burned area products can account for the difference in emission estimates. Twice the amount of particulates is released from biomass burning than from the industrial and energy sector (Table 9).

Table 8: Regional biomass burning emissions for southern Africa for September 2000 from MODIS, GBA-2000, GLOBSCAR and this study (Korontzi *et al*., 2004).

Method	MODIS		GBA-2000		GLOBSCAR		This study*	
Species	Woodland (Gg)	Grassland (Gg)	Woodland (Gg)	Grassland (Gg)	Woodland (Gg)	Grassland (Gg)	Woodland (Gg)	Grassland (Gg)
Carbon Dioxide (CO_2)	93393	40387	53935	36935	24951	5368	82993	54504
Methane (CH_4)	175	13.320.5	89	12	43	2	249	80
Carbon Monoxide (CO)	5100	767	2711	680	1284	109	5660	2552
Nonmethane hydrocarbons (NMHC)	138	21	75	18	35	3	302	114
Total Particulate Matter (TPM)	1077	101	562	89	268	15	931	220
Organic Particulate Carbon (OPC)	222	47	120	42	57	7	107	107
Black Carbon (BC)	26	4	14	3	7	1	30	16
Nitrous oxides (NO_x) as NO	190	70	108	63	50	9	159	171
Ammonia (NH_3)	19	3	10	3	5	0	74	30
Formaldehyde (HCHO)	75	14	40	13	19	2	116	15
Hydrogen Cyanide (HCN)	33	10	19	9	9	1	8	7
*Averaged values for September 2002-2006								

There are many uncertainties related to calculating emissions from biomass burning. The primary uncertainty is the amount of burned area. Burned area satellite products are not sufficiently validated to be reliable to accurately estimate burned area. Although some results were comparable with Scholes *et al*., (1996), the emissions calculated in this study are low in comparison to global estimates and other studies. The burned area calculated in this study is dependent on the number of active fires detected via MODIS and is possibly the primary factor responsible for the underestimation of emissions from biomass burning.

Table 9: Comparison of different combustion sources in South Africa per annum (adapted by Helas and Pienaar (1995) from Scholes and van der Merwe, (1994), Helas and Pienaar (1996), Wells *et al*. (1996), DEAT (2003).

Activity	CO_2 (Tg)	CO (Gg)	CH_4 (Gg)	NO_x (Gg)	Particulates (no.of particles)
Energy[a], industrial[a] burning, and other coal use[c] and Scheduled emissions[b]	843	57	44	2369	331
Agriculture[a] and Cane Sugar Burning[c]	4	95	26	18	-
Domestic coal and wood fires[c]	21.9	1848	30.4	62.4	-
All types of vehicles[c]	48	3428	15.9	519	-
Veld and Bushfires#[c]	64	4650	265	31	-
Biomass burning[d]	189	1152	463	375	610
- Value not known					
[a]DEAT, 2003, 1994 emissions					
[b]Wells *et al* , 1996					
[c]Helas & Pienaar, 1996					
# based on estimated total of 44.3Tg dry mass (DM) burnt per year, which equals 19.9Tg of carbon. DM concentrations are as follows: savanna (23.1Tg), grassland(18.3Tg), fynbos (2.9Tg)					
[1]for emission ratios measured during SAFARI 92 (Helas and Pienaar, 1995)					
[d]This study (average emissions between 2003 and 2006)					

Emissions of aerosols trace gases from biomass burning reach a peak during the dry season. CO_2 is the primary trace gas released from biomass burning. Woodland burning is extensive and is responsible for the greatest amount of emissions, whereas agriculture is the responsible for the least. The greatest number of CN is emitted by forest burning and savanna burning is responsible for the emission of most NO_x and HCN. Burned area and emission estimates in this study compare well with some studies for southern Africa but

poorly with others. Biomass burning makes a significant contribution to trace gas and aerosol emissions, especially with regards to CH_4. Although CO_2 emissions from biomass burning as calculated in this study do not exceed contributions from the industrial and energy sector, it still contributes two thirds of the amount from the above-mentioned sectors. Biomass burning also contributes significantly to the number of particulates emitted. The optimum way to refine emission estimates is to calculate burned biomass by using a combination of a burned area product and an active fire product (van der Werf *et al.,* 2003 and Ito and Penner, 2004), to include the modified combustion efficiency in calculations, and to use a consistent and refined vegetation classification and a consistent set of emission factors for specific vegetation types relevant to southern Africa.

Chapter 5

Summary and Conclusions

In this chapter the main findings of this study are summarised and concluded. The pattern of interannual and seasonal variation in fire activity over the study period is indicated. The pattern of biomass burning emissions across southern Africa is summarised and a comparison of calculated burned area and emission estimates is provided.

The main aim of this research is to investigate interannual and seasonal variations in fire occurrence across southern Africa, using active fire data from satellite imagery. Active fire counts are used to calculate estimates of aerosol and trace gas emissions from biomass burning. Conclusions are made regarding observed fire patterns and estimates of trace gases and aerosol emissions from various landcover types and are compared to those calculated in previous studies, and from other sources.

Biomass burning in southern Africa

Biomass burning in southern Africa contributes approximately 10% of biomass burned globally and approximately 40% of carbon released globally, according to the results from this study (Table 7). The burning season in southern Africa occurs during winter and spring and coincides with the dry season (May to October). Fire counts increase substantially in May and continue to increase, reaching a maximum in August and September.

- Fires start in the western part of the sub-continent in north-western Angola and the southern Democratic Republic of Congo (DRC) in March and fires burn extensively throughout the winter period between the Equator and Tropics.
- During late winter/early spring, burning in the eastern countries and east coast (Tanzania/Mozambique) increases and there is a decline in burning in the west and interior as drier conditions extend to the eastern coast of southern Africa

(Cahoon *et al*., 1992).

- By September, fires are widespread across southern Africa, and burning is particularly intense in Angola, DRC, Zambia, Zimbabwe and Mozambique (Cahoon *et al*., 1992) but are no longer burning as extensively in the northernmost parts of the Tropics, where burning is initiated.
- By November, most of the fires have ceased in the Tropics (Angola/DRC), except for a few isolated fires burning.
- The burning season in the south-western part of southern Africa occurs during summer, as this region receives winter rainfall.

Fire density in southern Africa

- The Angolan region has the highest fire density in southern Africa in autumn and winter.
- The main vegetation classes affected by fire in the Zambezi region in spring are agriculture, woodlands and forest. These vegetation types have a high biomass density that provides a large amount of fuel for burning. Natural vegetation is burned to clear land for agricultural purposes and land use changes.
- The lowest fire density for the sub-continent for each season occurs in the Namibian region, since vegetation density is low in this arid country.
- The Western Cape region of South Africa experiences burning during the summer/autumn months (December to February), as this is the dry season in this area.

Burning season for southern Africa

- A wet preceding rainy season allows for a greater amount of available biomass and a greater potential for burning. A particularly wet season followed by an extended or particularly dry season results in conditions most suitable for fire occurrence.
- The greatest interannual variations in fire counts occur in autumn.
- The most biomass burning occurs during winter which means that annual variations in burning reflect variations in winter burning.

- The timing of the onset of the rainy season is a factor that determines the length of the burning season and hence the total amount of burning for the burning season.
- A particularly dry burning season allows fire occurrence to be widespread.
- The correlation between rainfall and burning is inconsistent, which emphasises the influence of human activities on burning. The highest number of fires was detected in 2003, followed by 2005.

Interannual variability of fire occurrence and burning for southern Africa

Rainfall influences biomass burning, yet there are inconsistencies between the correlation of rainfall and fire incidence. This demonstrates the extent of fires that are anthropogenic in origin.

- The regional interannual variability pattern of burning is due to the dominance of woodland and savanna burning across southern Africa.
- Anthropogenic burning is particularly evident when there is a weak correlation between fire incidence and rainfall.
- Fires due to human activity can be attributed to deforestation and land use changes in Congo, agricultural burning in Zambezi and Namibia and anthropogenic woodland burning the East African and Angolan regions.
- Fire incidence and rainfall have an inverse relationship in the Zambezi region.
- The most consistent number of fires detected per square kilometre each year occurs in the Namibian region.
- South Africa has a two burning seasons. This is a consequence of winter rainfall and summer/autumn burning on the south west coast and adjacent lying area, and summer rainfall and winter/spring burning over the rest of the country.

Trace gases and aerosol emissions from biomass burning

The interannual and seasonal variations in emissions are primarily due to the occurrence of rainfall, the number of fires burning and agricultural practices.

- Carbon dioxide (CO_2), carbon monoxide (CO), methane (CH_4), ammonia (NH_3), total particulate carbon (TPC) and organic particulate carbon (OPC) exhibit a very similar pattern of burning interannually and seasonally, with woodland emitting the most, followed by forest and savanna and lastly agriculture. These trace gases are the most abundant of emissions from biomass burning.
- The burning of woodland and forest emits the most CO_2 per square kilometre due to the large number of fires (woodland) and the high biomass density and consequently fuel load (forest).
- The burning of savanna and woodland emit similar amounts of nitrogen oxides (NO_x) per square kilometre, considerably more than other land use types.
- Agricultural burning accounts for the lowest emissions per square kilometre for all species, other than NMHC, TPM and NO_x.
- The maximum amount of CN emissions originate from the burning of forest.
- Nitrous oxide (NO_x) and hydrogen cyanide (HCN) are emitted predominantly from savanna burning. Formaldehyde is emitted in minimal amounts in comparison to the other species.
- The greatest number of fires burn in woodland and savanna in southern Africa.
- Savanna and woodland burn extensively and efficiently as they dry out quickly and are easily combustible.
- Greatest quantities of most aerosols and trace gases are emitted from fires in woodland, savanna and forest.

Comparison of burned area and CO_2 emission estimates from biomass burning estimates with other studies

- Burned area estimates calculated in this study fall slightly below the average of estimates from previous studies for southern Africa. However, the CO_2 emissions fall close to the calculated average. Burned area products for

September 2000 (MODIS 500m burned area, GLOBSCAR and GBA-2000) show great discrepancies in burned area values. The MODIS burned area product detects a much higher burned area (9 269 200 km^2) than this study (2 528 300 km^2), GBA-2000 (268 500 km^2) and GLOBSCAR (59 800 km^2) (Korontzi *et al.,* 2004). There is also an inconsistency in the differences in burned area and the difference in emissions between products.

- CO_2 emissions from grassland burning are estimated to be much higher in this study that in most other studies. A large amount of vegetation was assigned as grassland in the vegetation classification, which can account for the higher estimate of emissions.
- Emissions calculated in this study compare well with those from the MODIS 500m burned area product for woodland for CO_2, CH_4, CO, OPC, NO_x and HCN.
- Estimates of TPM, NO_x and HCN of this study compare well with GBA-2000 woodland estimates
- Estimates of NMHC, BC, NH_3 emissions from this study are much higher than those from other studies.

Comparison of biomass burning emission estimates with emissions from other sectors

Biomass burning in South Africa makes a significant contribution to total trace gas and aerosol emissions

- Biomass burning makes a considerable contribution (approximately 463 $GgCH_4.yr^{-1}$) to total CH_4 emissions (approximately 844 $GgCH_4.yr^{-1}$).
- A considerable amount to total CO_2 emitted (189 $TgCO_2.yr^{-1}$), even though it is only approximately one quarter of the CO_2 emissions released by the industrial and the energy sector combined (843 $TgCO_2.yr^{-1}$).
- Biomass burning calculated in this study results in twice the amount of particulates (610.yr^{-1}) being released as the industrial and energy sector combined (331. yr^{-1}).
- Industrial burning, coal use, and scheduled emissions emit the greatest amount of CO_2 (843 $Tg.yr^{-1}$)and NO_x (2369 $Gg.yr^{-1}$)

There are many uncertainties related to calculating emissions from biomass burning. The primary uncertainty is the amount of burned area. The burned area calculated in this study is dependent on the number of active fires detected via MODIS and is possibly the primary factor responsible for the difference in burned area estimates and biomass burning emissions estimates compared to other studies. Burned area calculations can be refined by using a combination of a burned area and an active fire product (van der Werf *et al.,* 2003 and Ito and Penner, 2004). The refinement of trace gas and aerosol emission estimates can be achieved by the inclusion of the modified combustion efficiency in calculations. A consistent and refined vegetation classification and a consistent set of emission factors for specific vegetation types relevant to southern Africa is needed in order to allow for a systematic comparison of emissions.

Chapter 6

References

Albrecht, B.A., 1989: Aerosols, Cloud Microphysics, and Fractional Cloudiness, *Science,* 245, 1227-1230.

Alleaume, S., Hély, C., Le Roux, J., Korontzi, S., Swap,R.J., Schugart, H.H. and Justice, C.O., 2005:Using MODIS to evaluate hetrogeneity of biomass burning in southern Africa savannahs: a case study in Etosha, *International Journal of Remote Sensing,* 26(19), 4219-4237.

Anderson, B.E., Grant, W.B, Gregory, G.L., Browell, E.V., Collins Jnr, J.E., Sachse, G.W., Bagwell, D.R., Hudgins, C.H., Blake, D.R. and Blake, N.J. 1996: Aerosols from biomass burning over the tropical South Atlantic region: Distributions and impacts, *Journal of Geophysical Research*, 101, D19, 24,117-24,137.

Andreae, M.O., 1991: Biomass burning: It's history, use and distribution and its impact on environmental quality and global climate, in Levine, J.S., *Global Biomass Burning: Atmospheric, Climatic and Biospheric Implications,* MIT Press, Cambridge, Massachusetts, 3-21.

Andreae, M.O. and Merlet, P., 2001: Emission of trace gases and aerosols from biomass burning, *Global Biogeochemical Cycles*, 15, 955-966.

Anyamba, A., Justice, C.O., Tucker, C.J. and Mahoney, R., 2003: Seasonal to interannual variability of vegetation and fires at SAFARI 2000 sites inferred from advanced very high resolution radiometer time series data, *Journal of Geophysical Research* , 108, D13, 8507, doi: 10.1029/2002JD2464. SAF 43:1-26.

Author unknown, "AFIS User Guide", Advanced Fire Information System, CSIR Satellite Applications Centre. Available at : www.wamis.co.za/afis/afis.htm

Author unknown. "About FLAMBÉ: An Introduction to emissions." FLAMBÉ. 2003 <www.nrlmry.navy.mil/flambe>.

Author unknown, "Active fire monitoring with MSG Algorithm Theoretical basis document", EUMETSAT, April 2007, available at: www.eumetsat.int

Barbosa, L. A. G., Carta Fitogra´phica de Angola, 323 pp., Inst. de Invest. Cien. de Angola, Luanda, Angola, 1970.

Barbosa, P.M., Stroppiana, D., Grégoire, J-M. and Pereira, J.M.C., 1999: An assessment of vegetation fire in Africa (1981-1991): Burned areas, burned biomass, and atmospheric emissions, *Global Biochemical Cycles*, 13 (4), 933-950.

Bertschi, I., Yokelson, R.J., Ward, D.E., Babbit, R.E., Susott, R.A., Goode, J.G. and Hao, W.M., 2003, Trace gas and particle emissions from fires in large diameter and belowground biomass fuels, *Journal of Geophysical Research*, 108, D13, 8472, doi: 10.1029/2002JD002100.

Brown, S and Gatson, G., 1995: Use of forest inventories and geographic information systems to estimates biomass density of tropical forests: Application to tropical Africa, *Environmental Monitoring and Assessment*, 38, 157-168.

Bucini, G and Lambin, E.F., 2002: Fire Impacts on vegetation in Central Africa: a remote-sensing-based statistical analysis, *Applied Geography*, 22, 27-48.

Cachier, H., Liousse, C., Pertuisot, M.H., Gaudichet, A., Echalar, F. and Lacaux, J.P. 1996: African Fire Particulate Emissions and Atmospheric Influence, in Levine, J.S., *Biomass Burning and Global Change Volume 1: Remote Sensing, Modelling and Inventory Development, and Biomass Burning in Africa*, The MIT Press, Cambridge, Massachusetts.

Cahoon, R.C., Stocks, B.J., Levine, J.S, Cofer, W.R. and O'Neil, K.P. 1992: Seasonal distribution of African savanna fires, *Nature*, 359, 812-815.

Chandra, S., Ziemke, J.R., Bhartia, P.K., and Martin, R.V., 2002: Tropical Tropospheric ozone: Implications for dynamics and biomass burning, *Journal of Geophysical Research*, 107, D14, 10.1029/2001JD000447, ACH3:1-17.

Charlson, R.J., Schwartz, S.E., Hales, J.M., Cess, R.D., Coakley, J.A., Jnr, Hansen, J.E. and Hofmann, D.J. 1992: Climate Forcing by anthropogenic aerosols, *Science*, 255, 423-430.

Christopher, S.A., Kliche, D.V., Chou, J and Welch, R.M., 1996: First estimates of the radiative forcing of aerosols generated from biomass burning using satellite data, *Journal of Geophysical Research*, 101, D16, 21,265-21,273.

Christopher, S.A., Wang, M., Berendes, T.A. and Welch, R., M., 1998: The 1985 Biomass Burning season in South America: Satellite Remote Sensing of Fires, Smoke, and Regional Radiative Energy Budgets, *Journal of Applied Meteorology*, 37, 661-678.

Christopher, S.A. and Zhang, J., 2002: Daytime Variation of Shortwave Direct Radiative Forcing of Biomass Burning Aerosols from GOES-8 Imager, *Journal of Atmospheric Sciences*, 59, 681691.

Chrysoulakis, N. and Cartalis, C., 2000: A new approach for the detection of major fires caused by industrial accidents, using NOAA/AVHRR imagery, *International Journal of Remote Sensing*, 21 (8), 1743-1748.

Chu, D.A., Kaufman, Y.J., Ichoku, C., Remer, L.A., Tanré, D. and Holben, B.N., 2002: Validation of MODIS aerosol optical depth retrieval over land, *Geophysical Research Letters*, 29, 10.1029/2001GL013205, 2-1 – 2-4.

Conley, A.H. 1996: A synoptic view of water resources in Southern Africa, Monograph No 6: Sink or Swim?, October 1996. Available at: http://www.iss.co.za/Pubs/Monographs/No6/Conley.html

Delmas, R.A., Druilhet, A., Cros, B., Durand, P., Delon, C., Lacaux, J.P., Brustet, J.M., Serça, D., Affre, C., Guenther, A., Greenberg, J., Baugh, W., Harley, P., Kingler, L., Ginoux, P., Brasseur, G., Zimmerman, J.M., Grégoire, J-M., Janodet, E., Tournier, A., Perros., P., Marion, T., Gaudichet, A., Cachier, H., Ruellan, S., Masclet, P., Cautenet, S., Poulet, D., Bouka Biona, C., Nganga, D., Tathy, J.D., Minga, A., Loemba-Ndembi, J., and Ceccato, P., 1999: Experiment for regional sources and sinks of oxidants (EXPRESSO): An overview, *Journal of Geophysical Research*, 30609-30624.

DeFries, R. and Townshend, J.G.R., 1994: NDVI-derived land cover classifications at a global scale, *International Journal of Remote Sensing*, 15, 3567-3586.

Diab, R.D., Thompson, A.M., Zunckel, M., Coetzee, G.J.R., Combrink, J., Bodeker, G.E., Fishman, J., Sokolic, F., McNamara, D.P., Archer, C.B. and Nganga, D., 1996a: Vertical ozone distribution over southern Africa and adjacent oceans during SAFARI-92, *Journal of Geophysical Research*, 101 (D19), 23,823-23,833, doi:10.1029/96JD01267 .

Diab, R.D., Jury, M.J., Combrink, J. and Sokolic, F., 1996b: A comparison of anticyclone and trough influences on the vertical distribution of ozone and meteorological conditions during SAFARI-92, *Journal of Geophysical Research*, 101 (D19), 23,809-23,821, doi:10.1029/95JD01844.

Dozier, J., 1981: A Method for Satellite Identification of Surface Temperature Fields of Subpixel Resolution, *Remote Sensing of Environment*, 11, 221-229.

DeFries R.S., Townshend, J.R.G and Hansen, M.C., 1999: Continuous fields of vegetation characteristics at the global scale at 1-km resolution. *Journal of Geophysical Research*, 104, 16911–16923.

Dubovik, O., Holben, B., Eck, T.F., Smirnov, A., Kaufman, Y.F., King, M.D., Tanré, D and Slutsker, I., 2002: Variablity of Absorption and Optical Properties of key aerosol types observed in worldwide locations, Journal of Atmospheric Sciences, 59, 590-608.

Eck, T.F., Holben, B.N., Reid, J.S., Dubovik, O., Smirnov, A., O'Neill, N.T., Slutsker and Kinne, S., 1999: Wavelength dependence of the optical depth of biomass burning, urban, and desert aerosols, Journal of Geophysical Research, 104 (D24), 31,333-31,349.

Eck, T. F., Holben, B. N. , Ward, D. E., Mukelabai, M. M., Dubovik, O., Smirnov, A., Schafer, J. S., Hsu, N. C., Piketh, S. J. , Queface, A., Le Roux, J., Swap, R. J. , and Slutsker, I., 2003: Variability of biomass burning aerosol optical characteristics in southern Africa during the SAFARI 2000 dry season campaign and a comparison of single scattering albedo estimates from radiometric measurements, *Journal of Geophysical Research*, 108(D13), 8477, doi:10.1029/2002JD002321.

Edwards, D.P., Emmons, L.K., Gille, J.C., Attié, J.-L., Giglio, L., Wood, S.W., Haywood, J., Deeter, M.N., Massie, S.T., Ziskin, D.C., and Drummond, J.R., 2006: Satellite-observed pollution from southern hemisphere biomass burning, *Journal of Geophysical Research*, 111, D14312, doi: 10.1029/2005JD006655.

Eva, H. and Lambin, E.F., 1998a: Burnt area mapping in Central Africa using ATSR data, *International Journal of Remote Sensing*, 19, 3473-3497.

Eva, H. and Lambin, E.F., 1998b: Remote sensing of biomass burning in tropical regions: Sampling issues and multisensor approach, *Remote Sensing of the Environment*, 64, 292-315.

Ferek., R.J., Reid, J.S., Hobbs, P.V., Blake, D.R., and Louisse, C., 1998: Emission factors of hydrocarbons, trace gases and particles from biomass burning in Brazil, *Journal of Geophysical Research*, 103, 32 107-32 118.

Fishman, J., Fakhurzzaman, K., Cross, B and Nganga, D., 1991: Identification of widespread pollution in the southern hemisphere deduced from satellite analyses, *Science*, 252, 1693-1696.

Frieman, M.T. and Piketh, S.J., 2003: Air Transport into and out of the Industrial Highveld Region of South Africa, *Journal of Applied Meteorology*, 42, 994-1002.

Frost, P.G.H., 1999: Fire in southern African woodlands: origins, impacts, effects, and control. In *Proceedings of an FAO meeting on Public Policies Affecting Forest Fires*, FAO Forestry Paper 138, pp. 181-205.

Garstang, M., Tyson, P.D., Swap, R., Edwards, M., Kållberg, P. and Lindesay, J.A., 1996: Horizontal and vertical transport of air over southern Africa, *Journal of Geophysical Research,* 101, D19, 23721-23731.

Giglio, L., Descloitres, J., Justice, C.O and Kaufmann, Y, 2003: An enhanced contextual fire detection algorithm for MODIS, *Remote Sensing of Environment*, 87, 273-282.

Giglio, L., van der Werf, G.R., Randerson, J.T., Colltz, G.J. and Kaisibhatla, P., 2006: Global estimation of burned area using MODIS active fire observations, *Atmospheric Chemistry and Physics,* 6, 957-974.

Guild, L.S., Boone Kauffman, J., Ellington, L.J., Cummings, D.L., Babbit, R.E., and Ward, D.E., 1998: Dynamics associated with the total aboveground biomass, C nutrient pools, and biomass of primary forest and pasture in Rondônia, Brazil during SCAR-B, *Journal of Geophysical Research*, 103, D24, 32091-32100.

Hansen, M., De Fries,R. , Townshend, J.G.R. and Sohlberg, R., 1998: UMD Global Land Cover Classification, 1 kilometre, 1.0, Department of Geography, University of Maryland, College Park, Maryland, 1981-1994.

Hansen, M.C. and Reed, B., 2000: A comparison of the IGBP DISCover and University of Maryland 1 km global land cover products, *International Journal of Remote Sensing*, 21 (6&7), 1365-1373.

Hansen, M.C., De Fries, R.S., Townshend, J.G.R. and Sohlberg, R.,2000: Global land cover classification at 1km spatial resolution using a classification tree approach, *International Journal of Remote Sensing*, 21 (6&7), 1331-1364.

Hao, W.M., Liu, M.H., and Crutzen, P.J., 1990,Estimates of annual and regional release of CO_2 and other trace gases to the atmosphere from fires in the tropics, based on FAO statistics for the period 1975-1980, in J.G. Goldammer (ed.), *Fire in the tropical biota: ecosystem processes and global changes*, Springer-Verlag, Berlin- Heidelberg, pp.440-462.

Hao, W.M., Ward, D.E., Olbu., G., and Baker, S.P., 1996: Emissions of CO_2, CO and hydrocarbons from fires in diverse African savanna ecosystems, *Journal of Geophysical Research*, 101, 23577-23584.

Haywood, J and Boucher, O., 2000: Estimates of the direct and indirect radiative forcing due to tropospheric aerosols: A review, *Reviews of Geophysics*, 38 (4), 513–543.

Haywood, J., Francis, P., Dubovik, O., Glew, M., Holben, B., 2003: Comparison of aerosol size distributions, radiative properties, and optical depths determined by aircraft observations and Sun photometers during SAFARI 2000, *Journal of Geophysical Research*, 108 (D13), 8471, doi:10.1029/2002JD002250.

Helas, G and Pienaar, J.J., 1996 , “Biomass burning emissions”, in Held, G., Gore, B.J., Surridge, A.D., Tosen, G.R., Turner, C.R. and Walmsley, R.D. (eds), *Air pollution and its impacts on the South African Highveld,* Environmental Scientific Association, Cleveland, pp 12-15.

Hély, C., Dowty, P.R., Alleaume, S., Caylor, K.K., Korontzi, S., Swap, R.J., Shugart, H.H. and Justice, C.O., 2003b: Regional fuel load for two climatically contrasting years in southern Africa, Journal of Geophysical Research, 108 (D13), 8475, doi: 10.1029/2002JD02341.

Hély, C., Caylor, K., Alleaume, S., Swap, R.J. and Shugart, H.H., 2003a: Release of gaseous and particulate carbonaceous compounds from biomass burning during the SAFARI 2000 dry season field campaign, *Journal of Geophysical Research*, 108, D13, 8470, doi:10.1029/2002JD002482.

Holben, B.N., Setzer, A., Eck, T.F., Pereira, A. and Slutsker, I., 1996: Effect of dry season biomass burning on Amazon basin aerosol basin concentrations and optical properties, *Journal of Geophysical Research*, 101 (D14), 19,465-19,481.

Holben, B.N., Tanré, D., Smirnov, A., Eck, T.F., Slutsker, I., Abuhassan, N., Newcomb, W.W., Schafer, J.S., Chatenet, B., Lavenu, F., Kaufman, Y.J., Van de Castle, J., Setzer, A., Markham, B., Clark, D., Frouin, R., Halthore, R., Karneli, A., O'Neill, N.T., Pietras, C., Pinker, R.T., Voss, K., and. Zibordi, G., 2001: An emerging ground-based aerosol climatology: Aerosol Optical Depth from AERONE, *Journal of Geophysical Research*, 106, (D11), 12,067-12,097.

Hobbs, P.V., Reid, J.S., Kotchenruther, R.A., Ferek, R.J. and Weiss, R., 1997: Direct Radiative Forcing by Smoke from Biomass Burning, *Science*, 275, 1776-1778.

Hoelzemann, J.J., Schultz, M.G., Brasseur, G.P. and Granier, C., 2004: Global Wildland Fire Emission Model (GWEM): Evaluating the use of global burnt satellite data, *Journal of Geophysical Research*, 109 (D14S04), doi:10.1029/2003JD003666.

Huffman, G.J., Adler, R.F. Arkin, P., Chang,A., Ferraro,R., Gruber, A., Janowiak, J., McNab, A., Rudolf, B., and Schneider, U., 1997: The Global Precipitation Climatology Project (GPCP) combined precipitation dataset, *Bulletin of the American Meteorological Society,* 78(1), 5-20.

Ichoku, C., Remer, L.A., Kaufman, Y.J., Levy, R., Chu, D.A., Tanré, D and Holben, B.N., 2003: MODIS observation of aerosols and estimation of aerosol radiative forcing over southern Africa during SAFARI 2000, *Journal of Geophysical Research*, 108, D13, 8499, doi: 10.1029/2002JD002366, 35-1 – 35-13.

IPCC Report 2001: *Climate Change 2001: The Scientific Basis,* Contribution of Working Group I to the Third Assessment Report of Intergovernmental Panel on Climate Change (IPCC), Cambridge: University Press.

Ito, A. and Penner, J.E., 2004: Global estimates of biomass burning based on satellite imagery for the year 2000, *Journal of Geophysical Research*, 109 (D14S05), doi: 10.1029/2003JD004423

Justice, C.O., Giglio, L., Korontzi, S., Morisette, J.T., Roy, D., Descloitres, J., Alleaume, S., Petitcolin, F. and Y. Kaufman., 2002: The MODIS fire products, *Remote Sensing of Environment,* 83, 244-262.

Kasischke, E.S., Hewson, J.H., Stocks, B., van der Werf, G. and Randerson, J., 2003: The use of ATSR active fire counts for estimating relative patterns of biomass burning- a study from the boreal forest region, Geophysical Research Letters, 30 (18), 1969, doi: 10.1029/2003GL017859.

Kaufman, Y.J. and Fraser, R.S., 1997: The effect of smoke particles on clouds and climate forcing, *Science,* 277, 1636-1639.

Kaufman, Y.J., Justice, C.O., Flynn, L., Kendall, J., Prins, E., and Ward, D.E., 1998: Potential global fire monitoring from EOS_MODIS, *Journal of Geophysical Research*, 103, 32215-32238.

Kaufman, Y.J., Ichoku, C., Giglio, L., Korontzi, S., Chu, D.A., Hao, W.H., Li, R-R. and Justice, C.O., 2003: Fire and smoke observed from the Earth Observing System MODIS instrument- product, validation, and operational use. *International Journal of Remote Sensing,* 24 (8), 1765-1781.

Keil, A and Haywood, J.M., 2003: Solar radiative forcing biomass burning aerosol particles during SAFARI 2000: A case study based on measured aerosol and cloud properties, *Journal of Geophysical Research*, 108, D13, 8467, doi: 10.1029/2002JD002315, SAF 3:1-10.

Kiehl, J.T. 1999: Solving the aerosol puzzle, *Science*, 283, 1273-1275.

Korontzi, S., Justice, C.O., and Scholes, R.J., 2003a: Influence of timing and spatial extent of vegetation fires in southern Africa on atmospheric emissions, *Journal of Arid Environment*, 54, 395-404.

Korontzi, S., Ward, D.E., Susott, R.A., Yokelson, R.J., Justice, C.O., Hobbs, P.V., Smithwick, E., and Hao, W.M., 2003b, Seasonal variation and ecosystem dependence of emission factors for selected trace gases and $PM_{2.5}$ for southern Africa savanna fires, *Journal of Geophysical Research*, 108(D24), 4758, doi: 10.1029/2003JD003730.

Korontzi, S., Roy, D.P., Justice, C.O. and Ward, D.E., 2004: Modeling and sensitivity analysis of fire emissions in southern Africa during SAFARI 2000, *Remote Sensing of Environment*, 92, 255-275.

Levine, J.S., Cahoon, Jnr., D.R., Costulis, J.A., Couch, R.H., Davis, R.E., Garn, P.A., Jalink, Jnr., A., McAdoo, J.A., Robinson, D.M., Roettker, W.A., Sasamoto, W.A., Sherrill, R.T., and Smith, K.D. 1996: FireSat and the Global Monitoring of Biomass Burning, in Levine, J.S., *Biomass Burning and Global Change Volume 1: Remote Sensing, Modelling and Inventory Development, and Biomass Burning in Africa*, The MIT Press, Cambridge, Massachusetts.

Levine, J.S., 1994, Biomass burning and the production of greenhouse gases, in R.G.Zepp (ed.), *Climate Biosphere Interaction: biogenic emissions and environmental effects of climate change*, John Wiley and Sons, Inc.

Levine, J.S., Cofer III, W.R., Cahoon Jnr, D.R., Winstead, E.L., The Global Impact of Biomass Burning, *Environmental Science and Technology*, March 1995,

Li, J., Pósfai, M., Hobbs, P.V. and Buseck, P.R., 2003: Individual aerosol particles from biomass burning in southern Africa: 2. Compositions and aging in inorganic particles, *Journal of Geophysical Research,* 108, D13, 8484, doi: 10.1029/2002JD002310, 20-1 – 20-12.

Lindesay, J.A., Andreae, M.O., Goldammer, J.G., Harris, G., Annegarn. H., J., Garstang, M., Scholes, R.J. and van Wilgen, B.W., 1996: International Geosphere-Biosphere Programme/International Global Atmospheric Chemistry SAFARI-92 field experiment: Background and overview, *Journal of Geophysical Research,* 101, D19, 23,521-23,530.

Matson, M., and Dozier, J., 1981: Identification of subresolution high temperature sources using a thermal IR sensor, *Photogrammetric Engineering and Remote Sensing*, 47, 1311-1318.

Mayaux,P., Bartholomé, E., Massart, M., Van Cutsem, C., Cabral, A., Nonguierma, A., Diallo,O., Pretorius,C., Thompson, M., Cherlet, M., Pekel, J-F., Defourny, P., Vasconcelos, M., Di Gregorio, A., Fritz, S., De Grandi, G., Elvidge, C., Vogt,P., Belward, A., 2003: *GLC2000: A Land cover map of Africa*, EUR 20524 EN, European Commission, Luxembourg.

Mbow, C., GoÏta, K., and Bénié, G.B., 2004: Spectral indices and fire behaviour simulation for fire risk assessment in savanna ecosystems, *Remote Sensing of Environment*, 91, 1-13.

McCollum, J.R., Gruber, A., and Mamoudou B, BA., 2000: Discrepancy between Gauges and Satellite Estimates of Rainfall in Equatorial Africa, *Journal of Applied Meteorology*, 39, 666-679.

Menzel, W.P. and Prinz, E.M., 1996: Monitoring Biomass Burning with the New Generation of Geostationary Satellites, in Levine, J.S, *Biomass Burning and Global Change Volume 1: Remote Sensing, Modelling and Inventory Development, and Biomass Burning in Africa*, The MIT Press, Cambridge, Massachusetts.

Moeller, C.C., Revercomb, H.E., Ackerman, S.A., Menzel, W.P. and Knuteson, R.O., 2003: Evaluation of MODIS thermal IR and L1B radiances during SAFARI 2000, *Journal of Geophysical Research,* 108, D13, 8494, doi:1029/2002JD002323., 30-1 – 30-12.

Morisette, J.T., Giglio, L., Csiszar, I., Setzer, A., Schroeder, W., Morton, D and Justice, C.O., 2005: Validation of MODIS active fire detection products derived from two algorithms, *Earth Interactions*, 9, 1-25.

Moula, M., Brutstet, J.M., Eva, H.D., Lacaux, J.P., Grégoire, J.M. and Fontan, J., 1996: Contribution of the Spread-Fire Model in the Study of Savanna Fires, in Levine, J.S., *Biomass Burning and Global Change Volume 1: Remote Sensing, Modelling and Inventory Development, and Biomass Burning in Africa*, The MIT Press, Cambridge, Massachusetts, 270-277.

Otter, L., Guenther, A., Wiedinmyer, C., Fleming, G., Harley,P., and Greenberg, J., 2003: Spatial and temporal variations in biogenic volatile organic compound emissions for Africa south of the equator, *Journal of Geophysical Research*, 108, D13, 8505, doi:10.1029/2002JD002609.

Pak, B.C., Langenfelds, R.L., Young, S.A., Francey, R.J., Meyer, C.P., Kivlighon, L.M., Cooper, L.N., Dunse, B.L., Allison, C.E., Steele, L.P., Galbaly, I.E. and Weeks, I.A., 2003: Measurements of biomass burning influences in the troposphere over southeast Australia during the SAFARI 2000 dry season campaign, *Journal of Geophysical Research*, 108, D13, 8480, doi: 10.1029/2002JD002343, 16-1 – 16-10.

Penner, J.E., Dickinson, R.E., O'Neill, C.A., 1992: Effects of Aerosol from Biomass Burning on the Global Radiation Budget, *Science*, 256, 1432- 1433.

Piketh, S.J., Annegarn, H.J., and Keen, M.A., 1996: Regional Scale Impacts of Biomass Burning Emissions over southern Africa, in Levine, J.S., *Biomass Burning and Global Change Volume 1: Remote Sensing, Modelling and Inventory Development, and Biomass Burning in Africa*, The MIT Press, Cambridge, Massachusetts.

Piketh, S.J., Annegarn, H.J. and Tyson, P.D., 1999: Lower tropospheric aerosol loadings over South Africa: The relative contribution of Aeolian dust, industrial emissions, and biomass burning, *Journal of Geophysical Research,* 104, 1597-1607.

Piketh, S.J.,Swap, R.B., Maenhaut, W, Annegarn, H.J. and Formeti, P., 2002: Chemical evidence of long-range transport over southern Africa, Journal of Geophysical Research, 107 (D24), 4817, doi:10.1029/2002JD002056.

Piketh, S.J. and Walton, N.M., 2004: Characteristics of Atmospheric Transport of Air Pollution for Africa, *The Handbook of Environmental Chemistry Vol.4,* Part G, 173-195.

Prins, E.M. and Menzel, W.P., 1994: Trends in South American biomass burning detected with the GOES visible infrared spin scan radiometer atmospheric sounder from 1983 to 1991, *Journal of Geophysical Research,* 99, D8, 16,719-16,735.

Prins, E.M., Feltz, J.M., Menzel, W.P. and Ward, D.E., 1998: An overview of GOES-8 diurnal fire and smoke results for SCAR-B and 1995 fire season in South America, *Journal of Geophysical Research*, 103, D24, 31,821-31,835.

Queface, A.J., Piketh, S.J., Annegarn, H.J., Holben, B.N. and Uthui, R.J., 2003: Retrieval of aerosol optical thickness and size distribution from the CIMEL Sun photometer over Inhaca Island, Mozambique, *Journal of Geophysical Research*, 108, D13, 8509, doi:10.1029/2002JD002374, 45-1– 45-9.

Radke, L.F., Hegg, D.A., Lyons, J.H., Brock, C.A., and Hobbs, P.V., 1988: Airborne measurements on smokes from biomass burning in *Aerosols and Climatic,* edited by P.V. Hobbs and M.P. McCormick, pp. 411-422, A. Deepak, Hammpton, Va.

Reid, J.S., Hobbs, P.V., Liousse, C., Martins, J.V., Weiss, R.E., and Eck, T.F., 1998: Comparisons of techniques for measuring shortwave absorption and black carbon content of aerosols from biomass burning in Brazil, *Journal of Geophysical Research*, 103, D24, 32031-31040.

Reid, J.S, Hobbs, P.V., Rango, A.L. and Hegg, D.A., 1999: Relationships between cloud droplet effective radius, liquid water content, and droplet concentration for warm clouds in Brazil embedded in biomass smoke, *Journal of Geophysical Research*, 104, D6, 6145-6153.

Reid, J., 2002: Research proposal: **"**Analysis of Real Time Biomass-Burning Transport Model Data with Remote Sensing Products.**"** Submitted to NASA Earth Science Enterprise's Modelling and Data Analysis Research, NRA-02-OES-06: Interdisciplinary Science (IDS), EOS Interdisciplinary Science (EOS/IDS) program managed by Dr. Donald Anderson. *Unpublished paper*, Monterey, California.

Roberts, G, Wooster, M.J., Perry, G.L.W., Drake, N., Rebelo, L.-M. and Dipotso, F., 2005: Retrieval of biomass combustion rates and totals from fire radiative power observations: Application to southern Africa using geostationary SEVIRI imagery, *Journal of Geophysical Research*, 110, D21111, 1-19, doi: 10.1029/2005JD006018.

Ross, J.L., Hobbs, P.V. and Holben, B., 1998: Radiative characteristics of regional hazes dominated by smoke from biomass burning in Brazil: Closure tests and direct radiative forcing, *Journal of Geophysical Research*, 103, D24, 31,925-31,941.

Roy, D.P., Borak, J.S., Devadiga, S, Wolfe, R.E., Zheng, M. and Descloitres, J., 2002: The MODIS land product quality assessment approach, *Remote Sensing of Environment,* 83, 62-76.

Roy, D.P., Frost, P.G.H., Justice, C.O., Landman, T., Le Roux, J.L.,Gumbo, K., Makungwa, S., Dunham, K., Du Toit, R., Mhwandagara, K., Zacarias, A., Tacheba, B., Dube, O.P., Periera, J.M., Mushove, P., Morisette, J.T., Santhana Vanna, S.K., and Davies, D. 2005:The Southern Africa Fire Network (SAFNet) regional burned-area product-validation protocol, *International Journal of Remote Sensing,* 26 (19), 4265-4292.

Roy, D.P., Jin, Y., Lewis, P.E. and Justice, C.O, 2005a: Prototyping a global algorithm for systematic fire-affected area mapping using MODIS time series data, *Remote Sensing of the Environment,* 97, 137-162.

Roy D.P., Trigg, S.N., Bhima, R., Brockett, B.H., Dube, O.P., Frost, P., Govender, N, Landmann,T., Le Roux,J., Lepono, T., Macuacua, J., Mbow, C., Mhwandangara, K.L., Mosepele, B., Mutanga, O., Neo-Mahupeleng, G., Norman, M., and Virgilo., S., 2006: The utility of satellite fire rroduct accuracy information—perspectives and recommendations from the Southern Africa Fire Network, *IEEE Transactions on Geoscience and Remote Sensing*, 44 (7).

Schmetz, J., Pili, P., Tjemkes, S, Just, D, Kerkmann, J, Rota, S and Ratier, A. 2002: An Introduction to Meteosat Second Generation (MSG), *BAMS American Meteorological Society*, 978-992, EUMETSAT 2005 www.eumetsat.int

Schmid, B., Redemann, J., Russell, P.B., Hobbs, P.V., Hlavka, D.L., McGill, M.J., Holben, B.N., Welton, E.J., Campbell, J.R., Torres, O., Kahn, R.A., Diner, D.J., Helmlinger, M.C., Chu, D.A., Robles-Gonzalez, C.and de Leeuw, G., 2003: Coordinated airborne, spaceborne, and ground-based measurements of massive thick aerosol layers during the dry season in southern Africa, Journal of Geophysical Research, 108, 8496, doi:10.1029/2002JD002297.

Scholes, M. and Andreae, M.O., 2000: Biogenic and Pyrogenic Emissions from Africa and their Impact on Global Atmosphere, Ambio, 29 (1), 23-29.

Scholes, R.J. and Walker, B.H., 1993: *An African Savanna: Synthesis of the Nylsvley Study*, pp. 175-176, Cambridge University Press, New York.

Scholes, R.J., Ward, D.E. and Justice, C.O., 1996a: Emissions of trace gases and aerosol articles due to vegetation burning in southern hemisphere Africa, *Journal of Geophysical Research*, 101, D19, 23677-23682.

Scholes, R.J., Kendall, J and Justice, C.O. 1996b: The quantity of biomass burned in southern Africa, *Journal of Geophysical Research*, 101, D19, 23,667-23,676.

Scholes, R.J., 1997: *Savanna* in Vegetation of Southern Africa., R.M. Cowling, D.M. Richardson, and S.M. Pierce (Eds), pp. 258-277, Cambridge: Cambridge University Press.

Schultz, M.G., 2002: On the use of ATSR fire count data to estimate the seasonal and interannual variability of vegetation fires, *Atmospheric Chemisrty and Physics,* 2, 387-395.

Shea, R.W., Shea, B.W., Boone Kauffman, J., Ward, D.E., Haskins, C.I., and Scholes, M.C., 1996: Fuel biomass and combustion factors associated with fires in savanna ecosystems of Soth Africa and Zambia, *Journal of Gepphysical Research,* 101, D19, 23,551-23,568.

Simon, M., Plummer, S., Fierens, Hoelzemann, J.J., and Arino, O., 2004: Burnt area detection at global scale using ATSR-2: The GLOBSCAR products and their qualification, Journal of Geophysical Research, 109, D14S02, doi: 10.1029/2003JD003622

Sinha, P., Hobbs, P.V., Yokelson, R.J., Bertschi, I.T., Blake, D.R., Simpson, I.J., Gao, S., Kirchstetter, T.W. and Novakov, T., 2003: Emissions of trace gases and particles from savanna fires in southern Africa, *Journal of Geophysical Research*, 108, D13, 8487, doi: 10.1029/2002JD002325.

Swap, R.J., Annergarn, H.J., Suttles, J.T., Haywood, J., Helmlinger, M.C., Hely, C., Hobbs, P.V., Holben, B.N., Ji, J., King, M.D., Landman, T., Maenhaut, W., Otter, L., Pak,B., Piketh, S.J., Platnick, S., Privette, J., Roy, D., Thompson, A.M., Ward, D. and Yokelson, R., 2002b: The Southern African Regional Science Initiative (SAFARI 2000): Overview of dry season field campaign, *South African Journal of Science*, 98, 125-130.

Swap, R.J., Annegarn, H.J., and Otter, L., 2002a: Southern African Regional Science Initiative (SAFARI 2000): summary of science plan, *South African Journal of Science*, 98, 119-124

Swap, R.J., Annegarn, H.J., Suttles, J.T., King, M.D., Platnick, S., Privette, J.L. and Scholes, R.J. 2003: Africa burning: A thematic analysis of the southern African Regional Science Initiative (SAFARI 2000), *Journal of Geophysical Research*, 108, D13, 8465, doi: 10.1029/2003JD003747.

Tansey, K., Grégoire, J-M., Stroppiana, D., Sousa, A., Silva, J., Pereira, J.M.C., Boschetti, L., Maggi, M., Brivio, P.A., Fraser, R., Flasse, S., Ershov, D., Binaghi, E., Graetz, D., and Peduzzi, P., 2004: Vegetation burning in the year 2000: Global burned area estimates from SPOT VEGETATION data. *Journal of Geophysical Research*, 109, D14S03, doi: 10.1029/2003/JD003598.

Thompson, A.M., Diab, R.D., Bodeker, G.E., Zunckel, M., Coetzee, G.J.R., Archer, C.B., McNamara, D.P., Pickering, K.E., Combrink, J., Fishman, J.and Nganga, D, 1996: Ozone over southern Africa during SAFARI-92/TRACE A, *Journal of Geophysical Research*, 101 (D19), 23,793-23,807, doi:10.1029/95JD02459.

Tyson, P.D. and Von Gogh, R.G., 1976: The use of monastic acoustic radar to assess the stability of the lower atmosphere over Johannesburg, *South African Geographical Journal,* 58(1), 57-67.

Tyson P.D., 1986: *Climatic Change and Variability in Southern Africa,* Oxford University Press, Cape Town.

Tyson, P.D., Garstang, M., Swap, R., Källberg, P. and Edwards, M., 1996a: An Air Transport Climatology for Subtropical Southern Africa, *International Journal of Climatology*, 16, 265-291.

Tyson, P.D., Garstang, M and Swap, R., 1996b: Large-scale Recirculation of Air over Southern Africa, *Journal of Applied Meteorology,* 35, 2218-2236.

Tyson, P.D., Garstang, M., Swap, R., Kâllberg, P. and Edwards, M., 1998: An air transport climatology for subtropical southern Africa, *Journal of Climatology*, 16 (3), 265-291, doi: 10.1002/(SICI)1097-0088(199603)16:3<265::AID-JOC8>3.0.CO;2-M.

Tyson, P.D. and Preston-Whyte, R.A. 2000: *The Weather and Climate of Southern Africa* Oxford University Press, Cape Town.

Tyson, P.D. and Gatebe, C.K., 2001: The atmosphere, aerosols, trace gases and biogeochemical change in southern Africa: a regional integration, *South African Journal of Science*, 97, 106-118.

Van der Werf, G.R., Randerson, J.T., Collatz, G.J. and Giglios, L., 2003: Carbon emissions from fires in tropical and subtropical ecosystems, *Global Change Biology*, 9, 547-562.

Van der Werf, G.R., Randerson, J.T., Giglio, L., Colltz, G.J., Kasibhatla, P.S., and Arellano, A.F., 2006: Interannual variability in global biomass burning emissions from 1997 to 2004, *Atmospheric Chemistry and Physics*, 6, 3423-3441.

Walker, N.D., 1990: Links between South African Summer Rainfall and Temperature Variability of the Aghulas and Benguela Current systems, *Journal Of Geophysical Research*, 95 (C3), 3297-3319, doi: 10.1029/JC0951CO3p03297.

Ward, D.E. and Hardy, C.C., 1991: Smoke emissions from wildland fires, *Environmental Information*, 17, 117-134.

Ward, D.E. and Hao, W.M., 1992: *Air toxic emissions from burning of biomass globally-preliminary estimates*, in Proceedings: Air and Waste Management Association 85th Annual Meeting and Exhibition, Vancouver, British Columbia.

Ward, D.E. and Radke, L.F., 1993: Emission measurements from vegetation fires: A comparative evaluation of the results in *Fire in the environment: The Ecological, Atmospheric and Climatic Importance of Vegetation Fires,* edited by P.J. Crutzen and J.G. Goldammer, pp. 55-75, John Wiley, New York.

Ward, D. E., Hao, W. M., Susott, R. A. , Babbitt, R. E. Shea, R. W. , Kauffman, J. B., and Justice. C. O., 1996: Effect of fuel composition on combustion efficiency and emission factors for African savanna ecosystems, *Journal of Geophysical Research*, 101(D19): 23569-23576.

Watts, P.D., Allen, M.R., Mutlow, C.T. and Levoni, C., 2000: "Aerosol properties derived from Meteosat Second Generation (MSG) Observations: Final Report for Council for Central laboratory of Research Councils (CLRC)". <www.eumetsat.int>

Waugh, D., 1995. *Geography: An Integrated Approach*, Thomas Nelson and Sons Ltd.: UK.

White, F., 1983, The Vegetation of Africa: A descriptive memoir to accompany the UNESCO/AETFAT/UNSO vegetation map of Africa, 356 pp., UNESCO, Paris, 1983.

Wild, H., and L. A. G. Barbosa (eds.), Flora Zambesiaca (suppl.), in Vegetation Map of the Flora Zambesiaca Area, edited by H. Wild and H. Fernandes, 68 pp., M. O. Collins, Zimbabwe, 1968.

Yokelson, R.J., Bertschi, I.T., Christian, T.J., Hobbs, P.V., Ward, D.E. and Hao, W.M., 2003: Trace gas measurements in nascent, aged, and cloud-processed smoke from African savanna fires by airborne Fourier transformation infrared spectroscopy (AFTIR), *Journal of Geophysical Research*, 108, D13, 8478, doi: 10.1029/2002JD002322, 14-1 – 14-18.

Zunkel, M., Piketh, S and Freiman, T., 1999: Dry deposition of sulphur at a high altitude background station in South Africa, *Water, Air and Soil Pollution*, 115, 445-463.

Appendix

Table 10: Total biomass burning emissions for each region

2003	CO_2 (Tg)	CH_4 (Gg)	CO (Gg)	NMHC (Gg)	TPM (Gg)	TPC (Gg)	OC (Gg)	BC (Gg)	NO (Gg)	NH_3 (Gg)	HCN (Gg)	HCHO (Gg)	CN (number of particles)
Congo	200	740	13100	890	1300	790	790	80	300	170	100	20	4.4E+17
Angola	130	390	8800	500	1340	500	650	50	240	115	150	15	3.2E+17
East Africa	120	350	7500	430	1100	430	550	40	220	100	120	10	2.8E+17
Zambezi	60	120	3100	170	380	160	170	20	130	30	40	10	4.1E+17
South Africa	170	430	10600	600	1600	570	700	60	320	130	170	20	7.8E+17
Nambia	60	120	3150	170	460	160	190	20	120	40	50	10	3.7E+17
2004	CO_2 (Tg)	CH_4 (Gg)	CO (Gg)	NMHC (Gg)	TPM (Gg)	TPC (Gg)	OC (Gg)	BC (Gg)	NO (Gg)	NH_3 (Gg)	HCN (Gg)	HCHO (Gg)	CN (number of particles)
Congo	270	840	16350	1030	1540	950	930	100	530	210	120	30	5.9E+17
Angola	140	410	9200	520	1370	515	670	50	270	120	150	15	3.4E+17
East Africa	160	420	9700	520	1240	540	640	60	370	130	130	15	3.8E+17
Zambezi	140	260	7130	350	670	360	350	40	420	90	60	20	5.9E+17
South Africa	190	460	11550	650	1700	610	750	70	390	140	170	25	8.2E+17
Nambia	100	180	5200	260	600	260	280	30	260	60	60	10	4.6E+17
2005	CO_2 (Tg)	CH_4 (Gg)	CO (Gg)	NMHC (Gg)	TPM (Gg)	TPC (Gg)	OC (Gg)	BC (Gg)	NO (Gg)	NH_3 (Gg)	HCN (Gg)	HCHO (Gg)	CN (number of particles)
Congo	260	820	16000	990	1500	910	900	90	500	200	120	25	5.6E+17
Angola	140	400	9100	510	1400	510	660	50	270	120	150	15	3.4E+17
East Africa	160	410	10000	510	1200	520	630	50	360	120	130	15	3.7E+17
Zambezi	130	240	6800	330	650	330	330	40	390	80	50	20	5.7E+17
South Africa	190	460	11400	640	1680	600	740	70	380	140	170	25	8.0E+17
Nambia	90	170	5000	250	600	250	270	30	250	60	50	10	4.4E+17
2006	CO_2 (Tg)	CH_4 (Gg)	CO (Gg)	NMHC (Gg)	TPM (Gg)	TPC (Gg)	OC (Gg)	BC (Gg)	NO (Gg)	NH_3 (Gg)	HCN (Gg)	HCHO (Gg)	CN (number of particles)
Congo	300	930	18100	1140	1700	1050	1020	110	580	230	130	30	6.5E+17
Angola	150	440	10000	560	1500	560	720	60	290	130	170	15	3.7E+17
East Africa	180	460	10600	570	1350	580	700	60	410	140	140	20	4.2E+17
Zambezi	160	280	7900	380	750	390	380	50	460	100	60	20	6.6E+17
South Africa	210	500	12500	700	1800	660	810	70	420	160	190	30	9.0E+17
Nambia	110	200	5600	280	670	280	300	30	280	70	60	15	5.1E+17

Table 11: Biomass burning emissions per vegetation type

2002	CO2 (Tg)	CH4 (Gg)	CO (Gg)	NMHC (Gg)	TPM (Gg)	TPC (Gg)	OC (Gg)	BC (Gg)	NO (Gg)	NH3 (Gg)	HCN (Gg)	HCHO (Gg)	CN (number of particles)
Forest	20	110	1610	130	100	100	80	10	20	20	2	2	0.0E+00
Woodland	120	350	8000	430	1300	460	640	40	220	100	160	10	2.5E+17
Savanna	65	105	3270	150	290	150	140	25	220	42	20	10	3.8E+17
Agriculture	10	20	550	40	80	20	20	5	20	10	1	1	2.0E+16
2003	CO2 (Tg)	CH4 (Gg)	CO (Gg)	NMHC (Gg)	TPM (Gg)	TPC (Gg)	OC (Gg)	BC (Gg)	NO (Gg)	NH3 (Gg)	HCN (Gg)	HCHO (Gg)	CN (number of particles)
Forest	150	660	10100	790	630	640	500	60	150	130	15	10	3.3E+17
Woodland	500	1500	34000	1810	5600	1900	2700	180	1000	450	670	50	1.1E+18
Savanna	410	610	19400	870	1670	900	810	120	1310	230	120	50	2.1E+18
Agriculture	40	70	2300	170	320	100	80	20	60	30	5	5	8.4E+16
2004	CO2 (Tg)	CH4 (Gg)	CO (Gg)	NMHC (Gg)	TPM (Gg)	TPC (Gg)	OC (Gg)	BC (Gg)	NO (Gg)	NH3 (Gg)	HCN (Gg)	HCHO (Gg)	CN (number of particles)
Forest	150	660	10070	780	630	640	500	60	150	130	10	15	3.3E+17
Woodland	500	1500	34000	1810	5590	1900	2730	180	950	440	700	50	1.1E+18
Savanna	410	610	19390	870	1680	900	820	120	1300	230	120	60	2.1E+18
Agriculture	40	90	2280	170	320	100	80	20	60	30	5	5	8.4E+16
2005	CO2 (Tg)	CH4 (Gg)	CO (Gg)	NMHC (Gg)	TPM (Gg)	TPC (Gg)	OC (Gg)	BC (Gg)	NO (Gg)	NH3 (Gg)	HCN (Gg)	HCHO (Gg)	CN (number of particles)
Forest	150	640	9720	760	610	620	490	60	150	120	10	10	3.2E+17
Woodland	540	1610	36700	1960	6040	2100	2950	190	1030	480	760	50	1.2E+18
Savanna	380	560	17860	800	1570	820	750	110	1190	210	110	50	2.0E+18
Agriculture	40	70	2420	190	340	110	90	20	70	30	5	5	9.0E+16
2006	CO2 (Tg)	CH4 (Gg)	CO (Gg)	NMHC (Gg)	TPM (Gg)	TPC (Gg)	OC (Gg)	BC (Gg)	NO (Gg)	NH3 (Gg)	HCN (Gg)	HCHO (Gg)	CN (number of particles)
Forest	170	740	11310	880	710	720	570	70	170	140	15	20	3.7E+17
Woodland	610	1840	41900	2230	6890	2390	3400	220	1170	550	860	60	1.3E+18
Savanna	455	660	21200	950	1850	980	900	130	1410	250	130	60	2.4E+18
Agriculture	40	70	2410	180	340	110	90	20	70	30	5	5	8.9E+16